Structure and Function in Early Glaucoma

by

Carmen Balian

A thesis

presented to the University of Waterloo

in the fulfillment of the

thesis requirement for the degree of

Doctor of Philosophy

in

Vision Science

Waterloo, Ontario, Canada, 2017

I hereby declare that I am the sole author of this thesis. This is a true copy of the thesis, including any required final revisions, as accepted by my examiners.

I understand that my thesis may be made electronically available to the public.

Abstract

Glaucoma is a general term that includes an array of ocular conditions that cause a specific neuropathy of the optic nerve (Greenfield, Bagga, et al. 2003) of which abnormalities associated with this disorder are localized at the level of the retinal ganglion cell layer (Epstein 1997; Quigley & Broman 2006). This structure-function relationship is not clear as it relies on several factors such as variability from the structural and functional tests, differences in measurement scales between the two modalities (Greaney et al. 2002; Katz 1999; Drance 1985; Hood et al. 2007) and physiological variation amongst individuals (Pan & Swanson 2006).

The global aim of this thesis was to relate visual function of the retinal ganglion cells to structure of the optic nerve head and retinal nerve fiber layer with respect to the following perimetry techniques: i) standard automated perimetry (SAP), ii) frequency doubling technology (FDT), iii) flicker defined form (FDF), and iv) the motion detection test (MDT), and the following imaging instruments: i) confocal scanning laser ophthalmoscopy (HRT), ii) optical coherence tomography (OCT), and iii) scanning laser polarimetry (GDx VCC).

The specific purpose of this study was to i) compare the test-retest characteristics of the perimetry techniques, ii) determine which may be more sensitive for early detection, iii) evaluate the structure-function relationship between measures of retinal nerve fiber layer and visual function, and iv) perform a preliminary study to determine which

techniques may be most suitable to monitor progression, in patients with early stage glaucoma.

MDT showed little change in the 1-year follow-up study thus being unsuitable for monitoring change. FDT and FDF gave a similar performance and are likely optimal for the detection of early functional damage.

Poor diagnostic agreement was seen between the HRT and each perimetry technique. Because no one perimetry test showed both high sensitivity and high specificity, it is recommended that a combination of FDF with either SAP, FDT or MDT be used as the functional component in the diagnosis and follow-up of patients with glaucoma.

The strongest global structure-function correlations for OCT were seen with SAP, FDT and MDT; for GDx, the strongest association was seen with FDF. These results suggest that FDF and GDx used in combination are best to detect early glaucomatous changes.

Acknowledgements

First and foremost I would like to thank my supervisors, Dr. John G. Flanagan and Dr. Natalie Hutchings, from whom I have learned so much. I am honored for the opportunity to work with them and for their contributions to my studies have been invaluable.

In addition, I would also like to thank the remaining members of my committee, Dr. Daphne McCulloch, Dr. Michael Beazely and Dr. Shaban Demirel for their time and dedication.

Special thanks to Dr. Christoph Kranemann, Dr. Areef Nurani and their staff who offered their support and encouragement during the collection of my data.

The dedication of the patients involved in this study is greatly appreciated; if it were not for them, this study will not have been possible.

Words cannot express the gratitude I feel towards you all.

Dedication

To Mom, Dad and Lina, who have always believed and supported me in everything I have done. I could not have done it without your love and support.

Table of Contents

List of Figures

List of Tables

List of Abbreviations

AGIS	Advanced Glaucoma Intervention Study
AH	aqueous humor
ANOVA	analysis of variance
asp	apostilbs
ASTA	adaptive staircase thresholding algorithm
AUROC	area under receiving operator curve
BCVA	best corrected visual acuity
BES	Baltimore Eye Study
BL	borderline
BMES	Blue Mountain Eye Study
CCT	central corneal thickness
CGS	Canadian Glaucoma Study
C/D	cup to disc ratio
CI	confidence interval
CIGTS	Collaborative Initial Glaucoma Treatment Study
CNTGS	Collaborative Normal Tension Glaucoma Study
CL	confidence limit
CoR	coefficient of repeatability
CoV	coefficient of variability
CSLO	confocal scanning laser ophthalmoscopy

D	diopters
dB	decibels
ECC	enhanced corneal compensation
EMGT	Early Manifest Glaucoma Trial
FD	Frequency Doubling
FDF	Flicker Defined Form
FDT	Frequency Doubling Technology
FL	fixation losses
FN	false negative
FP	false positive
FT	full threshold
GCP	glaucoma change probability
GCPM	glaucoma change probability map
GDx VCC	nerve fiber analyzer with variable corneal compensation
GHT	glaucoma hemifield test
GPA	glaucoma progression analysis
GPS	glaucoma probability score
GSS	glaucoma staging system
HD-OCT	high definition optical coherence topography
HEP	Heidelberg Edge Perimeter
HFA	Humphrey Field Analyzer
HRT	Heidelberg Retina Tomography

Hz	hertz
I	inferior
ILM	inner limiting membrane
IN	inferionasal
IOP	intraocular pressure
IT	inferiotemporal
LoA	limits of agreement
LOCS	Lens Opacity Classification System
LR	likelihood ratio
M cells	magnocellular ganglion cells
MD	mean deviation
MDT	Motion Detection Threshold
MinArc	minutes of arc
MOBS	modified binary search
MRA	Moorfields Regression Analysis
MS	mean sensitivity
N	nasal
NFI	nerve fiber index
NFL	nerve fiber layer
nm	nanometer
NRA	neuroretinal rim area
OCT	optical coherence tomography

OD	right eye
OHTS	Ocular Hypertension Treatment Study
ONH	optic nerve head
ONL	outside normal limits
OS	left eye
PCA	principal curve analysis
pdf	probability density function
PD	pattern deviation
PERG	pattern electroretinogram
POAG	primary open angle glaucoma
PSD	pattern standard deviation
RNFL	retinal nerve fiber layer
RGC	retinal ganglion cells
S	superior
SAP	standard automated perimetry
SD	standard deviation
SD-OCT	spectral domain optical coherence tomography
SITA	Swedish interactive test algorithm
SLP	scanning laser polarimetry
SN	superionasal
SS	SITA standard
ST	superiotemporal

SWAP	short-wavelength automated perimetry
SWS	short-wavelength sensitivity
T	temporal
TCA	topographic change analysis
TD	total deviation
TD-OCT	time domain optical coherence tomography
VA	visual acuity
VCC	variable corneal compensation
VF	visual field
VFI	visual field index
vs	versus
WEBS	weighted binary search
WNL	within normal limits
WW	white-on-white perimetry
ZEST	zippy estimation of sequential testing

1. Introduction

1.1 Glaucoma

Glaucoma is a general term that includes an array of ocular conditions that cause a specific neuropathy of the optic nerve (Gupta & Chen 2016) of which abnormalities associated with this disorder are localized at the level of the retinal ganglion cell layer (Epstein 1997; Quigley & Broman 2006). The early stage of glaucoma is a very gradual process; depressions of sensitivity noted in the patients' visual field often appear and disappear before becoming stable defects (Heijl & Patella 2002). Once stabilized, these defects, referred to as scotomas, begin to enlarge and pursue the arcuate pattern of the retinal nerve fibers. In the later stages, large scotomas from the superior and inferior field reach into the peripheral field and connect leaving only the central or temporal visual field intact (Weber et al. 1989; Quigley et al. 1989). Many times, the patients will not be able to detect any loss of vision until the later stages as a relative loss in sensitivity is difficult to be detected by the patient even with a relatively large scotoma.

The loss of retinal ganglion cells (RGC) and their axons is the essential pathological process in this disease (Quigley et al. 1989; Johnson 2009). Histopathologic studies of both human and animal eyes have shown that the primary site for glaucoma damage is the RGC axons at the lamina cribrosa (Burgoyne 2011; Quigley & Anderson 1976; Quigley et al. 1981; Minckler et al. 1977; Guedes et al. 2003). Progressive

glaucomatous loss of RGC causes characteristic optic nerve, retinal nerve fiber layer (RNFL) and visual field abnormalities (Epstein 1997; Johnson 2009; Nicolela et al. 2001; Quigley 1993). The RNFL is composed of retinal ganglion cells, neuroglia and astrocytes (Epstein 1997).

In glaucoma, RGCs have been shown to die by apoptosis after going through morphologic changes of dendritic field size reduction, axon atrophy and soma shrinkage (Almasieh et al. 2012; Quigley et al. 1995; Garcia-Valenzuela et al. 1995). This gradual morphogenesis leading to apoptosis leads some to believe that this time can allow for neuroprotective intervention and hence salvage the RGCs (Kwon et al. 2009). This stresses the importance and need for instruments which detect glaucoma early in the disease.

1.2 Primary Open Angle Glaucoma

Primary Open Angle Glaucoma (POAG) is the most common form of glaucoma (Allingham et al. 2005) and is characteristic of an open iridocorneal angle in which aqueous humor (AH) outflow is diminished and cupping of the optic nerve head (ONH) occurs with corresponding loss of visual field (Kwon et al. 2009; Allingham et al. 2005) in the characteristic pattern described above.

1.3 Structure in Glaucoma

Destruction of nerve fibers results in loss of normal NFL architecture therefore, evaluation of RNFL thickness is important for the early detection of glaucoma (Quigley et al. 1994; Lim et al. 2016, Fingeret et al., 2005; Kotowski et al., 2014; Quigley et al., 1992). A review by Greenfield and Weinreb (2008) have highlighted the importance of optic nerve head documentation in monitoring glaucoma.

Optic nerve topography is dependent upon the number, size and orientation of nerve fiber axons entering it from the retina (Jonas et al. 1992). Both age (Mikelberg et al. 1989; Repka & Quigley 1989; Balazsi et al. 1984; Poinoosawmy et al. 1997; Quigley et al. 1991) and ONH size (Mikelberg et al. 1989; Chen et al. 2009) determine the number of ganglion cells and nerve fibers present.

Several patterns of glaucomatous optic disc and nerve fiber layer damage have been described (Airaksinen et al. 1984; Drance et al. 1986; Caprioli et al. 1987; Jonas et al. 1988; Caprioli 1989; Tuulonen & Airaksinen 1991; King et al. 2000). Structural changes in glaucoma include enlargement of the optic cup size (Minckler et al. 1977; Airaksinen et al. 1984; Airaksinen & Heijl 1983; Zeyen & Caprioli 1993; Drance et al. 1977), morphological changes to the lamina cribrosa (Burgoyne 2004; Morgan-Davies et al. 2004; Faridi et al. 2014), large or asymmetric cup-to-disc (C/D) ratios and changes over time (Quigley et al. 1994), disc hemorrhages (Quigley et al. 1994; Airaksinen & Tuulonen 1984; Diehl et al. 1990; Bengtsson 1990; Sommer et al. 1991), NFL abnormalities (TG & Caprioli 1993; Quigley et al. 1992; Tuulonen et al. 1993; Chandra

et al. 2013; GDx VCC Primer 2004), damage (Johnson 2009) and decrease in the number of optic nerve head fibers (Harwerth et al. 1999), rim thinning, notching and excavation (Quigley et al. 1994; AW & Bailey 1993). Loss of neuroretinal rim and increase in optic cupping are parallel with the loss of optic nerve axons in glaucoma (Teal et al. 1972; Airaksinen & Drance 1985).

Clinically, distinguishing between normal and glaucomatous optic nerve is a challenge. The difficulty in detecting early to moderate ONH damage is for the most part due to the large variability of the ONH size and appearance in normal individuals (Jonas et al. 1988; Bengtsson 1976); rim area and cup size vary significantly due to variation in disc size (Jonas et al. 1988; Bengtsson 1976; Quigley et al. 1990) and ethnic origin (Beck et al. 1985; Chi et al. 1989; Varma et al. 1994; J 1971). There also exists a large variability between glaucoma experts in evaluating the optic disc for glaucoma diagnosis or signs of progression (Lichter 1976; Pederson & Anderson 1980; Zeyen et al. 2003; Tanna et al. 2011). Thus, a more objective method of ONH and RNFL documentation is needed.

The two main applications for optic nerve head analysis in the diagnosis and treatment for glaucoma are i) distinguishing between normal and disease of optic nerve heads and ii) identifying progression with successive tests (Fingeret, Medeiros, et al. 2005). Both accurate and reproducible measurements are essential for early diagnosis and detection of progression (Fingeret, Medeiros, et al. 2005).

Various imaging techniques available for recording the structure of the optic nerve head and retina use different properties of light and are aimed at detecting different characteristics of retinal tissue in order to quantitatively assess topography and other structural properties of the ONH and RNFL (Ventura et al. 2006; Weinreb 1999; Weinreb et al. 1990; Weinreb et al. 1993; Huang et al. 1991; Hoh et al. 2000; Greenfield 2002; Kotera et al. 2008; Zangwill et al. 2000; Niessen et al. 1996; Chang & Budenz 2008). Such techniques include, optical coherence tomography (OCT) (Schuman, Hee, Arya, et al. 1995; Schuman et al. 1996; Strouthidis & Garway-Heath 2008), confocal scanning laser ophthalmoscopy (CSLO) (Fechtner et al. 1993; Uchida et al. 1996; Zangwill et al. 1996; Lemij & Reus 2008), and scanning laser polarimetry (SLP) (Zeimer et al. 1998). These techniques can provide precise and objective quantitative measurements of the RNFL and ONH (Wollstein et al. 1998; Swanson et al. 1993; Teal et al. 1972; Hoh et al. 2000; Drexler et al. 1999; Weinreb, Shakiba & Zangwill 1995; Weinreb, Shakiba, Sample, et al. 1995) which can help with the diagnosis and monitoring of diseases that affect the optic nerve (Samarawickrama et al. 2012) and have been shown to discriminate between normal, OHT, POAG, and NTG subjects (Zangwill et al. 1996; Anton et al. 2007). Both hardware and software upgrades have been applied to all these instruments since their earlier versions which have allowed for more sensitive detection and monitoring of glaucoma (Fechtner & Lama 1999). Patients were more accurately screened for early perimetric glaucoma when parameters from more than one instrument were combined (Greaney et al. 2002).

In early glaucoma, structural damage is more readily detectable in larger optic discs (Quigley et al., 1982; Zangwill et al., 2000). Both clinical and experimental observations of the peripapillary NFL region have shown that the earliest signs of NFL damage as a result of glaucoma are along the superiotemporal and inferiotemporal bundles (Leung et al., 2010). In normal adults, the neuroretinal rim width is greatest inferiorly, then superiorly, nasally then temporally (Quigley et al. 1990) resulting in a horizontally oval cup shape. Any changes to this configuration can be due to glaucoma hence, identifying the neuroretinal rim width is key in the diagnosis and monitoring of glaucoma (Hoyt & Newman 1972).

Measuring macular thickness is becoming a useful tool in detecting early glaucomatous damage as it is highly dense with RGCs (Aref 2013; Zeimer et al. 1998; Greenfield, Bagga, et al. 2003). A recent study suggests using a perimetry technique with a more dense test grid pattern in the macular region to detect macular damage caused by glaucoma (Grillo et al. 2016).

1.4 Function in Glaucoma

One of the most common measures of visual function is static automated perimetry (Garway-Heath et al. 2002; Flammer et al. 1985) which measure the extent and depth of visual field damage by determining the eye's ability to detect small points of light

projected onto both the central and peripheral areas of the field of vision. The purpose of a visual field examination in glaucoma is to detect defects and determine the specific pattern of visual field loss for diagnostic purposes, and monitor patients for evidence of visual function deficit progression (Chauhan et al. 1990; Spry et al. 2001; Spry & Johnson 2002).

The use of automated perimeters has allowed for detection of relative scotomas within the visual field. The neural-sensitivity hypothesis states that the proportion of RGC loss determines perimetry thresholds (Tate 1985; Frisén 1993; Bartz-Schmidt & Weber 1993; Harwerth et al. 2004; Kerrigan-Baumrind et al. 2000; Harwerth et al. 2007; Harwerth & Quigley 2010; Garway-Heath et al. 2002; AGIS Investigators 1994) therefore, through psychophysical testing, the ocular effects of glaucoma can be quantified (Katz 1999) giving a functional correlate to the damage.

Evaluating a patient's glaucoma status based on his or her visual field results requires statistical analysis to determine how the results differ from expected values and how it is related to the RGCs and helps estimate glaucoma severity (AGIS Investigators 1994). This thesis will be comparing different perimetry techniques to determine the ability of each at detecting functional changes due to glaucoma and determine which may be more suitable for early detection.

1.6 Structure and Function in Glaucoma

Defining the relationship between structural and functional loss in glaucoma has been of great interest since the 1850s (Drance 1974). Von Graefe, Jaeger, Weber and Mackenzie were among the group who founded the relationship between the appearance of the optic nerve and glaucomatous visual field defects (Duke-Elder 1941). The relationship between structure and function of the retinal ganglion cells is not very accurate (Harwerth et al. 2007; Harwerth & Quigley 2006; Harwerth et al. 2002; Johnson et al. 2000) as it relies on several factors such as variability from the structural and functional tests, differences in measurement scales between the two modalities (Garway-Heath et al. 2002; Katz 1999; Drance 1985; Hood & Kardon 2007), spatial summation (Drance 1985; Hood & Kardon 2007; Budenz et al. 2002; Pan & Swanson 2006) and physiological variation amongst individuals (Pan & Swanson 2006).

Correlation between structural and functional changes in glaucoma can be seen in less than 50% of glaucoma cases, even with the use of advanced diagnostic and analytic procedures (Drance 1985; Turpin et al. 2009; Gardiner et al. 2005; Garway-Heath, Caprioli, et al. 2000; Strouthidis, Vinciotti, et al. 2006). Many studies have shown that structural changes can be observed before any functional change is detected (Johnson 2009; Harwerth et al. 1999; Drance et al. 1977; Quigley et al. 1992; WC 1990; Johnson 1994; Breton & B 1989; Chauhan et al. 2001; Aptel et al. 2010; Sung et al. 2011; Harwerth 2008) i.e. thinning of the RNFL or neuroretinal rim is often seen in patients

with normal standard automated perimetry measures (Sung et al. 2011; Airaksinen & Heijl 1983; Airaksinen & Drance 1985; Lan et al. 2003), while other studies have shown either parameter can change before the other or simultaneously (Kass et al. 2002; Heijl et al. 2002; Malik et al. 2012a).

In patients with glaucoma, the observed patterns of visual field abnormalities correspond to the anatomy of the RNFL and its projections to the ONH (Breton & Drum 1989; Choplin 2007). Initial studies were conducted by Quigley who demonstrated that 40% axonal loss may occur before any noticeable changes in visual function (Quigley et al. 1982). Further studies showed that 20% to 50% of retinal ganglion cell loss is required to first detect any significant visual function defect and that this value varies with retinal eccentricity (Quigley et al. 1982; Harwerth et al. 2007).

Strong evidence suggests that glaucoma can progress to a moderate a stage before a visual field defect is seen on SAP (Johnson 2009; Harwerth et al. 1999; Zeyen & Caprioli 1993; Quigley et al. 1992; Tuulonen et al. 1993; Chandra et al. 2013; Hart et al. 1978; Sommer et al. 1979a) and structural changes are present before any visual field damage is detected by SAP (Kuang et al. 2015; Quigley et al. 1992; Chandra et al. 2013; Wilensky & Kolker 1976; Leung et al. 2005; Kanamori et al. 2008; Reus et al. 2006; Bowd et al. 2006a). Recent studies have reported less RGC loss with SAP (Fechtner & Lama 1999; Ventura et al. 2006; Park et al. 2011; Jung et al. 2012). Thus, techniques that are more sensitive to measuring RNFL are needed to help with the accurate diagnosis and monitoring of glaucoma (Medeiros & Weinreb 2002).

The OHTS (Keltner et al. 2006) and the European Glaucoma Prevention Study (Miglior 2005) have found that initial glaucomatous damage can be either structural, functional or both. Factors such as age (Honjo et al. 2015; Zueva et al. 2016) and the presence of initial functional changes (Öhnell et al. 2016) can influence the diagnostic capabilities of each parameter. Measurement of structural changes to the ONH and RNFL offers the prospect of improved early detection and monitoring of glaucoma (Quigley 1986; Drance 1985; Bowd et al. 2001). Therefore, it is imperative to use both structural and functional measurements comprehensively to make clinical decisions regarding the disease (Garway-Heath 2007; Airaksinen et al. 1985; Airaksinen & Drance 1985).

It should also be noted that dissociation between structural and functional measurements occur, such that some structural changes are not associated with loss of RGCs and functional changes are not related to cell loss but cell dysfunction (Garway-Heath 2007). Cell shrinkage and methods used to determine number of ganglion cells could affect retinal ganglion cell count (Airaksinen & Alanko 1983). Different types of perimetric techniques require loss of varying numbers of ganglion cells to show different depths of visual field defect (Johnson 1994; AGIS Investigators 1994) explaining the discrepancy seen amongst perimetry techniques in detecting glaucomatous changes.

Harwerth et al (2005) have described that the structure-function relationship is different at different stages of the disease. This relationship has been proposed to be curvilinear

when plotted in linear/logarithmic units (Hood et al. 2007). Hence, functional changes are smaller per unit structure in the early stages than later in the course of the disease (Artes 2008). Thus, it has been proposed that early stages of glaucoma should be monitored with structural measurements and later stages should be followed with functional tests.

Studies have shown that structural damage does not occur without functional consequences (Harwerth & Quigley 2006; Kanamori et al. 2006) and both structure and function test should be used together to help with the follow up of patients with glaucoma (Artes & Chauhan 2005a; Strouthidis, Vinciotti, et al. 2006). Recent studies confirm the hypothesis that the structure-function relationship changes with age (Ren et al. 2014; Honjo et al. 2015).

The RGC redundancy hypothesis (also known as, RGC functional reserve hypothesis) presents a theory regarding the structure-function relationship in early glaucoma (Ventura et al. 2006). It proposes that as much >25% of RGCs and their axons can be lost (Kerrigan-Baumrind et al. 2000; Quigley et al. 1992) before SAP detects loss in visual function (Ventura et al. 2006), i.e significant retinal thinning can occur but not be corroborated by visual field testing (Medeiros et al. 2004; Asrani et al. 2003). Studies in monkeys with experimental glaucoma have reported a progressive functional loss in SAP with increasing loss of RGCs above 50% (Harwerth et al. 2002). However,

in some areas of the retina, sensitivity losses of 6-12dB were seen on SAP with 0-10% RGC loss (Harwerth et al. 2002).

The impression of a functional-reserve hypothesis is due to the difference in scaling between structural (percentage) and functional (decibel, dB) measurements (Garway-Heath et al. 2002; Reus & Lemij 2004b; Garway-Heath, Caprioli, et al. 2000); because visual function is measured on a dB (nonlinear) scale, structural changes occur at a faster rate than VF changes in the early stages and this relation is reversed in the later stages (Airaksinen & Drance 1985).

Neural density (measured in %-age loss) and visual sensitivity (measured by dB) have a curvilinear relationship (Garway-Heath et al. 2002; Airaksinen & Drance 1985; Bartz-Schmidt et al. 1999; Jonas & Grundler 1997). A logarithmic transformation of either variable produces a linear relationship for prediction of structural loss from functional measurements (Harwerth et al. 2004). However, the accuracy of this model is best suited for moderate to advanced glaucomatous neuropathy during which subjective perimetric measurements are more accurate than objective structural measurements (Sommer et al. 1991; Drance 1975; Sanchez-Galeana et al. 2001; Johnson et al. 2003; Matsumoto et al. 2003). Hence automated perimetry is likely to remain the gold standard for assessment of stage of neural damage from glaucoma (Johnson 1996). Because structural changes of the RNFL and ONH often precede development of visual

field loss in glaucoma (Repka & Quigley 1989; Kerrigan-Baumrind et al. 2000), the detection of damage to RNFL and ONH is critical for the early diagnosis of glaucoma.

Several studies have suggested that decreasing IOP can reverse RGC dysfunction (Ventura & Porciatti 2005; Gandolfi et al. 2005). Looking at these studies together gives rise to the "dysfunction-preceding-death hypothesis" (Ventura et al. 2006). In RGC losses of less than 50%, there are only small changes (in decibels) of visual loss, whereas in RGC losses greater than 50%, the visual sensitivity is more closely correlated (Garway-Heath et al. 2002). This may arise because visual sensitivity loss is measured in dB whereas RGC loss is measured in percentage. If both variables were measured with a linear scale, a linear relationship may be noted between RGC and visual sensitivity loss regardless of the stage of glaucoma (Garway-Heath et al. 2002; Swanson et al. 2004; Schlottmann et al. 2004).

The development of more objective, quantitative methods of combining structural and functional information has been of interest to several investigative groups (Harwerth et al. 2007; Drance 1985; Strouthidis, Vinciotti, et al. 2006; Turpin et al. 2009; Mardin et al. 2006; Ronald S. Harwerth et al. 2005). This thesis will investigate the structure function relationship amongst several perimetry techniques and imaging modalities to determine which pair of instruments shows the strongest correlation.

1.6 Standard Automated Perimetry: Humphrey Field Analyzer

1.6.1 HFA: Instrument Specifications

Standard Automated Perimetry (SAP), also known as white-on white perimetry, is currently the gold standard for detecting glaucomatous visual field loss (Nicolela et al. 2001; Quigley 1993; Sommer et al. 1991; Johnson 1996; Bayer & Erb 2002; Anderson 1987; Alexander 1991; Johnson & Sample 2003; Sekhar et al. 2000). The Humphrey Field Analyzer (HFA; Carl Zeiss Meditec, Dublin, CA, USA) uses differential light sensitivity to measure the eye's ability to detect small flashes of white light (usually 0.43˚ diameter, Goldmann size III) on a background luminance of 10 cd/m^2 or 31.5 asb. The Goldmann size III stimulus is most commonly used as it provides a valid assessment of neural loss (Harwerth et al. 2002) and the specific background illumination was chosen as it is the minimum amount of light needed to stimulate both cone and rod photoreceptors (Heijl & Patella 2002).

The 24-2 stimulus pattern available on the HFA tests 54 points within the central 24 degrees of the field of vision with an extension of 30 degrees in the nasal region; each test location is separated by 6˚ and offset by 3˚ from both the horizontal and vertical meridians (Zalta 1991). The HFA is installed with a statistical software package, STATPAC, which provides a rapid analysis of the patient's visual field along with a comparison of the patient's sensitivity values with that of an age-matched normal population (Heijl & Patella 2002).

1.6.2 HFA: Bracketing Strategy

The standard algorithm of the HFA uses a bracketing strategy, a 4-2-2 dB staircase, to estimate threshold levels (Walsh 1990). Depending on the patient's response to the initial stimulus presented at each location, the proceeding stimulus intensity will increase or decrease (Delgado et al. 2002) by 4 dB. When the patient's response pattern changes at a given test location, the intensity will be altered by a smaller interval of 2 dB; this reversal is repeated several times until consistent responses are obtained and the threshold is determined. The threshold expresses the intensity of light that the patient can see 50% of the time the stimulus is presented at the specified retinal location.

1.6.3 HFA: SITA

The Swedish Interactive Test Algorithm (SITA) is a family of test algorithms designed to reduce threshold estimation test time for the stimulus patterns available on HFA without compromising the data quality (Sekhar et al. 2000; Bengtsson et al. 1998; Wild et al. 1999). Studies have shown that lengthier tests result in lower threshold estimates as a result of fatigue (Wild et al. 1999; Heijl et al. 2000; Bengtsson, Olsson, et al. 1997). The SITA algorithms use maximum likelihood methods to estimate threshold values (Bengtsson, Olsson, et al. 1997).

Unlike the full threshold (4-2-2 dB staircase) techniques where each test location presents a stimulus with a specified intensity, SITA calculates the initial intensity for test locations based on the known relationship of location sensitivity in the normal visual field (Bengtsson, Olsson, et al. 1997). SITA has allowed perimetry testing to be more reliable and accurate with significantly shorter test duration (Sekhar et al. 2000). A study by Artes et al. (2002) has shown that SITA Standard may be superior to the Full Threshold algorithm when measuring patients with visual field loss; this could be attributed to less fatigue experienced by the patient during the test.

1.7 Function Specific Perimetry

As stated previously, studies have shown that RNFL and ONH changes can be detected before changes to the visual field as noted by standard automated perimetry (Harwerth et al. 1999; Kerrigan-Baumrind et al. 2000; Johnson 1994; Sommer et al. 1991; Ronald S. Harwerth et al. 2005; Lan et al. 2003; Johnson et al. 2003; Okubo 1986). The emergence of new functional tests that are more sensitive than SAP lead to the possibility that functional loss may occur with, or even before, structural loss (Airaksinen & Alanko 1983; Fortune et al. 2012).

The development of new perimetry techniques has been aimed at selectively testing subsets of ganglion cells to better reflect ganglion cell loss (selective testing hypothesis)

(Johnson 1994), or testing subsets of ganglion cells that may be more prone to glaucomatous damage (selective loss hypothesis) (Alward 2000), or testing higher order cognitive functions that appear to be more prone to early disease.

It has been shown that SAP with Goldmann size III stimulus provides a more accurate assessment of advanced RGC loss than mild RGC loss especially in threshold losses greater than 15 dB, in excess of 50% RGC loss (AGIS Investigators 1994; Hart et al. 1990). This promotes Johnson's Reduced Redundancy Hypothesis (Johnson 1994) which states that early functional loss can be detected if testing for a select subpopulation of ganglion cells which are preferably damaged earlier in the disease stage (Stewart 1990) or have a sparse distribution throughout the retina (Johnson 1994). This testing approach may be more suitable in detecting change earlier than using a stimulus with the potential of stimulating a subset of ganglion cells.

Whether or not glaucoma affects retinal ganglion cells preferentially (Alward 2000; Quigley et al. 1988) or non-preferentially (Johnson 1994), it should be understood that there is a difference between preferential anatomic loss and preferential psychophysical loss which reflects the functional properties of ganglion cell subtypes (Sample 2001). The magnocellular ganglion cells (M cells) in the retina are principally, but not exclusively, responsible for the detection of motion and flicker (Breton & Drum 1989; Schiller et al. 1994). M-cells account for only 10% of ganglion cells in the retina (Perry et al. 1984) therefore, testing cells of the M pathway might enable detection of early

glaucomatous loss whether or not glaucoma selectively damages ganglion cells of the magnocellular pathway. Theoretically, testing the function of M-cells should be able to detect the earliest form of glaucomatous damage (Chauhan & Johnson 1999; Artes, Hutchison, et al. 2005).

M-cells have been shown to have larger soma and thicker axons (Kaplan & Shapley 1986) and are believed to be damaged first in the glaucomatous process (Quigley et al. 1989; Alward 2000; Quigley et al. 1987; Dandona et al. 1991; Glovinsky, Quigley, et al. 1991; Glovinsky, Quigley, et al. 1991; Silverman et al. 1990; Bullimore et al. 1993; Tyler 1981). M-cells are mediated by low spatial and high temporal frequencies (Kaplan & Shapley 1986). Hence the use of perimetric tests which utilize flicker (Johnson 2009; Harwerth et al. 1999; Tyler 1981; Lachenmayer et al. 1989; Horn et al. 1997) and motion (Silverman et al. 1990; Wall & Ketoff 1995; Bosworth et al. 1997) have been proposed for the early detection of glaucoma. In glaucoma, abnormality in spatial and contrast sensitivity have also been described (Tyler 1981; Sample et al. 1991). Several techniques such as Frequency Doubling Technology (FDT), Flicker Defined Form (FDF) and Moorfields Motion Detection Test (MDT) have been developed that are aimed at selectively testing ganglion cells of the magnocellular pathway, and its cortical processing (Swanson et al. 2004). However, in a study by Swanson et al. (2011) they looked at the differences in contrast gain between M and P cells using both SAP size III and the frequency doubling stimulus. They concluded that SAP size III is superior to the frequency doubling stimulus at preferentially stimulating cells of the magnocellular

pathway. This casts doubt on the reason for the diagnostic performance of these new tests being related to preferential stimulation of the M-cells, and that higher order cognitive factors may play a more important role in determining their sensitivity to early disease.

1.7.1 Frequency Doubling Technology (FDT)

It has been proposed that FDT selectively tests magnocellular cells, by using a flicker detection task (Anderson & Johnson 2002; Quaid et al. 2005; White et al. 2002). However, FDT perimetry does not depend on the perception of the frequency-doubling illusion to detect visual field loss but on changes in contrast sensitivity of a flickering stimulus (Quaid et al. 2005; White et al. 2002). Masking experiments were able to establish that the diagnostic performance of FDT is more likely due to a cortical response than a retinal response (Quaid et al. 2005). Studies have shown that the contrast sensitivity produced by the FD illusion is reduced in patients with glaucoma (King-Smith et al. 1994). Hence, it may be an optimum means of detecting and monitoring glaucoma, especially in the early stages of the disease. FDT has been shown to be equally repeatable across all threshold estimates (Spry et al. 2003; Artes & Chauhan 2005b) and therefore also may be more suitable than SAP to measure progressive glaucomatous visual field loss (Spry et al. 2001; Chauhan & Johnson 1999). However, it should be noted that the repeatability is much greater than SAP in the

nearly normal range. In addition the range of possible sensitivities is greatly reduced in FDT, ensuring that the relative repeatability is difficult to compare with SAP.

1.7.1.1 FDT: Instrument Specifications

Frequency Doubling Technology (FDT) is a perimetry-like technique which simultaneously exploits the utility of contrast sensitivity, spatial frequency and temporal modulation (Sponsel et al. 1998). The FDT target is made up of a sinusoidal grating undergoing counterphase flicker (Sponsel et al. 1998). The FD phenomenon is perceived when a high temporal frequency counter phase flicker is combined with a low spatial frequency sinusoidal grating (Sample et al. 1991; Garway-Heath, Caprioli, et al. 2000; Verdon-Roe et al. 2006; Baez et al. 1995). Thus, the subject perceives the stimulus as having twice the number of bands and each band is half the width of the original (Yu et al. 2003). Figure 1.1 shows a schematic diagram of the FD illusion. However the perception threshold described above is not possible to be reliably measured clinically and therefore is not the threshold criterion used in FDT. Instead, the flicker detection threshold is used, i.e. the patient is asked to respond to the presence of a flickering target rather than to the perception of 8 rather than 4 bars. It is the flicker detection threshold values that are used in the FDT normative values (Baez et al. 1995).

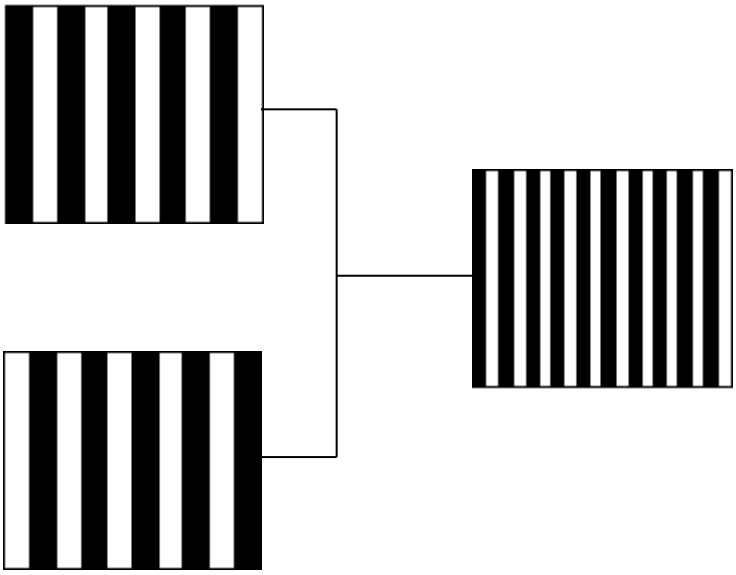

Figure 1.1: Schematic diagram of the Frequency Doubling Illusion.

1.7.1.2 FDT: Test Procedures

1.7.1.2.1 FDT: MOBS

The full threshold test on the initial commercially available FDT screening instrument (FDT I) uses the Modified Binary Search (MOBS) test procedure (Turpin et al. 2002a; Tyrrell & Owens 1988). The FDT is programmed to present a 10^{o} stimulus with a spatial frequency of 0.25 cycles/deg and a temporal frequency of 25Hz. A range of possible thresholds sets the upper and lower thresholds for the patient at each test location. An average contrast value of the upper and lower threshold limit is calculated as the target contrast for the initial presented stimulus. The patient's response to the target determines the interval from which the contrast for the proceeding stimulus at that

location will be calculated. This reversal is continued until the difference between the upper and lower threshold is equal to or less than a predetermined interval (Tyrrell & Owens 1988); this information is used to calculate the threshold values. An advantage of MOBS is that it can recover quickly from response error and it can make large jumps to remain close to the correct location of threshold (Tyrrell & Owens 1988).

1.7.1.2.2 FDT vs SAP

FDT has demonstrated a superior performance to SAP for the detection of early disease and comparable performance in later-stage disease (Johnson & Sample 2003). Abnormalities on FDT perimetry have been shown to precede detectable SAP damage by several years (Kim et al. 2007; Landers et al. 2003; Medeiros et al. 2004). High sensitivity and specificity values have been shown with the FDT in early, moderate and late stages of glaucoma (Cello et al. 2000). Despite its short duration as compared with conventional perimetry tests (Turpin et al. 2002b), MD and PSD values of FDT 30-2 show a strong linear correlation with that of the Humphrey 30-2 technique (Sponsel et al. 1998); thus promising a possibility that FDT can be used to detect and differentiate the severity of glaucomatous visual field loss (Cello et al. 2000).

Several studies have concluded that FDT is a promising screening tool for early glaucoma (Alward 2000; F. A. Medeiros et al. 2004; Cello et al. 2000; Trible et al. 2000; Johnson & Samuels 1997; Quigley 1998) and can be effective at detecting moderate to

severe cases of glaucoma (Alward 2000; Cello et al. 2000; Trible et al. 2000). A longitudinal study looking at the rates of change in FDT PSD values showed that FDT may be useful for risk stratification in patients with suspected glaucoma and evaluation for glaucoma progression (Meira-Freitas et al. 2014). FDT is an attractive alternative to SAP in the clinical setting because the test is more resilient to refractive errors and blur (Alward 2000; Cello et al. 2000), it has a large dynamic range, and the threshold test strategies are short in duration (Cello et al. 2000; Medeiros et al. 2004). Good repeatability (Spry et al. 2003) and high sensitivity and specificity values (Cello et al. 2000; Medeiros et al. 2006) have been shown with the FDT in early, moderate and late stages of glaucoma.

The Matrix, also known as FDT II (Welch Allyn, Skaneateles Falls, NY; Carl Zeiss, Meditec, Dublin CA) is an updated version of the FDT; it was developed as a means of improving efficiency and accuracy. In comparison to FDT, the Matrix uses a smaller stimulus size, allowing for more test locations to be tested thereby giving more detail on the spatial distribution of the visual field loss (Artes, Hutchison, et al. 2005). The commercially available Matrix is programmed to present a 5^{o} stimulus with a spatial frequency of 0.5 cycles/deg and temporal frequency of 15Hz on a background luminance of 100 cd/m^2.

1.7.1.2.3 FDT: ZEST

Threshold values for the Matrix are calculated using an adaptation of the Zippy Estimation of Sequential Threshold (ZEST) procedure (Artes, Hutchison, et al. 2005; McKendrick 2005). At each test location, 4 stimuli are presented, each with a predetermined intensity and corresponding probability density function (pdf) curve (King-Smith et al. 1994; Turpin et al. 2002a), which estimates the probability of subsequent threshold values based on previously collected data; the pdf curve is modified for the next presentation with respect to the patients' response ("seen" or "not seen") (Artes, Hutchison, et al. 2005). The 15 possible combinations of "seen/not seen" responses to the 4 stimuli presented determine the threshold estimates ranging from 0 to 38 dB (Artes et al. 2005), i.e. a frequency-of-seeing curve is obtained (King-Smith et al. 1994). Maximum-likelihood strategies are used to measure threshold values (Turpin et al. 2002a), by presenting only 4 stimuli at each location. This is why the test duration is independent of disease severity (Artes et al. 2005).

1.8 Flicker Defined Form

1.8.1 FDF: Instrument Specifications

The Heidelberg Edge Perimeter (HEP; Heidelberg Engineering, Germany) is a new perimetry instrument which provides both SAP and Flicker Defined Form (FDF) techniques (Flanagan et al. 1994; Ramchandran & Rogers-Ramchandaran 1991;

Livingstone & Hubel 1987). FDF is an illusionary stimulus, capable of preferentially stimulating the magnocellular pathway and is generated when a background of random dots flickers at a high temporal frequency (15 Hz) in counterphase with a 5º stimulus region (Heidelberg Engineering, 2010). The mean luminance of the background is set at 50 cd/m^2, the background and stimulus dot luminance differ from the mean luminance by a set amount known as the amplitude. The counterphase flickering of the background and stimulus dots gives rise to the illusion of a grey circle against a mean luminance background (Heidelberg Engineering, 2010) (Figure 1.2). Changes in the amplitude of the background and stimulus dots creates stimuli with different contrasts. FDF is believed to predominantly stimulate RGCs of the magnocellular pathway because the illusion is not perceived at chromatic luminance and is resistant to blur (up to 6D) (Heidelberg Engineering, 2010). Thus, it may be a good indicator for early glaucoma damage. It is likely that the illusion is cortically generated and requires involvement of the entire dorsal stream to be perceived. Sensitivity of FDF improves with increasing temporal frequency, eccentricity, dot density, target size and target area (Quaid & Flanagan 2005).

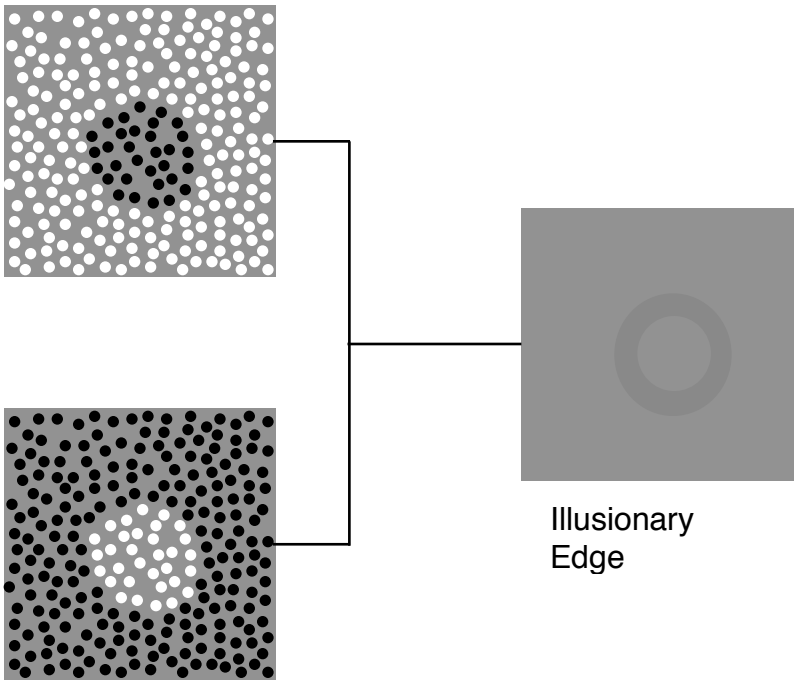

Figure 1.2: Schematic Diagram of Flicker Defined Form

1.8.2 FDF: Test procedures

1.8.2.1 FDF: ASTA

The Adaptive Staircase Thresholding Algorithm (ASTA) (Heidelberg Engineering, 2010) is an algorithm employed by the FDF that uses likelihood estimates from normal data distributions to determine the end point of threshold estimates. In each quadrant, seed points located at 15º by 15º are measured using a 4-2-2 dB algorithm. Neighbouring points then use the estimated sensitivity calculated at the seed points to complete a 2-2 dB staircase. If the crossings at each point lie within that of the expected age-matched

limits, further testing at that location is terminated. If locations appear significantly reduced or different from neighbouring points within the same hemifield, they will be retested.

The FDF ASTA Standard algorithm shows equivalent test-retest variability throughout the dynamic range to that of SAP (Heidelberg Engineering, 2010) . FDF has been shown to detect glaucomatous damage when no defect was detected by SAP (Horn et al. 2016; Hasler & Stürmer 2012; Reznicek et al. 2015).

1.9 Moorfields Motion Displacement Test (MDT)

1.9.1 MDT: Instrument Specifications

Moorfields MDT is a new perimetric motion-displacement test used to diagnose glaucoma in the early stages (Verdon-Roe et al. 2006). Moorfields MDT uses 32 lines each scaled to the ganglion cell density (Garway-Heath et al. 2000; Garway-Heath et al. 2000) at its corresponding retinal location defined by the Garway-Heath map (Garway-Heath, Poinoosawmy, et al. 2000) of the anatomic relationship between the visual field and optic nerve head (Figure 1.3). The white lines (124 cd/m^2) are presented on a grey background (10 cd/m^2) and undergo brief lateral displacements of different magnitudes; 10 random displacements ranging from 0 to 18 minutes of an arc displaced at 2.5 Hz (Baez et al. 1995). These displacements give rise to the sensation of motion (Scobey &

Horowitz 1976). Like other perimetry techniques, the patient is asked to fixate on a centrally located target and press a button every time he or she detects a line on the screen to move. The threshold, measured in minutes of arc, is the minimum displacement detected at each test location (Baez et al. 1995); the smaller the displacement detected, the greater the sensitivity at that location. The ability to detect motion is the first to diminish in patients with glaucoma (Silverman et al. 1990) hence, the MDT proposes ideal for early detection of the disease.

MDT has been shown to be more sensitive to glaucoma detection than SAP (Baez et al. 1995; Fitzke et al. 1987; Fitzke et al. 1989; Ruben & Fitzke 1994; Poinoosawmy et al. 1992) and less effected from cataract than either SAP or FDT (Membrey et al. 1998; Bergin et al. 2011).

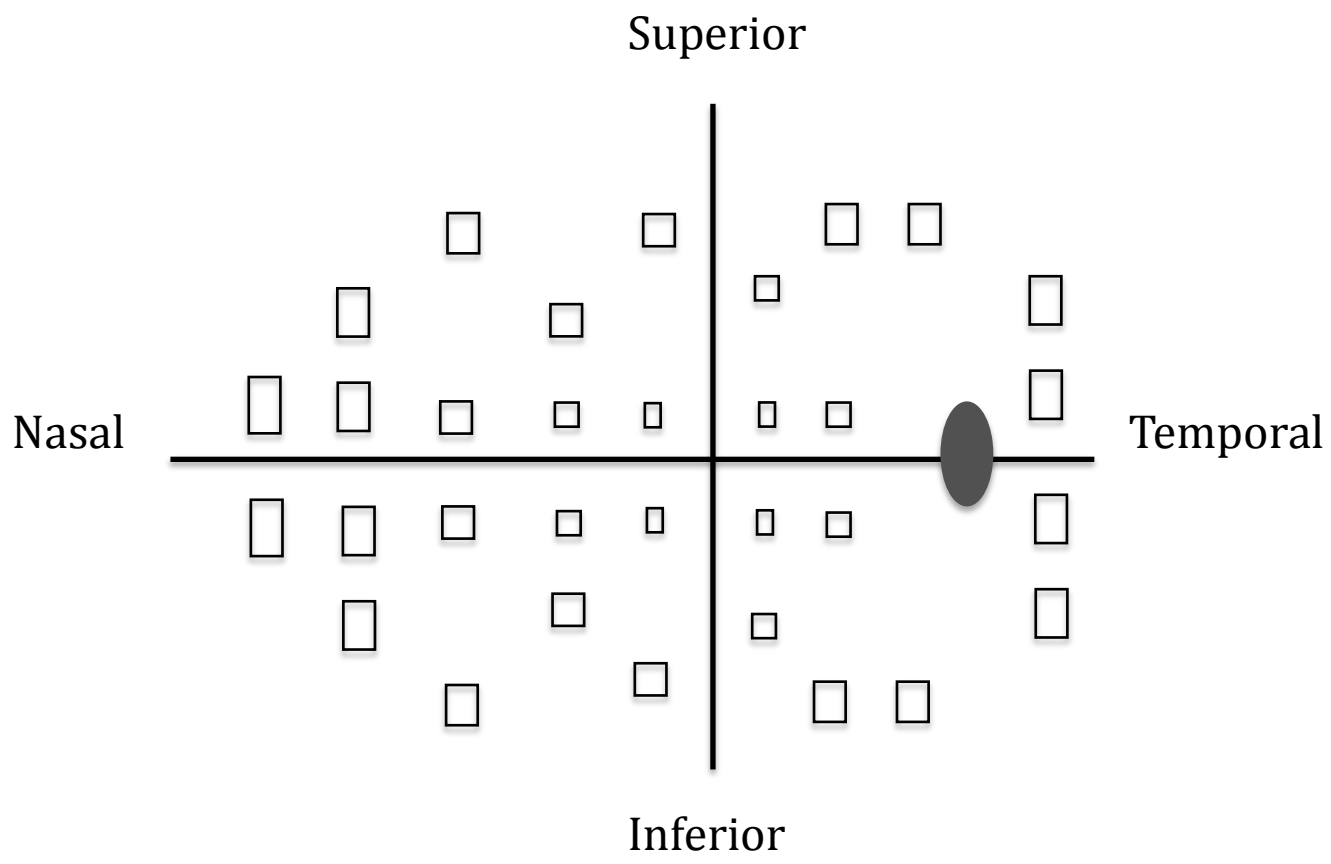

Figure 1.3: Diagrammatic representation of the MDT testing screen. The open squares represent the locations of the stimulus; each stimulus size corresponds inversely to the density of the receptor cells at that location. The closed oval represents the blind spot.

1.9.1.1 MDT: WEBS

A weighted binary search (WEBS) threshold strategy is employed by the MDT to measure retinal sensitivity. Each time the patient responds to a detection of motion, a

frequency of seeing curve is generated and used to calculate the threshold at that location (Membrey et al. 1998).

1.10 Sensitivity Values

Threshold and visual sensitivity, as measured by decibels (dB), are inverse functions. The dB scale is a logarithmic scale that is inversely related to luminance; each dB is equal to 0.1 log units with SAP, 0.05 log units with the Matrix (Artes, Hutchison, et al. 2005) and 0.1/√2 log units for the FDF. For the most part, neighbouring points in the visual field have similar thresholds (Heijl et al. 1980). Moorfields MDT measures sensitivity in minutes of arc (MinArc) ((Moorfield Eye Hospital 2015). The probability of seeing a stimulus presented at threshold is 50% (Turpin et al. 2002a; Turpin et al. 2002b).

1.11 Reliability Parameters

Sensitivity thresholds are influenced by patients' response fluctuations, experience, and fatigue (Bebie et al. 1976; Wild et al. 1989). In order to accurately evaluate visual field loss with perimetry tests, it is crucial to know how reliable the test results are. Reliability depends to a great extent on the patient's ability to consistently perform the perimetric task (Delgado et al. 2002; Bickler-Bluth et al. 1989; Bengtsson 2000) and the reproducibility of its results (Bengtsson 2000). Fixation losses (FL), false positive (FP),

and false negative (FN) calculations, as reported on the perimetry test printout, are an indication of the reliability and validity of the test.

Fixation losses provide a relative idea of how well the patient kept his or her eye fixed on the fixation target during the test. Throughout the test, at random intervals, a stimulus is projected in the area of the blind spot where the stimulus should not be seen (the instrument locates the area of the blind spot at the beginning of the test) (Drance & Anderson 1985) at maximum intensity; the number of times the patient reports seeing such stimuli is recorded alongside the other reliability indices (Heijl & Patella 2002; Cello et al. 2000). This method is known as the Heijl-Krakau method (Heijl & Patella 2002) for determining fixation loss and is employed by SAP and FDT. The FDF calculates fixation loss by using a video eye tracker to monitor eye movements; any movement greater than 5 degrees from central fixation is recorded as loss of fixation (Heidelberg Engineering GmbH, 2010).

The false positive rate (FP) is presented as a ratio of the total number of times the subject responds without a stimulus being presented to the total number of times the instrument pauses without presenting a stimulus (Heijl et al. 1989). A patient is termed "trigger happy" when he/she has a high false positive rate, i.e. frequently clicks the button when no stimulus is presented. False negative errors usually result when the subject fails to respond to a distinctly visible stimulus (Heijl & Patella 2002) in a location outside of the determined blind spot.

The false negative rate (FN) is presented as a ratio of the total number of times the subject fails to respond when a stimulus of 9 dB higher than the previously determined threshold at that location is presented to the total number of such presentations (Heijl et al. 1989), i.e. failing to respond to stimulus with 100% contrast. In the presence of severe visual field loss, FN is not used to define reliability due to the low number of catch trials (Zalta 1991).

The SITA algorithm calculates FP and FN differently than described above. False positives are calculated by recording positive responses when none are expected, i.e. within the minimum reaction time interval after a stimulus is shown (de Boer et al. 1982). False negatives are calculated based on the patient's pattern of responses after the test is completed (Olsson et al. 1988). Data from FP and FN defined in this way are combined and the maximum likelihood method is used to calculate FP and FN responses as a percentage (Olsson et al. 1988). This method of estimating the frequency of FP and FN responses helps reduce testing time by reducing the number of presentations. Moorfields MDT only calculates FP and it does this by counting the number of responses that were recorded within 180ms from the stimulus presentation, the physiological minimum response time, against the total number of stimulus presentations (Olsson et al. 1997).

Vertex Monitoring and Gaze Tracking are features available on HFA II and HEP. The former ensures that the patient's eye is centered behind the lens at a distance that

allows for greatest focus of the stimulus, eliminating the trial lens as a possible source for unreliable results. The latter is used to determine the patients' fixation during the test. This is done by using real-time image analysis. A gaze tracking graph is displayed on the printout where deviations in gaze are indicated by a line which extends upwards (Heijl & Patella 2002); the proportion of the spike is proportional to the amount of fixation loss to a maximum of 10 degrees (Heijl & Patella 2002).

1.12 Statistical Plots

Probability maps are used to evaluate the normality of the data (Heijl et al. 1989). They compare the threshold values of the patient with that of the age-matched normal database, if one is available for the technique.

Total deviation (TD) values and its related probability plot are calculated on techniques that have a normal database available. The TD plot is composed of positive and negative integers which correspond to the difference in sensitivity between the subject and age-matched normal data at each point of the visual field (Heijl & Patella 2002; Bernhard et al. 1993). TD plots are useful because they accentuate areas of the visual field which fall outside the normal range (Heijl & Patella 2002). Its corresponding probability map indicates how different the given results are from that of the normal (Walsh 1990; Werner et al. 1989).

A pattern deviation (PD) plot and its related probability plot are also calculated with respect to a normal database. This particular plot allows for the field test results to be compensated with respect to the subject's height of the hill of vision (Heijl & Patella 2002), i.e. it eliminates defects caused by a generalized shift in MD (Bernhard et al. 1993). Thus, it signifies the difference in shape of the measured hill-of-vision as compared with that of the normal population (Heijl et al. 1989). This allows for differentiation of localized visual field loss from that resulting from age-related conditions such as small pupils and cataract formation (Heijl & Patella 2002).

1.13 Global Indices

Statistical analysis of visual fields has become useful in interpreting the results from automated perimetry (Brenton & Argus 1987). Visual field indices are statistical review of the retinal light sensitivities which are designed to recognize and evaluate the extent of visual field damage (Chauhan et al. 1990). They are used to facilitate interpretation of the results from a single perimetric examination (Chauhan et al. 1990). It assists the interpreter with defining visual field loss by summarizing the data obtained from the test (Flanagan et al. 1993). Visual field indices, Mean Deviation (MD) and Pattern Standard Deviation (PSD) are calculated based on previously acquired normal data (Trible et al. 2000). MD is calculated by averaging the deviation from normal for all points tested (Bickler-Bluth et al. 1989). It quantifies overall change of visual field loss with respect to normal data of age-matched controls (Lindenmuth et al. 1990; Spry & Johnson 2002;

Trible et al. 2000; Katz et al. 1991). Pattern standard deviation (PSD) measures the extent to which the tested field deviates from the shape of the "normal hill of vision" (Bickler-Bluth et al. 1989). It is an index for showing localized change in the visual field (Lindenmuth et al. 1990; Trible et al. 2000; Katz et al. 1991).

The visual field index (VFI) is a newer global index available on HFA, which evaluates the level of visual function (Giraud et al. 2010) and has been shown to correlate linearly with MD calculations (Artes et al. 2011). The VFI calculates the overall severity of the visual field and, unlike MD, its calculation is weighted depending on eccentricity with respect to ganglion cell density. The index is given as a percentage from 0 to 100 where 0% represents severe glaucoma and 100% represents a normal visual field. Studies are underway to determine its effectiveness in predicting glaucoma progression (Bengtsson et al. 2009; Ernest et al. 2016; Banegas et al. 2016).

1.14 Structural Assessment

In the past, stereo photography was used to evaluate and document the structure of the optic nerve head. Analysis of stereophotos have been shown to have great inter-variability among non-expert and expert observers (Breusegem et al. 2011). Today, imaging of the ONH and RNFL by computerized methods has become common practice in addition to visual field tests (Greenfield 2002; Zangwill & Bowd 2006; Stein et al.

2012) however, diagnosis by expert observer still remains the best reference standard (Prum et al. 2016).

1.14.1 Scanning Laser Tomography

The Heidelberg Retina Tomograph (HRT) (Heidelberg Engineering GmbH, Heidelberg, Germany) uses the principles of confocal scanning laser ophthalmoscopy (CSLO) to acquire images of the optic nerve head (ONH) and macula (Weinreb 1993) and measure height of the internal limiting membrane (Eid et al. 1997). Figure 1.4 is a schematic diagram of the CSLO principle. It provides three-dimensional images of the optic disc and peripapillary retina for the detection and monitoring of changes in glaucoma (Chauhan et al. 2000). The HRT has been shown to acquire repeatable and reliable measurements of the ONH (Mikelberg et al. 1993; Rohrschneider et al. 1994; Chauhan et al. 1994), provide reasonable levels of sensitivity and specificity (Mikelberg et al. 1995; Bathija et al. 1998; Uchida et al. 1996; Zangwill et al. 2007) and be in agreement with an ophthalmologist's clinical examination (Yaghoubi et al. 2015).

The HRT III uses a 675 nm diode laser as a light source which measures the reflectivity of 147, 456 points in 0.024 seconds per plane. In summary, a pinhole is placed in front of the light source and the laser beam is focused onto the retina at a predetermined depth by use of a converging lens. The laser scans an image field 15˚ horizontally and 15˚ vertically along the xy-plane of the retina in a raster pattern and a 2-dimensional

cross-section of the ONH is obtained, composed of pixels that are in and out of focus. The laser is successively lowered along the z-axis in small increments and each xy-plane is scanned. The scan depth is automatically selected and ranges from 1.0mm to 4.0mm. For each millimeter along the z-axis, 16 xy-planes are scanned; the data are then computed to form a 3-dimentional image. Magnification errors between patients are corrected by inputting the corneal curvature measurements prior to obtaining the measurements.

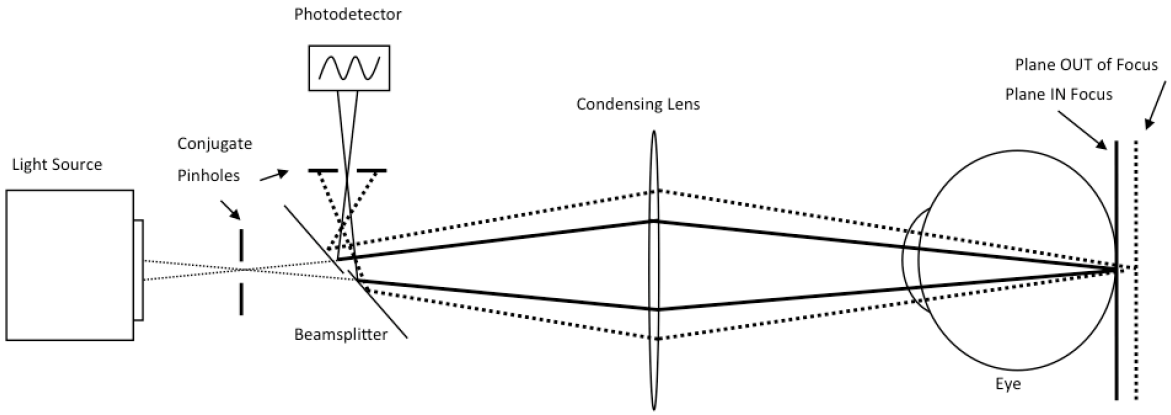

Figure 1.4: Schematic diagram of confocal scanning laser ophthalmoscopy (CSLO) as utilized by Heidelberg Retina Tomograph (HRT). A 675 nm diode laser is focused on the retina at a predetermined depth. The xy-plane of the retina is scanned in a raster pattern. The laser is successively lowered along the z-axis in small increments; for every 1 mm of depth along the z-axis, 16 xy-planes are scanned. All scanned planes are then computed to form a 3-dimensional image.

The HRT software computes such indices as neuroretinal rim area, cup volume, NFL thickness, and cup-shape measure (Mikelberg et al. 1993). Cup shape measure, as calculated by the HRT, is an important parameter to detect change (Brigatti & Caprioli

1995) and most predictive when comparing normal and glaucomatous optic discs (Iester et al. 1997).

In comparison to the HRT II, HRT III, has a larger normative database and introduction of ethnic-specific stratification, a new classification system, the Glaucoma Probability Score (GPS), and an improved image scaling and alignment algorithm (Strouthidis & Garway-Heath 2008).

The HRT II & III are equipped with software, which determined whether a given ONH falls within the age-matched normal range. Moorfields regression analysis (MRA) is a calculation based on comparison of the subject's rim area with that of a normal database (Wollstein et al. 1998). The Glaucoma Probability Score (GPS) classification algorithm (Swindale et al. 2000) discriminates between normal and glaucomatous ONH using a mathematical model of ONH shape for comparison purposes (Strouthidis & Garway-Heath 2008). It is operator independent, as it does not need a contour line to be drawn around the ONH; the option for drawing a contour line is also available. Sensitivity and specificity of GPS and MRA are similar (Strouthidis & Garway-Heath 2008). Optic disc size has been shown to have a significant effect on GPS classification but a lesser effect on MRA classification (Coops et al. 2006; DeLeón Ortega et al. 2007; Zangwill et al. 2007; Ferreras et al. 2007). Disease severity influences GPS and MRA classification (Strouthidis & Garway-Heath 2008). GPS has higher sensitivity and lower

specificity than MRA in patients with mild glaucomatous VF loss (Strouthidis & Garway-Heath 2008); MRA better discrimination in severe glaucoma (Ferreras et al. 2007).

Previous studies have shown that HRT parameters are a good indicator of glaucomatous ONH damage (Iester et al. 1997). In studies where HRT was used to measure structural damage in early glaucoma, damage is detected more readily in larger optic discs than smaller ones (Emdadi et al. 1998; Iester et al. 1996). Hence, patients with reproducible focal visual field defects that have small optic discs can have structural damage that is not detected by the HRT (Emdadi et al. 1998) and underlies the importance of combining structural and functional testing for glaucoma detection and management.

The amount of neuroretinal rim loss as measured by the HRT has showed the best correlation, among the other parameters, with histologic optic nerve fiber count in a study with monkeys (Yucel et al. 1998).

1.14.2 Optical Coherence Tomography

Optical Coherence Tomography (OCT) is a non-invasive imaging technique which allows for cross-sectional imaging of the human retina (Guedes et al. 2003) and resolution of the individual layers. The instrument was initially used for measuring RNFL thickness but recent improvements have allowed it to quantitatively examine the

optic disc and retina (Medeiros et al. 2005) to evaluate ONH topography and macular thickness for diagnosis (Schuman et al. 1995a; Schuman et al. 1995b) and follow-up of patients with glaucoma (Medeiros et al. 2005).

The OCT uses low-coherence interferometry to produce cross-sectional images of the retina with quantitative assessment of retinal and retinal nerve fiber layer (RNFL) thickness (Greenfield et al. 2003; Schuman et al. 1995a). The original OCT was based on a time-delay interferometry procedure; more recent developments have incorporated spectral-domain procedures.

In the time-domain OCT (TD-OCT) a low coherence light beam is divided by an optical beam splitter into a reference beam and a measurement beam and is directed into a Michelson interferometer set-up (Figure 1.5). The reference beam is directed to a mirror whose position and distance is known; the measurement beam is directed into the patient's eye where it is reflected from the surface different microstructures of the retina. Both the reference and measurement beams are reflected to a mirror where they recombine and are transmitted to a photosensitive detector. The time delay between the two beams is used to calculate the thickness of different intraocular structures at the point along the z-axis of the retina.

Measuring RNFL thickness by OCT is influenced by the reflective properties of the ILM (Hess et al. 2005). The ILM can vary greatly in its optical properties, especially in cases

of glaucomatous damage hence, loss of reflectivity of NFL in advanced glaucoma cases may contribute to the inaccuracy of thickness as measured by the OCT (Pons et al. 2000).

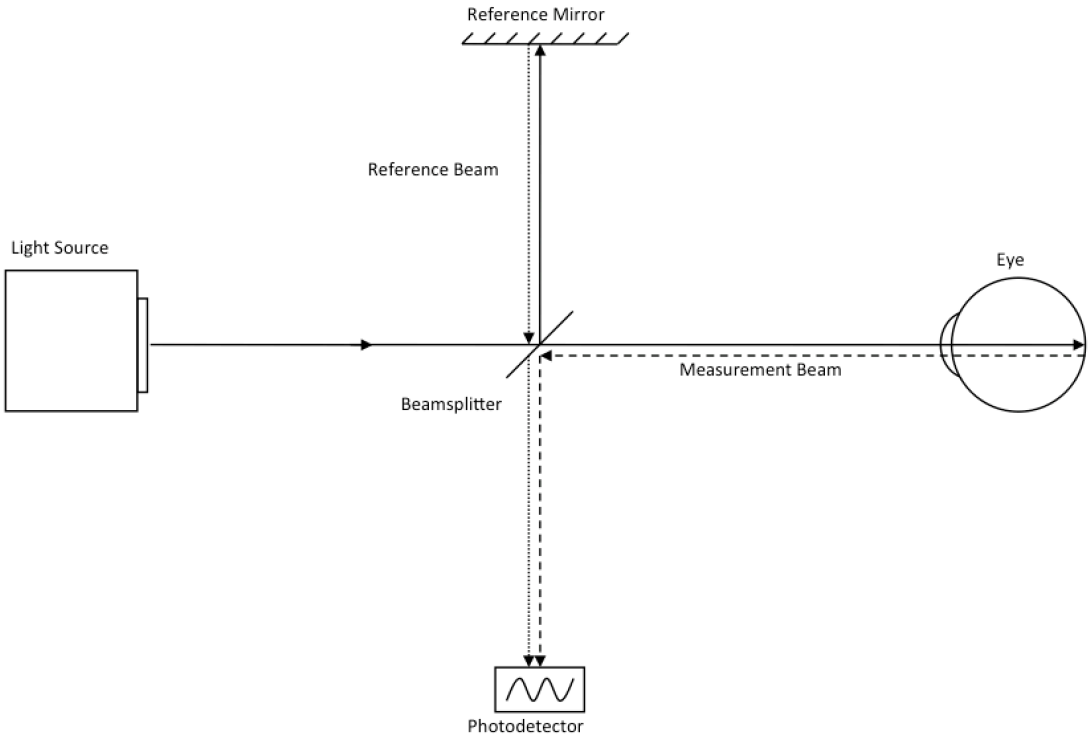

Figure 1.5: Schematic diagram of the Optical Coherence Tomography (OCT). The infrared light emitted from the source is divided by an optical beam splitter into a reference beam and a measurement beam. The reference beam is reflected to a reference mirror and then back to the beam splitter. The measurement beam is reflected into the patient's eye and reflected back from surfaces of the different ocular structures. This reflected measurement beam is composed of multiple echoes from each of the different intraocular surfaces. The time delay between the reflected beams is used to calculate the thickness of the different intraocular structures.

It has been shown that OCT provides reliable and reproducible measurements of the RNFL, retinal thickness and optic nerve head in human eyes (Blumenthal et al. 2000; Carpineto et al. 2003; Schuman et al. 1996).

Traditional OCT is the time domain OCT (TD-OCT) (Huang et al. 1991; Hee et al. 1995; Puliafito et al. 1995; Thomas & Duguid 2004) which measures thickness of the retina with respect to a reference beam after a longitudinal translation in time (Forte et al. 2009). Spectral domain OCT (SD-OCT) measures retinal thickness as a function of optical frequencies which requires less time for data acquisition and allows for more measurements per unit area which provides greater resolution (Drexler et al. 2003; Wojtkowski et al. 2005; Wojtkowski et al. 2004; Koizumi et al. 2008; Knight et al. 2009). Both TD-OCT and SD-OCT are used to detect and monitor glaucoma. It has been shown that SD-OCT can better detect preperimetric glaucoma than TD-OCT (Jeoung et al. 2014). However, a study by Schrems et al. (2015) found high levels of agreement between TD- and SD-OCT.

A review by (Abe et al. 2015) demonstrated that the SD-OCT has the potential for serving as a “biomarker” for glaucomatous damage. Recent advances in OCT technology such as OCT Angiography may be useful for the detection and monitoring of progression in glaucoma (Jia et al. 2015.; Liu et al. 2015).

1.14.3 Scanning Laser Polarimetry

Scanning laser polarimetry provides an objective means of measuring RNFL thickness. The GDx VCC (Laser Diagnostic Technologies, San Diego, CA) is a scanning laser polarimeter, which measures thickness of the nerve fiber layer in the peripapillary area by using the birefringent properties of the RGC axons (Weinreb et al. 1995b). It provides quantitative measurements of the RNFL (Weinreb et al. 1990; Weinreb 1995a) that correspond to the properties of the RNFL (Weinreb et al. 1995a). RNFL is known to be thicker in the superior and inferior peripapillary regions (Morgan & Waldock 2000; Varma et al. 1996; Dichtl et al. 1999), the GDx has been shown to agree with these measures in normal subjects (Weinreb, Shakiba & Zangwill 1995; Morgan & Waldock 2000; Tjon-Fo-Sang et al. 1996; Brandt 2004). SLP provides a good and objective method for RNFL thickness evaluation (Chen et al. 2009) as it has shown a good correlation with histological measurements (Blumenthal et al. 2009; Cohen et al. 2008).

The GDx uses a 780-798 nm diode laser which acquires its measurements in 0.8 seconds. It is based on the principle that, as polarized light passes through the microtubules of the nerve fiber layer the phase shift, or retardation, caused by the birefringent properties of the RNFL, is proportional to its thickness (Weinreb et al. 1990), i.e. birefringence due to the oriented cylindrical structure of RGC axons is proportional to the histologically measured RNFL thickness (Figure 1.6). Areas that are thicker have more retardation than thinner nerve fiber layers (Quigley et al. 1982).

However, birefringence, as measured by SLP, is also influenced by the density and/or composition of axonal organelles (Hemenger 1989; Zhou & Knighton 1997), which vary around the ONH (Huang et al. 2004) and may vary during different stages of the disease (Weinreb et al. 2003; Bagga et al. 2003; Guedes et al. 2003; Mohammadi et al. 2004). Although this technique was a promising predictor of glaucomatous visual field loss, birefringence of the cornea has a great effect on the calculation of RNFL thickness. The Variable Corneal Compensation (VCC) algorithm was introduced to compensate partially for the corneal birefringence. The VCC cancels out the specific effects of the cornea as per patient (Zhou & Weinreb 2002). This has helped improve glaucoma detection (Zhou & Weinreb 2002; Weinreb et al. 2003; Greenfield, Knighton, et al. 2003; Medeiros et al. 2003; Greenfield et al. 2002; Choplin et al. 2003) and shows a stronger correlation with other structural measures (Reus et al. 2006; Bagga et al. 2003; Schlottmann et al. 2004). Atypical retardation patterns, ones that do not follow the normal birefringence pattern of highest retardation in the superior and inferior sectors (Bagga et al. 2005), are seen in 25% and 51% of normal and glaucomatous eyes, respectively (Bagga et al. 2005). These atypical retardation patterns result in poor signal-to-noise ratios (Susanna & Medeiros 2006) and result in diagnostic discrepancy. The Enhanced Corneal Compensation (GDx ECC) algorithm was developed to overcome this problem by improving the neutralization of the atypical retardation patterns (Bagga et al. 2005; Medeiros et al. 2007). This has improved the detection of

glaucoma in patients with severe cases of atypical retardation patterns (Medeiros et al. 2007; Mai et al. 2007).

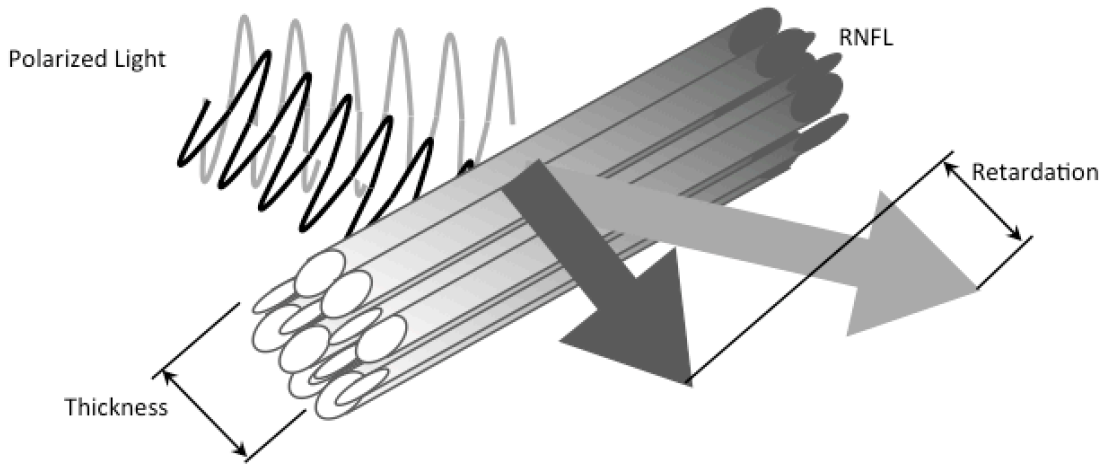

Figure 1.6: Schematic Diagram of GDx VCC

The GDx VCC calculates an index called the nerve fiber indicator (NFI) which integrates the overall indices of the RNFL. It ranges between 0 and 100, with 100 representing patients with severe glaucoma. The NFI on the GDx VCC is the best discriminating parameter between normal and glaucomatous eyes (Reus & Lemij 2004a).

1.15 Progression in Glaucoma

One of the most difficult tasks in the management of glaucoma is detection of progression (Banegas et al. 2016; Haymes et al. 2005; Vesti et al. 2003), which relies on the detection of a worsening structural and/or functional measurement (European

Glaucoma Society 2008). Early detection of glaucoma progression is just as important as early detection of the disease (Ansari et al. 2000), as progression can significantly impact visual function (Gupta & Weinreb 1997) and quality of life (Abe et al. 2016). Progression is determined by either i) trend analysis, which looks at regression of a parameter over time, or ii) event analysis, which performs a point-by-point comparison between baseline and follow-up examinations (Vesti et al. 2003).

For progression to be detected on any instrument, measurement "noise" must be distinguished from change due to glaucoma (Strouthidis et al. 2006). As Spry and Johnson have said in an article outlining the guidelines for the clinical management of glaucoma, "developing a standardized method of determining glaucomatous progression and the rate of progression remains a challenge" (Spry & Johnson 2002). Several studies have shown that the difference in test performance to detect glaucoma progression is dependent on the stage of the disease (Leung et al. 2010; Vizzeri et al. 2010; Kerrigan-Baumrind et al. 2000; Suh et al. 2012; Rao et al. 2011; Banegas et al. 2016).

Several statistical approaches have been developed and several criteria have been used with major clinical trials on determining visual field progression (AGIS Investigators 1994; Anderson et al. 1998; Gordon & Kass 1999; Leske et al. 1999; Spry & Johnson 2002). These differences in methodology give rise to difficulties in comparing the

results of the studies to each other, in addition to the absence of a gold standard (Nouri-Mahdavi et al. 1997; McNaught et al. 1996).

Progression studies are cross-sectional and determine the average of many patients seen at one time (Artes 2008) thus, the amount of change over time will follow a characteristic pattern (Bengtsson & Heijl 2008). Individually, change over time as measured for each patient may be different (Artes 2008) as only extreme cases may follow this pattern (Artes 2008; Artes & Chauhan 2005a).

1.15.1 Functional Progression

The key to managing a patient with glaucoma is to determine whether or not the patient's visual status has progressed (Johnson 2009); changes in visual field have been used to determine progression of glaucoma (AGIS Investigators 1994; Anderson et al. 1998; Gordon & Kass 1999; Leske et al. 1999; Glaucoma & Group 2006; Musch et al. 1999)._Various methods have been used to define and classify glaucomatous visual field defects (AGIS Investigators 1994; Katz 1999; Anderson et al. 1998; Gordon & Kass 1999; Leske et al. 1999), and progression (Katz et al. 1997; Katz 1999; Anderson et al. 1998; Leske et al. 1999; Bengtsson, Lindgren, et al. 1997; Fitzke et al. 1996; Smith et al. 1996). Detecting glaucomatous visual field progression is a challenge as it is difficult to detect true change in visual status (signal) from variability (noise) (Bebie et al. 1976; Artes, Nicolela, et al. 2005). Variability can be both within (short-term fluctuation) and

between (long-term fluctuation) tests (Flammer et al. 1984; Stewart & Hunt 1993). Other factors such as eccentricity (Heijl et al. 1987; Heijl et al. 1989), defect depth (Heijl et al. 1989; Flammer et al. 1984), test duration (Heijl & Drance 1983), experience (Wild et al. 1989) and fatigue (Hudson et al. 1994) also contribute to the test's variability. The amount of initial visual field loss and both inter- and intra-test variability contribute to how well a specific method can detect progression (Flammer 1985). For example, some methods may detect progression only in the early stages, while other methods detect progression when extensive damage already exists (Vesti et al. 2003).

Trend analysis measures the amount of change from baseline using all tests that are available. Several procedures use this method of analysis to measure visual field progression including, mean deviation, pattern standard deviation, PROGRESSOR (Viswanathan et al. 1997) and the visual field index (VFI) (Bengtsson & Heijl 2008). MD and PSD indicate change over time of the overall visual field can accurately detect significant change if there is a general depression in sensitivity or a very large localized change that is evident when all the data points are averaged (Bengtsson & Heijl 2008; Viswanathan et al. 1997).

The use of global indices to measure visual function and global statistics to measure structure may, however, be inadequate to follow more subtle progress changes as global measures cause loss of spatial information and result in poor sensitivity to identify localized change (Chauhan et al. 1990). Thus, small localized changes in the visual

field will go unnoticed with this type of analysis. PROGRESSOR looks at individual test locations over successive perimetric examinations using linear regression of sensitivity on time (Bengtsson & Heijl 2008). This method is very useful in determining localized change over time and has been shown to detect and predict future glaucomatous visual field loss (Viswanathan et al. 1997).

The Humphrey Field Analyzer is equipped with the STATPAC software which calculates glaucoma change probability (GCP) as described by Artes et al (2011) and Heijl et al (1991). GCP and glaucoma progression analysis (GPA) programs (Carl Zeiss Meditec, Inc., Dublin, CA) are statistical analysis software equipped in the HFA which compare baseline to follow-up examinations and flag points that lie outside of the 90% confidence interval in the total deviation and pattern deviation probability plots. These calculations combine the first two visual field test results to obtain a mean baseline and then compare this calculated baseline to the subsequent tests as such they employ event analysis (Artes et al. 2011; Heijl et al. 1991; Spry & Johnson 2002). If threshold values of the follow-up test are outside the 5th and 95th percentile of test-retest variability of stable glaucoma patients, then the points are highlighted as probable improvement or progression, respectively. An advantage of this technique is that it can identify progression with as little as three visits (Spry & Johnson 2002). On the other hand, the techniques allow only determination of change and do not calculate the magnitude or rate of change; the amount of change required to be considered as progressing must exceed the test-retest variability (Spry & Johnson 2002). Patients with glaucoma have

greater test-retest variability making it more difficult for subtle changes to be noted as progression (Spry & Johnson 2002).

In glaucoma, perimetry testing may be the only means of detecting progression in the later stages as the optic disc will no longer be a reliable or accurate indicator for progression (Katsumori et al. 1985), as minute changes in neuroretinal rim anatomy are difficult to quantify. The problem in comparing methods of visual field progression is that there is no set gold standard (Nouri-Mahdavi et al. 1997). There is weak evidence supporting the notion that SWAP and FDT are more sensitive than SAP at detecting progression (Demirel & Johnson 2001; Haymes et al. 2005). Function specific perimetry tests become less sensitive with increasing loss of RGCs therefore SAP may not be the most sensitive technique to monitor glaucomatous progression at the end-stage (Chauhan et al. 2001).

1.15.2 Structural Progression

Progressive optic neuropathy is the hallmark of glaucoma (Fechtner & Lama 1999). An alternative method to determining glaucomatous progression with visual fields is to clinically assess the characteristics of the optic nerve head (Spry & Johnson 2002). Characteristic traits of structural glaucoma progression include increasing ONH excavation and RNFL thinning (Drance 1975; Schwartz 1976; Spaeth et al. 1976). .

Event analysis (glaucoma change probability) and trend analysis (Moorfields regression analysis) appear to be the most commonly used procedures (Fingeret et al. 2005) in detecting structural progression. HRT uses Topographic Change Analysis (TCA) to determine progression by comparing a 4x4 array of 16 pixels from baseline and follow-up and determine whether or not the 16 pixels fall within the 95% confidence interval of variability (red worse, green better) (Sommer et al. 1977; Chauhan et al. 2000; Chauhan et al. 2001). Both SLP and OCT use event analysis (Guided Progression Analysis) which compare baseline to follow-up images to determine change outside of the 95% confidence limit in the RNFL and ONH respectively (Alencar et al. 2010; Leung et al. 2010).

Changes in optic disc topography can be detected more readily than changes in visual function as assessed by SAP (Chauhan et al. 2001) in the early stages of glaucoma. This is supported by the OHTS where 52% of the patients who developed POAG showed structural signs of progression and only 7% later developed functional damage (Keltner et al. 2006).

A study by Harwerth et al (2004) has shown a good correlation between structural and functional loss in experimental glaucoma when eccentricity factors are included.
The study by Bowd et al (2006b) suggest that Stratus OCT RNFL thickness measurements may provide better cross-sectional representation of visual function than

HRT II and GDx VCC measurements however, these results may have been affected by the different normative database available for each instrument.

Associations of RNFL/disc topography and visual sensitivity are dependent upon the instruments being tested, the locations being tested as well as the characteristics of the study population (Bowd et al. 2006). The stage of the disease also plays a role in variability and repeatability of test parameters within each instrument (Michelessi et al. 2015). For example, one study compared the effects of glaucoma severity on repeatability of CSLO, SLP and OCT (DeLeón Ortega et al. 2007) and found that global RNFL and vertical C/D ratio as measured with GDX VCC and HRT III, respectively, was stable across disease severity; unlike rim area which increased with disease severity. These findings suggest that global RNFL and vertical C/D ratio be used to monitor glaucoma progression in the later stages as opposed to rim area.

Imaging devices such as HRT, OCT and GDx VCC which identify glaucoma at the earliest signs of visual field damage have a sensitivity of 70% with 90-95% specificity with respect to clinical evaluation and results obtained from SAP 24-2 (Medeiros et al. 2004; Zangwill et al. 2001; Ford et al. 2003) and both imaging devices and clinicians have the same ability to identify structural damage caused by glaucoma (Wollstein et al. 2000; Mistlberger et al. 1999; Yaghoubi et al. 2015; Kourkoutas et al. 2007) and that imaging instruments can assist clinicians in diagnosing and monitoring glaucoma (Reus et al. 2007).

1.16 Rationale

In summary, early detection of glaucomatous damage and its progression over time is one of the most important clinical challenges in glaucoma (Hood & Kardon 2007). Both perimetry and structural imaging tests are essential for the management of glaucoma (Garway-Heath 2007; Airaksinen et al. 1985; Airaksinen & Drance 1985). The developments of new perimetry techniques and imaging instruments are aimed at providing optimum sensitivity and specificity in detecting the disease early and monitoring its progression. We want to compare the diagnostic abilities of SAP, FDT, FDF and MDT to see which technique is better able to pick-up glaucomatous damage earlier also, compare these functional measures to structural measures of the HRT, OCT and GDx.

1.17 Purpose

A two-fold approach was taken to address the study purpose: i) cross-sectional comparison of perimetry tests and imaging techniques to evaluate structure-function relationship between measures of RNFL, ONH and visual function, and ii) preliminary longitudinal comparison of perimetry tests and imaging techniques to determine which instrument being studied detects progression in patients with early stage glaucoma. The first part of this study was conducted as a multi-center study with four different

study sites. However, the longitudinal study was conducted by only one of the four centers (Toronto, Ontario location). In each study center, patients with glaucoma and control subjects were recruited based on the inclusion and exclusion criteria described below.

The data collected were used to look at test-retest within techniques, the structure-function relationship between the various imaging and structural tests, and to determine the ability of each technique to measure progression.

1.18 Research Questions

Does choice of perimetry affect repeatability and detection of characteristics of visual field abnormalities in patients with early stage glaucoma?
Does there exist and structure-function relationship between RNFL and visual function?

1.19 Objectives

The global aim of this thesis is to determine whether or not visual function of the RGCs correspond to structure of the ONH and RNFL and which technique is more sensitive for the early detection of glaucoma. The following perimetry techniques were used: i) SAP,

ii) FDT, iii) FDF, and iv) MDT; the following imaging instruments were used: i) HRT, ii) OCT, iii) GDx.

The primary objectives of this study was to determine which perimetry technique, SAP, FDT, FDF, or MDT, is more reliable and sensitive to early detection of glaucoma and whether or not visual function as measured by these techniques corresponds to the ONH and RNFL structure as measured by the HRT, OCT and GDx.

1.20 Hypotheses

1. Function specific perimetry techniques show earlier and deeper defects than SAP.
2. HRT shows greater agreement with function specific perimetry techniques than with SAP.
3. There are differences in the structure function relationship of different ONH sectors.
4. There are differences in the structure function relationship of different ONH sectors between OCT, GDx VCC and measures of visual function.
5. Function specific perimetry shows more change in one year than SAP.

2. Methods

2.1 Sample Size

The sample size for this study was calculated with the following formula:

$$\eta = \frac{2[(a+b)^2 \sigma^2}{E^2}$$

where η is the sample size, σ is the population standard deviation obtained from previous studies and E is the margin of error (maximum difference between techniques). Similar studies performed previously have reported σ =3.30. For this study, we chose a 95% confidence interval (α=0.05), power of 80% (β=0.80) thus a= 1.96, and b=0.842 and E=1.

Substituting these values into the equation we get:

$$\eta = \frac{2[(1.96+0.842)^2(3.30)^2}{1^2}$$

$$=171$$

Although our sample size calculation indicates that an η of 171 will provide statistically significant results; however, 194 subjects were recruited for this study.

2.1.1 Study Sample Demographics

Table 2.1 describes the study sample demographics recruited for the study. All subjects were included in the test-retest study and a subgroup of these subjects were used for the structure-function and progression studies. The details of these subgroups are described below. The sample consisted of 104 males and 90 females, 95 glaucoma and 99 controls. 109 right eyes and 85 left eyes were included. The age ranged from 18 to 84 years with a mean age and standard deviation of 60.99 $\pm$ 11.51 years.

Table 2.1: Study sample demographics for test-retest study.

	Ratio	Average	Minimum	Maximum
Males: Females	104: 90	---	---	---
Glaucoma : Control	95: 99	---	---	---
Eyes (Right: Left)	109: 85	---	---	---
Age (years)	---	60.99 $\pm$ 11.51	18	84
Time Elapsed Between Visits (days)	---	88 + 27	1	109
Time Elapsed Between Visits (weeks)	---	12 $\pm$ 4	<1	16

Table 2.2: Study sample demographics for the subgroup of patients included in the study comparing HRT to SAP, FDT, FDF and MDT.

	Ratio	Average	Maximum	Minimum
Males: Females	82: 75	---	---	---
Glaucoma: Control	70: 87	---	---	---
Eyes (Right: Left)	86: 71	---	---	---
Age (years)	---	59.99 $\pm$ 11.24	78	18

Table 2.3: Study sample demographics for the subgroup of patients included in the study comparing OCT and GDx to SAP, FDT, FDF and MDT.

	Ratio	Average	Maximum	Minimum
Males : Females	27 : 11	---	---	---
Eyes (Right : Left)	22 : 16	---	---	---
Age (Years)	---	64.82 $\pm$ 11.50	85	30

Table 2.4: Study sample demographics for subgroup of patients included in the progression study.

	Ratio	Average	Maximum	Minimum
Males : Females	27 : 11	---	---	---
Eyes (Right : Left)	22 : 16	---	---	---
Age (Years)	---	64.82 $\pm$ 11.50	85	30
Time Elapsed Between Visits (days)	---	420 $\pm$ 39	510	367
Time Elapsed Between Visits (weeks)		60 $\pm$ 6	73	52

2.1.2 Inclusion/Exclusion Criteria

Patients with characteristic glaucomatous visual field defects were considered as possible candidates for participation in the study. Glaucomatous visual field defects were defined as defects within the visual field whose pattern reflected the anatomy of the RNFL.

To be included in the study, the following criteria were: i) HRT results with image quality standard deviation <40 microns, ii) reliable SITA SAP results, i.e. false positive and false negative rates of <15% and fixation loss <30%, iii) visual acuity of 6/12 or better in the study eye, iv) refractive error less than $\pm$ 6.0 D sphere and/or less than $\pm$ 3.0 D cylinder, v) tolerant to dilating drops, vi) able and willing to make the required visits, vii) able and willing to give consent and properly follow given instruction. The subject was excluded

from the study if he or she had at least one of the following conditions: i) a suspicion or actual defect in the visual field of the eye being tested that was explained by the patients ocular status or history for a condition other than glaucoma ('glaucoma' subjects only), ii) any history of disease or use of medication that may affect visual field reliability and/or imaging of the RNFL, e.g. media opacities such as dense cataract, iii) past history of stroke or diabetic retinopathy, iv) previous ocular surgery other than uncomplicated cataract surgery. For glaucoma subjects, the eye with the least damage was chosen as the study eye; for control subjects, the eye to be tested was chosen at random.

For the Toronto, Ontario site, the glaucoma subjects were recruited from the Ophthalmology Clinic of Dr. Christoph Kranemann Medicine Professional Inc. based on judgment by the treating ophthalmologist. Control subjects were recruited from the Optometry Clinic of Dr. Areef Nurani based on judgment by the treating optometrist. The control group was recruited to calculate sensitivity and specificity values of the techniques used. In most of the data analysis, the data from both the glaucoma and control subjects were pooled into a single database.

2.2 Definition of Disease Stage

For the purposes of this study, the Heidelberg Retina Tomograph and Goldmann Applanation Tonometry were used to categorize control subjects and those with early stage glaucoma.

The patients were classified into the 'Control' group if his or her HRT results were classified as "Within Normal Limits" and IOP was <21 mmHg without treatment. The patients were classified into the 'Glaucoma' group if his or her HRT results were classified as "Outside Normal Limits" with rim area >0.8 mm^2 and disc area "Within Normal Limits", and IOP measured >21 mmHg before they had started any treatment and <26 mmHg at time of testing.

2.3 Ethics

The study was approved by the University of Waterloo, Office of Research Ethics. Written consent was obtained from each of the subjects prior to enrollment in the study.

2.4 Procedures

Upon obtaining consent, subjects were given an ophthalmic examination consisting of the following: measurement of visual acuity, Goldmann applanation tonometry, slit lamp examination of the anterior segment of the eye and dilated ophthalmic examination including evaluation of the crystalline lens using LOCS III classification.

The cross-sectional study compared the structure of RNFL and function of RGCs using the following instruments: i) confocal scanning laser ophthalmoscopy (HRT III, Heidelberg Engineering, software version 3.1.2), ii) interferometry (OCT Cirrus, Carl

Zeiss Meditec, Dublin, CA, software version 3.0.0.64), iii) Scanning Laser Polarimetry (GDx VCC, Carl Zeiss Meditec, Dublin, CA, software version 6.0.0) iv) Flicker Defined Form, (Heidelberg Engineering, software version 2.0.1.12), v) Standard Automated Perimetry (SAP, Humphrey Field Analyzer, Carl Zeiss Meditec, software version 4.2), vi) Matrix (Carl Zeiss Meditec, software version M02.02.01), and vii) Moorfields Motion Displacement Test (Moorfields Eye Hospital, London). Each instrument represents the current commercially available version for clinical use. The purpose was to determine if a correlation exists between structure of the RNFL and function of RGCs in patients with and without glaucoma as measured with the instruments used in this study.

All tests performed in Toronto were administered by one technician (CB). Contour lines for HRT were drawn by the primary observer (CB).

For the cross-sectional study, each subject attended 2 visits within a 16-week period. At each visit one eye from each subject was examined with the three imaging techniques and four perimetry tests. The order of image acquisition was not considered relevant as the techniques are not subjective. The order of perimetry testing was randomized but remained constant for each patient; this was done to eliminate any bias that may be caused from the carryover effect. Subjects were given at least 5 minutes to rest between tests in an attempt to eliminate the effect of fatigue on subsequent tests.

For the longitudinal study, glaucoma subjects from the Toronto site attended 2 additional visits, approximately 12 weeks apart, at least 12 months after the last visit (Visit 2). At the subsequent visits the same procedures as in Visits 1 and 2 were carried out. Table 2.5 provides an overview of the techniques used at each of the visits.

Table 2.5: Techniques used for each visit.

	Qualifying Exam	HRT	Cirrus OCT *	GDx VCC*	SAP	FDT	FDF	MDT
Visit 1	√	√	√	√	√	√	√	√
Visit 2			√	√	√	√	√	√
Visit 3					√	√	√	√
Visit 4					√	√	√	√

* Cirrus OCT and GDx VCC were only performed on the subjects from the Toronto site.

2.5 Analysis

All threshold estimates with a value less than 0 dB were given a value of 0 dB.

Test-retest was tested with all function tests from all centers.

Structure-function analysis with HRT and the four function techniques was done with subjects from all centers. Structure-functional analysis of OCT and GDx was done only with the subjects from the Toronto site.

Progression between examinations for each of the four function tests was analyzed only for the glaucoma subjects from the Toronto site.

The functional tests, SAP, FDT, FDT and MDT measure a total of 54, 55, 53 and 32 test locations, respectively. The test grids for each of the techniques were superimposed and only those that overlapped with all four test grids were used. Thus, a total of 32 points were used that corresponded to the MDT test grid.

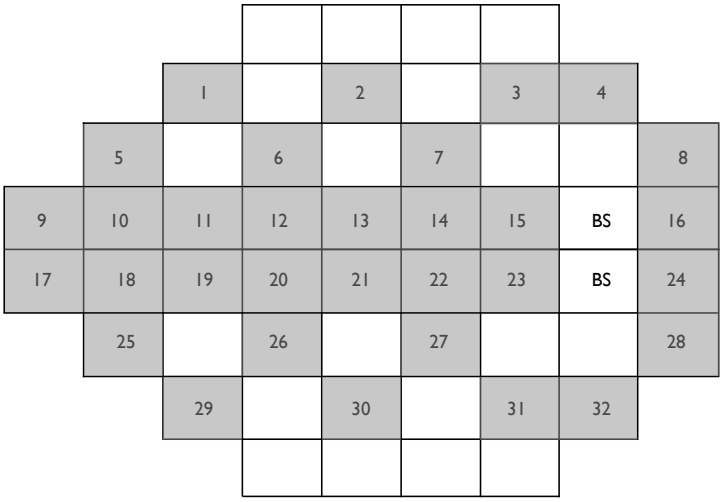

Figure 2.1: Overlapping Coordinates. Stimulus locations for the 24-2 algorithms for SAP, FDT, FDF and MDT. For comparison purposes, the test grids from all techniques were superimposed and only the 32 locations which were common to all four techniques was used; illustrated in grey (BS- blind spot). The centers of overlapping points from all four test grids for each of the test point locations were less than 2^{o} apart.

2.5.1 Test-retest

Test-retest variability plots analyze the variability between tests. This type of analysis can be a valid measure of variability only if no actual change has taken place, i.e. no progression of glaucoma. Test-retest variability analysis shows, for the range of measurement values, the variability upon repeated measurement.

Bland-Altman (Bland & Altman 1986) plots compare the average of two repeated measurements with their difference and they are used in method-comparison and validity studies in the medical literature. The mean difference, and the 5th and 95th percent confidence limits of the difference are marked on the plots to define the range of differences in which 90% confidence interval into which the follow-up data fall. Lower variability between measurements results in a narrower interval the technique is regarded more repeatable when compared to a test that has a wider confidence interval.

The frequency of differences in threshold points between visits was calculated within each technique. The frequency of data points was calculated globally and for threshold values in the range of near-normal, moderate to near-normal, severe to moderate and severe threshold values.

2.5.2 Structure-Function Correlation

For the structure-function analysis, the maps created by (Garway-Heath et al. (2000) were used (Figure 2.2). The points on the visual function tests were grouped according to the ONH sector they corresponded to.

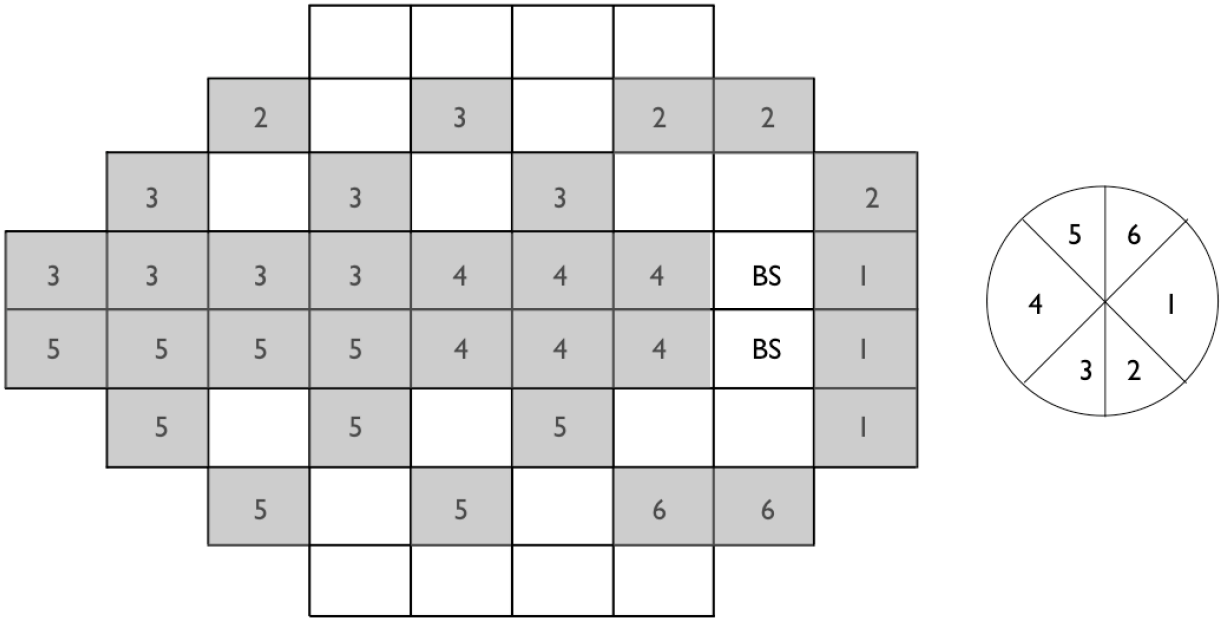

Figure 2.2: Structure-function relationship of the 32 test locations tested with the 6 sectors of the optic nerve head based on the structure-function map of Garway-Heath et al (2000). Sectors 1, 2, 3, 4, 5, and 6 represent the nasal, inferionasal, inferiotemporal, temporal, superiotemporal, and superionasal sectors, respectively.

2.5.3 Progression

Progression was determined between a visual function examination at Visit 1 or Visit 2 and a corresponding examination at Visit 3 or Visit 4; the test that had better reliability

was used for analysis; if both tests had equal reliability, which was the fact in most cases, then the test to be analyzed was chosen at random. Reliability was assessed using the reliability indices for each of the functional tests. The time difference between Visit 2 and Visit 3 was approximately 1 year.

Because each visual field instrument uses a different scale to measure threshold values, pattern deviation probability plots were used to compare progression. Only probability levels of $p>0.05$, $p<0.05$ and $p<0.02$ were used, these were common between all devices and was limited to the probability levels used by the MDT. Ordinal scores of 0, 2 and 5 were assigned to the $p>0.05$, $p<0.05$ and $p<0.02$ probability levels, respectively; this approach is similar to that used to weigh the Glaucoma Hemifield scores (Asman & Heijl 1992). Scores from Visit 1/2 (relabeled as Visit A) and Visit 3/4 (relabeled as Visit B) were compared to detect progression.

The difference between ordinal scores for each point was calculated.
Because only one set of follow-up data was available for this study, a point-by-point analysis was done and change was defined based on event-analysis.

3 Test-retest of Perimetry Tests in Early Glaucoma

3.1 Overview

Purpose: To compare the test-retest characteristics of SAP, FDT, FDF and MDT to determine which is more suitable to measure visual field loss and potentially monitor its progression.

Methods: 95 subjects with early glaucoma and 99 controls were enrolled in the study. Each subject attended 2 visits. During each visit, one eye was examined with SAP, FDT, FDF and MDT. Results from both visits were compared using paired Student's t-test, test-retest plots, frequency of difference plot, and Bland & Altman plots.

Results: Both SAP and MDT showed least variability in areas of near-normal sensitivity with increasing variability as sensitivity decreased. FDT and FDF both showed constant variability throughout the dynamic range with FDF having a narrower 95% confidence interval.

Conclusion: SAP is not able to detect abnormality as readily as FDT or FDF. However, SAP may be better at monitoring change in the near-normal range and FDF in the moderate to severe range of glaucoma.

3.2 Introduction

The purpose of a visual field examination in glaucoma is to detect defects and determine the specific pattern of visual field loss for diagnostic purposes, and monitor

patients for evidence of visual function defect progression (Chauhan et al. 1990; Spry et al. 2001; Spry & Johnson 2002).

The current gold standard perimetry technique, SAP, has been shown to detect visual field defects after glaucoma has progressed to a moderate stage (Zeyen & Caprioli 1993; C. Johnson 2009; Harwerth et al. 1999; Tuulonen et al. 1993; Chandra et al. 2013; Jonas et al. 1989; Quigley et al. 1995; Hart et al. 1978; Sommer et al. 1979b). The development of new perimetry techniques have been aimed at selectively testing subsets of ganglion cells to better reflect ganglion cell loss (selective testing hypothesis) (Johnson 1994), test subsets of ganglion cells that may be more prone to glaucomatous damage (selective loss hypothesis) (Alward 2000), or test cognitive functions driven by selective input to the visual cortex that appear to be more prone to early disease (Swanson et al. 2004).

Perimetry techniques such as Frequency Doubling Technology (FDT), Flicker Defined Form (FDF) and the Moorfields Motion Detection Test (MDT) are aimed at selectively testing the magnocellular pathway, and its cortical processing (Swanson et al., 2004) however, SAP has been shown to also test the function of M cells (Swanson, Sun, Lee & Cao 2011).

The Heidelberg Edge Perimeter (HEP; Heidelberg Engineering, Germany) is a new perimetry instrument which uses both Standard Automated Perimetry and Flicker

Defined Form (FDF) (Ramchandran & Rogers-Ramchandaran 1991; Flanagan et al. 1994), an illusionary stimulus. Flicker Defined Form stimulus is believed to predominantly stimulate RGCs of the magnocellular pathway because the illusion is not perceived using equiluminant chromatic stimuli and is resistant to blur (up to 6D) (Heidelberg Edge Perimeter 2010), thus it may be a good indicator for early glaucoma damage.

Moorfields MDT is a new perimetric motion-displacement test designed to diagnose glaucoma in the early stages (Verdon-Roe et al. 2006) using stimuli generated on a laptop computer. The ability to detect motion is believed to diminish early in glaucoma (Silverman et al. 1990). Hence, the MDT also has potential for early detection. Accurately detecting functional change is important to the management of glaucoma. The purpose of this study is to compare the test-retest characteristics of four measures of visual function to determine which is more suitable to measure visual field loss and potentially monitor its progression.

In order to determine test-retest variability of the perimetry tests, comparisons were made using global indices and threshold estimates.

3.3 Methods

The recruitment criterion was as described in Chapter 2 section 2.2. The study sample demographics are shown in Table 2.2. The procedures are explained in section 2.5.

3.4 Analysis

The patient's age and severity of visual field, ONH and RENFL defect were considered as separate between-subject factors.

Table 3.1 displays the mean and standard deviation for the visual field indices Mean Deviation (MD), Pattern Standard Deviation (PSD), and test duration; MDT does not calculate MD and PSD. The Student's t-Test was used to compare these indices from Visit 1 with Visit 2.

Table 3.1: Mean Deviation (MD), Pattern Standard Deviation (PSD) and Examination Duration.

Index	Visit	SAP	FDT	FDF	MDT
MD	1	-1.62 $\pm$ 3.36	-2.36 $\pm$ 4.75	-5.03 $\pm$ 5.29	---
	2	-1.49 $\pm$ 3.44	-2.08 $\pm$ 4.61	-4.56 $\pm$ 5.36	---
PSD	1	2.89 $\pm$ 2.54	3.42 $\pm$ 1.49	3.39 $\pm$ 1.56	---
	2	2.67 $\pm$ 2.31	3.44 $\pm$ 1.47	3.28 $\pm$ 1.57	---
Examination Duration	1	5.14 $\pm$ 0.77	5.14 $\pm$ 0.38	5.23 $\pm$ 1.42	6.65 $\pm$ 0.92
(minutes)	2	5.05 $\pm$ 0.71	5.16 $\pm$ 0.22	5.91 $\pm$ 1.47	6.64 $\pm$ 0.99

The Paired Student's t-test was sued to compare sector averages between visits for each technique (Table 3.2).

Table 3.2: Paired Student's t-Test p-values: Visit 1 vs Visit 2.

Technique	S1	S2	S3	S4	S5	S6	MS
SAP	0.394(N)	0.303(N)	0.211(N)	0.089(N)	0.308(N)	0.105(N)	0.478(N)
FDT	0.834(N)	0.741(N)	0.481(N)	0.777(N)	0.593(N)	0.821(N)	0.778(N)
FDF	0.154(N)	0.227(N)	0.020(N)	0.064(N)	0.027(N)	0.232(N)	0.094(N)
MDT	0.757(N)	0.721(N)	0.215(N)	0.948(N)	0.206(N)	0.482(N)	0.031(N)

Average of sectors and mean sensitivity (MS). N=not reject H_0.

Test-retest variability for each technique was plotted as a function of visual field sensitivity or threshold for Visit 1 to Visit 2 (Figure 3.3). The analysis describes the 5th and 95th confidence limits into which 90% of follow-up threshold estimates are likely to fall, provided no real change has occurred.

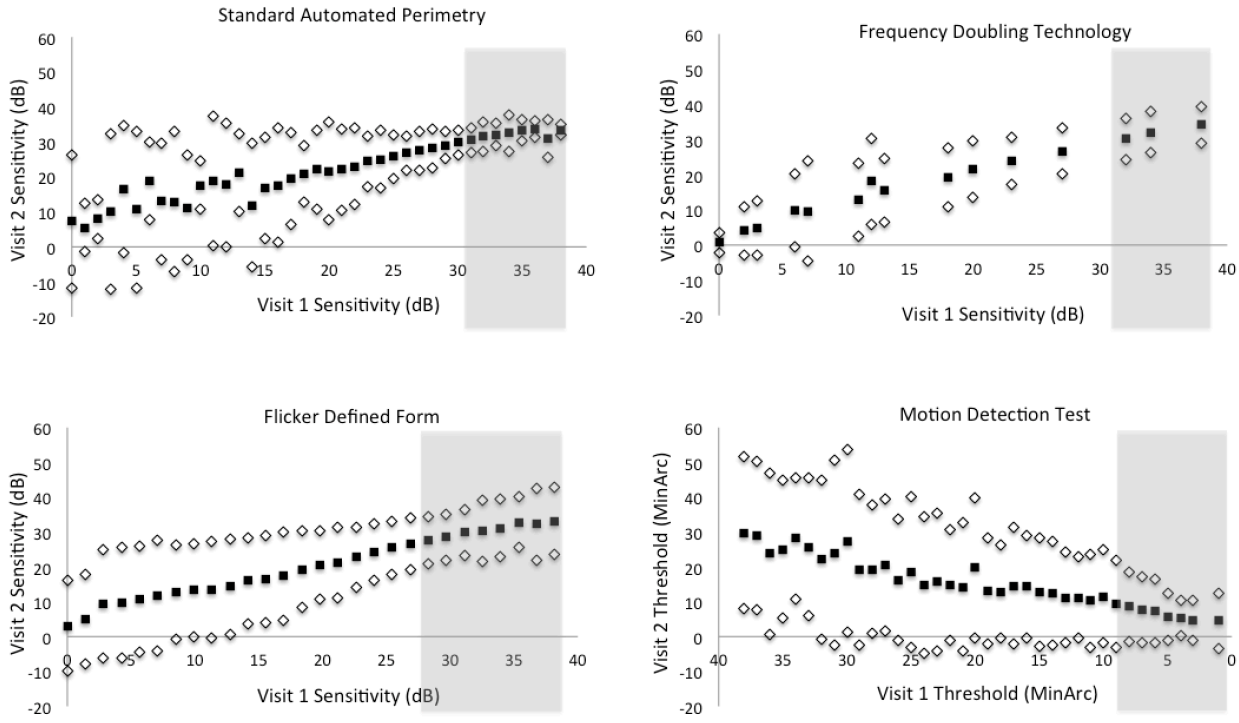

Figure 3.1: Test-retest plots showing the 95th, 50th and 5th percentiles for the distribution of retest sensitivity across the range of sensitivities measured, collapsed across all spatial locations for each technique. The threshold sensitivity from Visit 2 for each given location is plotted with respect to the threshold sensitivity value of Visit 1 (i.e. within-algorithm, between-visit analysis). The shaded areas denote the near- normal sensitivity range for each of the techniques.

The frequency of data points as a function of threshold difference between Visits 1 and 2 was plotted to illustrate which perimetry technique had the most number of points with no difference and at what threshold difference most of the data points fall within. Table 3.3 summarizes the data from Figure 3.2. The frequency of threshold estimates with 0 difference between visits and the maximum threshold difference for 90% of the data for each of the techniques is provided.

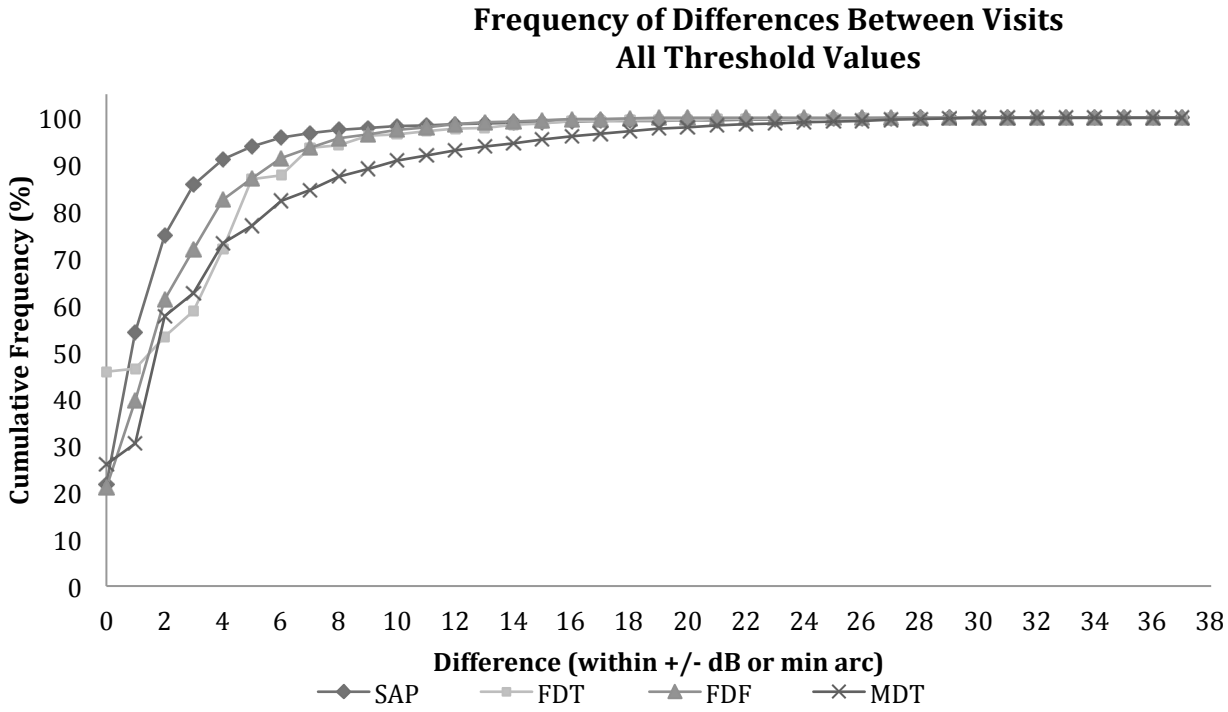

Figure 3.2: Global frequency of difference for all threshold points between Visits 1 and 2.

Table 3.3: Summary data from frequency of differences graphs.

Technique	Test locations with 0 dB/MinArc difference (%)	Maximum threshold difference of 90% of data (dB/MinArc)
SAP	22	4
FDT	46	7
FDF	21	8
MDT	26	10

Bland & Altman (1996) plots comparing repeatability of threshold estimates are shown in Figure 3.3. The mean, and $\pm$1.96 SD were noted on the graphs. The data is summarized in Table 3.4. This table includes the 90% confidence interval of the upper and lower limits of agreement as described by Carkeet (2015).

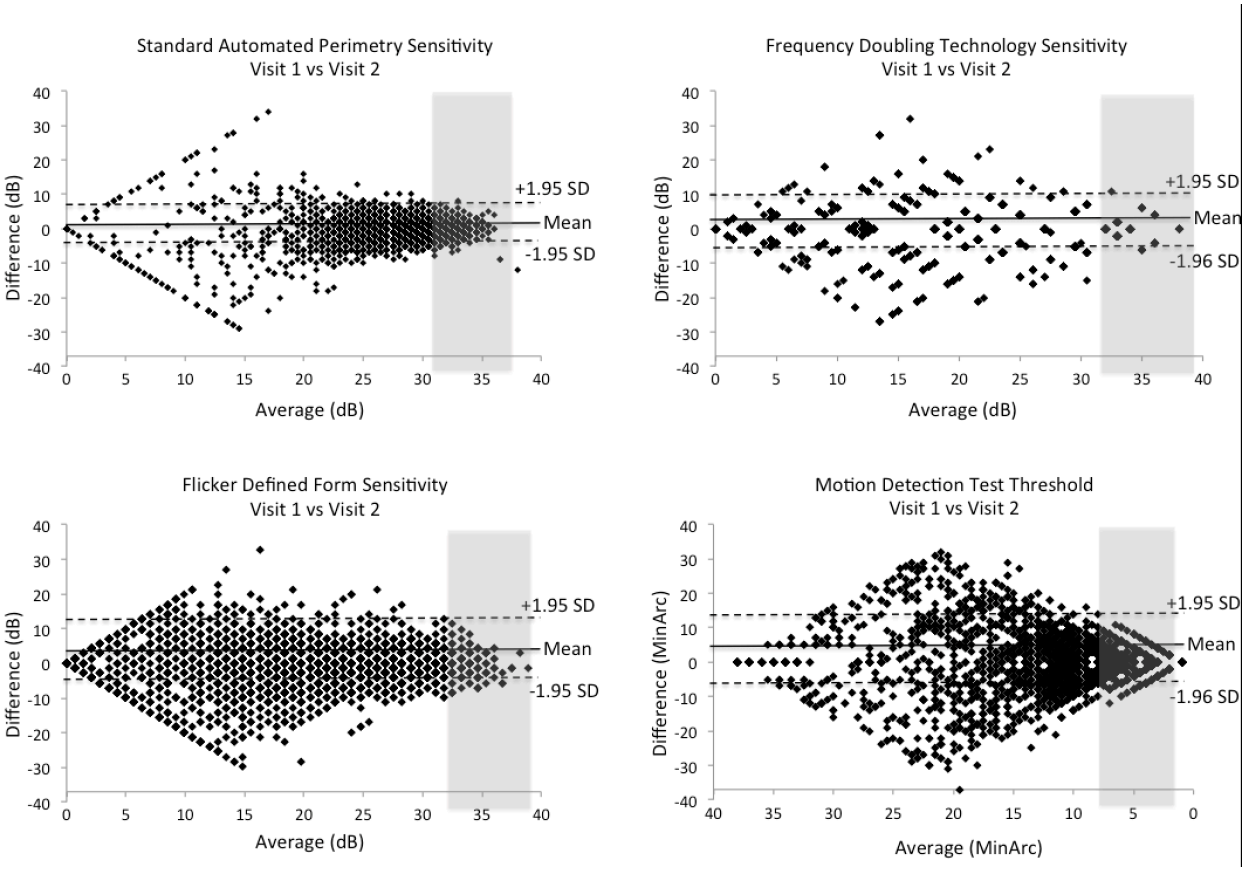

Figure 3.3: Bland & Altman shows the sensitivity values with respect to stimulus sensitivity or threshold of Visit 1 and Visit 2 for each technique with mean and ±1.96 standard deviations. The differences between Visits 1 and 2 (Visit 1 – Visit 2) are plotted with respect to the average of the two sensitivity values. The shaded areas denote the near-normal sensitivity range for each technique.

Table 3.4: Statistics from Bland & Altman Plots

Technique	MoD	-1.96 SD (95% CL)	+1.96 SD (95% CL)	Limits of Agreement (90% CI)
SAP	2.05	-3.05 (-2.97, -4.09)	7.60 (7.04, 8.15)	10.65
FDT	2.84	-4.22 (-3.60, -5.04)	9.90 (9.34, 10.78)	14.12
FDF	3.82	-4.14 (-3.43, -5.04)	11.79 (11.08, 12.69)	15.92
MDT	3.93	-5.93 (-5.08, -7.09)	13.79 (13.04, 15.05)	19.72

All values are in decibels (dB) except MDT which is in minutes of arc (MinArc).
MoD = mean of differences, CI = confidence interval, CL= confidence limit.

3.5 Results

Table 3.1 lists the global indices and test duration for each of the techniques studied. MDT was not included in the global indices comparison, as it does not calculate global indices. No significant difference within test was found between Visit 1 and Visit 2 for any of the parameters ($p>0.05$) except for MDT being approximately 1 minute longer than the rest of the techniques. Paired Student's t-test (Table 3.2) for the average of each sector and mean sensitivity showed no significant difference between Visit 1 and Visit 2.

Figure 3.1 displays the mean, 5% and 95% confidence limits for the range of values recorded in Visit 2 for a specific stimulus level in Visit 1. The SAP technique showed least variability in areas of normal to near normal sensitivity with increasing variability as sensitivity decreased. Moorfields MDT showed a similar trend to that of SAP but with greater variability throughout its dynamic range. Both FDT and FDF showed consistent variability throughout the instruments' dynamic range with FDT having a narrower range into which 90% of the follow-up data fall.

Figures 3.2 plot the global frequency of data points as a function of dB difference between visits. FDT showed the greatest fraction of threshold locations with a 0 dB difference between visits; however, SAP showed the most number of points with the least difference, followed by FDT. Moorfields MDT showed the greatest variability; this was in agreement with the test-retest plots.

Bland & Altman plots were calculated between visits for each technique (Figure 3.3); the average of two corresponding points was plotted against their difference (Visit 1 – Visit 2). The mean of differences and the Limits of Agreement (90% confidence intervals) are shown in Table 3.4. The diamond pattern is observed as a result of the floor effect (Wall et al. 2010) where below a certain sensitivity value, 0dB is the most frequent value on retest. This value is specific to each technique and defines the limit of the techniques dynamic range. For example, if the values from the two visits span the entire dynamic range (i.e. 0 and 40), the difference and average of these values will be 40 and 20, respectively. As the average of the two values deviates from the median, the difference between the values starts to decline. Thus, the further away the average of the two values is, the closer the difference will be to 0, giving rise to the diamond pattern. The difference in distribution of points within each technique is due to its unique properties. For both the FDT and FDF, variability is constant throughout the dynamic range that results in the fairly even distribution of points within the diamond pattern. Due to its limited number of final threshold estimates, the data points of the FDT are more sparse. In SAP, variability is less in the near-normal range, resulting in a narrow difference interval. Both SAP and MDT also have more points in the near-normal range explaining the higher density of points in this area.

Both FDT and FDF showed an even distribution of variability throughout the dynamic range with FDF showing a narrower interval. These results are in agreement with those seen with the test-retest plots.

3.6 Discussion

In perimetry, test-retest variability is dependent upon the stage of visual field defect being studied (Heijl et al. 1989), the stimulus characteristics (Wall et al. 1997) and, the algorithm used to estimate the sensitivity (Bengtsson et al. 1997). It has been previously noted that following disease progression in glaucoma is problematic as high levels of test-retest variability have been shown in moderate to severe stages of this disease (Chauhan & Johnson 1999; a Heijl et al. 1989). Thus, it is imperative to determine variability within a technique to determine whether or not it is suitable to measure visual field loss and monitor its progression. Previous studies have shown that the Matrix has uniform test-retest variability across its dynamic range (Artes, Hutchison, et al. 2005); in comparison to SAP, repeatability is greater in the normal range but gets worse in advanced defect. The FDF has also been shown to have uniform variability throughout its dynamic range; variability is similar to SAP in the normal range and improves in areas of increased defect (Heidelberg Engineering 2010). The main objective of this study was to test repeatability and test-retest characteristics of SAP, FDT, FDF and MDT to determine which technique is better suited to detect early glaucoma and monitor its progression.

The point-by-point analysis in Figure 3.1 describes the repeatability of each technique across the various sensitivity estimates. SAP and MDT variability increases as sensitivity decreases. This is in agreement with several previously published studies on

SAP test-retest characteristics (Henson et al. 1997; Russell et al. 2012); test-retest variability in SAP has also been shown to increase with increasing defect depth and eccentricity (Weber & Rau 1992; Olsson et al. 1993; Chauhan et al. 1993; Henson et al. 1997; Chauhan & Johnson 1999; Smith et al. 1996; Katz et al. 1997). MDT showed a slightly greater variability; however, both FDT and FDF showed uniform variability throughout the instruments' dynamic range with FDF having a narrower 90% confidence interval. This is also in agreement with previously published studies (Artes et al. 2005; Heidelberg Engineering 2010) where test-retest variability of FDT does not increase as much as SAP with an increase in defect severity (Spry et al. 2001). SAP has shown to be a poor diagnostic test for patients with early glaucoma, however, its performance improves (Spry et al. 2003) and variability increases (Harwerth et al. 2002; Weber & Rau 1992; Olsson et al. 1993; Wall et al. 1997; Chauhan et al. 1993; Henson et al. 1997) as sensitivity is reduced.

Frequencies of dB differences between visits are shown in Figure 3.2. FDT showed the highest fraction of 0 dB difference, which can be attributed to the fact that FDT has a smaller number of final threshold estimates compared to the other techniques (i.e. 15 vs 29 or 39). All techniques showed increasing variability with increasing disease severity with FDF having the least difference between threshold values from Visit 1 and Visit 2.

The Bland-Altman plots (Figure 3.3) showed greatest test-retest variability in the moderate defect range with all techniques; MDT was calculated to have the greatest

limits of agreement and mean of differences. SAP had the smallest values in both these parameters followed by FDT and FDF. The distribution described by the Bland-Altman plots (Figure 3.3) is in agreement with the trends seen in test-retest plots (Figure 3.1). In patients with open angle glaucoma, threshold values can vary as much as 10 dB and 21 dB, at locations with normal and moderate initial threshold values, respectively (Chauhan & Johnson 1999; Heijl et al. 1989; Holmin & Krakau 1979; Werner et al. 1982; Wilensky & Joondeph 1984; Katz & Sommer 1986; Lewis et al. 1986). In some cases, test-retest variability can span the entire dynamic range (Heijl et al. 1989) which makes it difficult to distinguish variability from true change (Haymes et al. 2005; Artes, Hutchison, et al. 2005).

The trends seen with the various techniques in this study indicates that SAP may be better at monitoring change in the near-normal range and FDF may be better for monitoring change in the moderate to severe range of glaucoma. However, the fact that more abnormal points are seen with FDT and FDF in comparison to SAP, as suggested by the MD and PSD calculations in Table 3.1, is evidence that SAP may not able to detect abnormality as readily as FDT and or FDF. This is in agreement with previous studies comparing the dynamic range of various perimetric techniques (Wall et al. 2010). FDF has been shown to detect glaucomatous damage when no defect was detected by SAP (Horn et al. 2016; Hasler & Stürmer 2012; Reznicek et al. 2015). However, SAP may be a suitable technique for monitoring progression in the moderate to late stages of glaucoma.

Early detection of glaucomatous damage and its progression over time is one of the most important clinical challenges in glaucoma (Hood & Kardon 2007). Thus, it is crucial to have tests that not only detect defect but also are repeatable in order to show true progression. A major limitation of this study was the fact that each technique has a unique threshold scale onto which its sensitivity values are calculated.

4 Structure-function relationship between Heidelberg Retina Tomograph with SAP, FDT, FDF and MDT

4.1 Overview

Purpose: The purpose of this study was to determine which perimetry technique best correlates with the structure of the ONH, both global and sectoral, as measured by the HRT.

Methods: 70 patients with early glaucoma and 87 controls were enrolled in the study. Each subject attended 1 visit during which one eye was measured with HRT and visual function was determined using SAP, FDT, FDF and MDT. In order to determine agreement between HRT and the perimetry tests, comparisons were made using sectoral and global analysis of the ONH sectors. Venn diagrams were used to show the diagnostic overlap amongst the HRT and 4 perimetry tests. Concordance charts were used to show the global and sectoral diagnostic overlap of the perimetry tests with that of the HRT.

Results: More agreement is seen with perimetry tests and the HRT when global classification of the ONH by HRT is outside normal limits. Sectorally, FDF showed greatest agreement with HRT when the sector was classified as outside normal limits and least agreement when the sector was classified as WNL. Sensitivities of 60.0, 60.0, 87.1 and 62.8 and specificities of 73.6, 75.9, 54.0 and 69.0 were calculated for SAP, FDT, FDF and MDT, respectively.

Conclusion: The poor diagnostic agreement seen between the HRT and each perimetry test may be due to the fact that each technique is identifying a different characteristic of glaucomatous damage. Because no one perimetry test has both high sensitivity and high specificity, it is recommended that a combination of FDF with either SAP, FDT or MDT be used as the functional component in the diagnosis and follow-up of patients with glaucoma.

4.2 Introduction

Understanding the structure-function relationship in glaucoma is necessary for understanding the natural history of the condition and grading of its severity (Malik et al. 2012b). Defining the structure-function relationship in glaucoma is currently the topic of ongoing research; considerable variation exists between the structure-function relationships in glaucoma (Ventura et al. 2006).

Imaging of the ONH and RNFL by computerized methods has become common practice in the detection and management of glaucoma in addition to the field tests (Breusegem et al. 2011; Greenfield 2002).

Confocal SLO provides accurate topographic maps of the optic disc and peripapillary retina and provides objective and reproducible data for analysis (Burgoyne 2004; Mikelberg et al. 1993; Rohrschneider et al. 1994) and discrimination between patients with and without glaucoma (Chauhan et al. 1994; Bathija et al. 1998; Mikelberg et al. 1995).

The purpose of this study was to determine which perimetry instruments best correlate with the structure of the optic nerve, both globally and sectorally, as measured by the HRT. For the purposes of this study, the Moorfields Regression Analysis computed by the HRT and IOP measurements defined the presence or absence of glaucoma.

4.3 Methods

The recruitment criterion was as described in Chapter 2 in section 2.2. The study sample demographics are listed in Table 2.3. The procedures are explained in section 2.5.

In order to determine agreement between HRT parameters and perimetry tests, comparisons were made using sectoral and global analysis of the HRT as described in Figure 2.2.

4.4 Analysis

Visual field sectors and entire visual fields were classified as within normal limits (WNL), or outside normal limits (ONL) based on the criteria listed in Table 4.1. Venn diagrams of overlapping agreement between visual field tests were made. This was stratified on the basis of the global classification of HRT being WNL or ONL.

Table 4.1: Visual field classification criteria.

Classification	Sector	Entire Field
WNL	≤ 30% of points at p<0.05	< 1 sector ONL
ONL	> 30% of points at p<0.05 **OR** ≥1 point at p<0.02	≥ 1 sectors ONL

WNL- within normal limits, ONL – outside normal limits

Diagnostic overlap between HRT and function specific perimetry were illustrated using pie charts. Figure 4.1 displays global comparison while figure 4.2 compares the diagnosis by sector.

Table 4.2: Sensitivity, specificity, Positive and Negative Predictive Values from global concordance and discordance.

	SAP	FDT	FDF	MDT
Sensitivity	60.0	60.0	87.1	62.8
Specificity	73.6	75.9	54.0	69.0
Positive Predictive Value	70.0	70.2	83.9	70.0
Negative Predictive Value	64.6	66.7	60.4	62.0

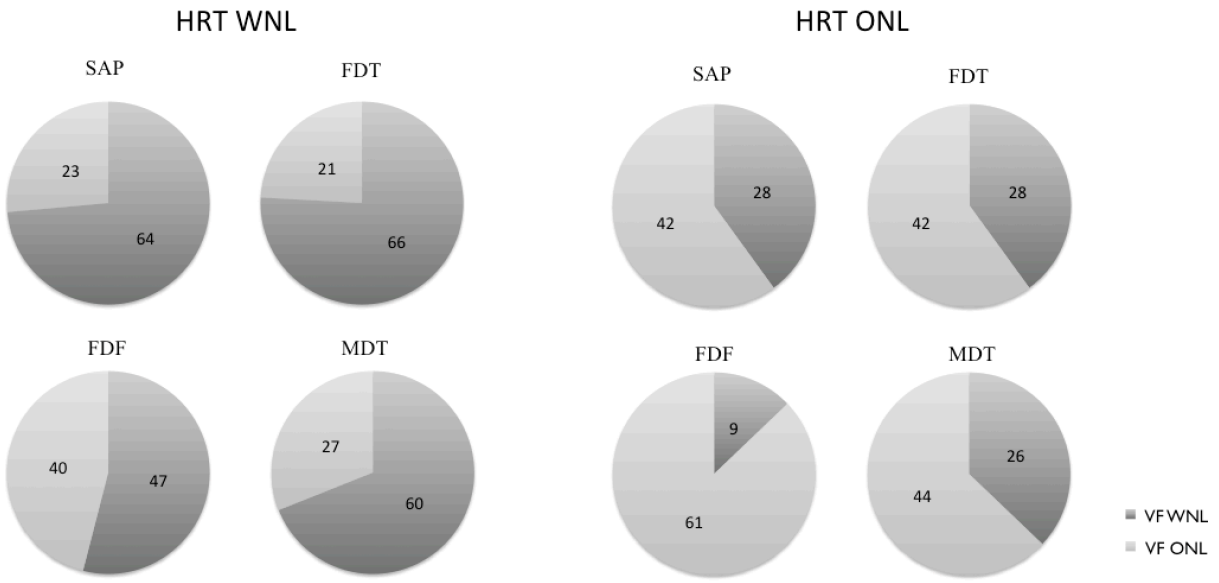

Figure 4.1: Global concordance and discordance between HRT and perimetry.

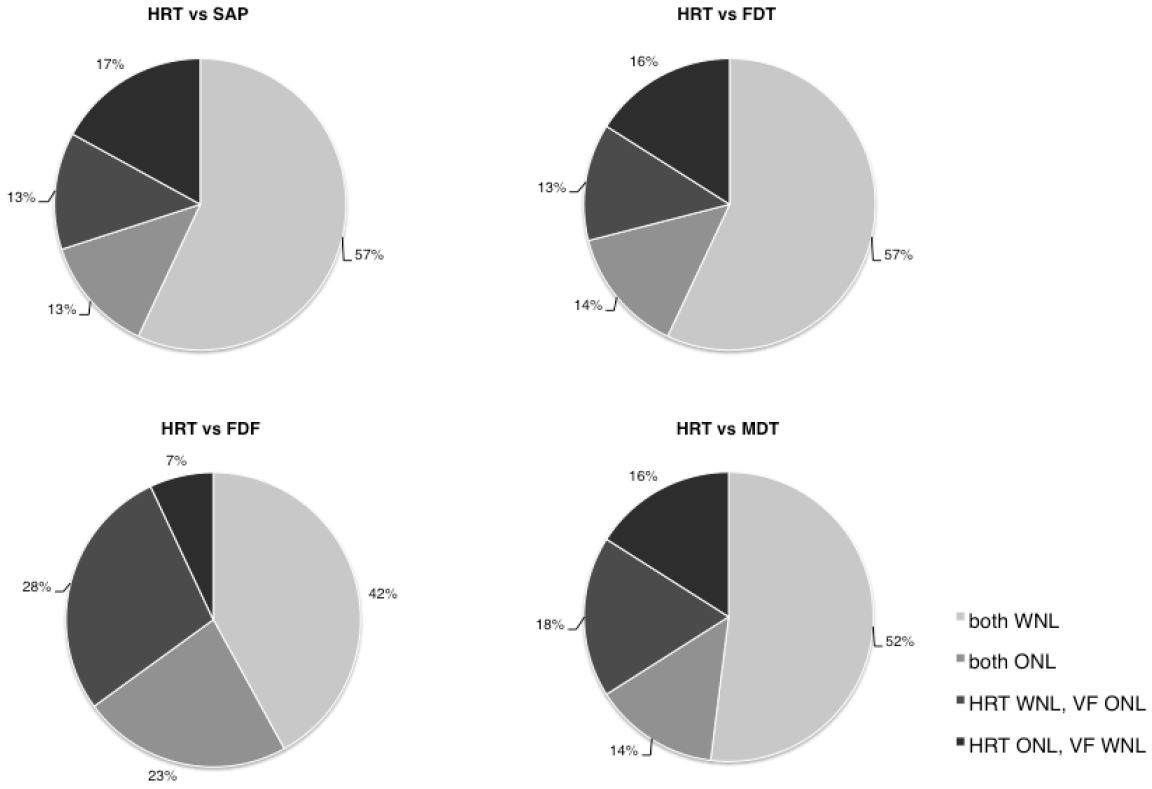

Figure 4.2: Illustration of the concordance and discordance between HRT and each visual field by sector.

Venn diagrams were constructed to show the diagnostic overlap of the four perimetry techniques to the HRT classifications of WNL and ONL (Figure 4.3).

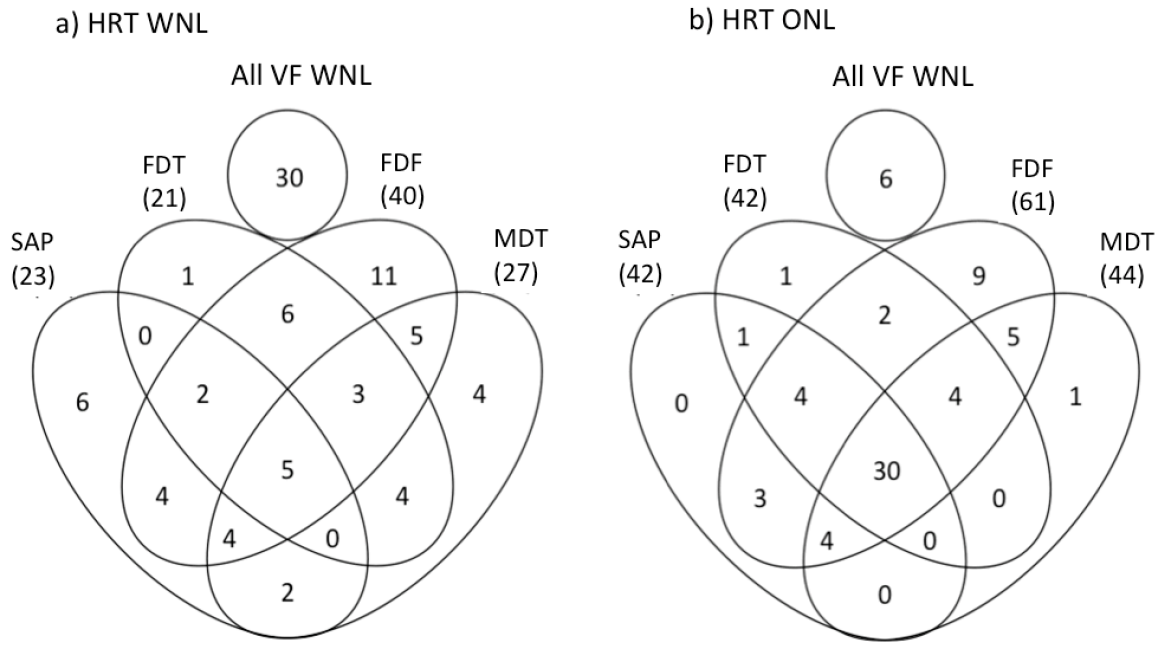

Figure 4.3: Venn diagram showing global diagnostic overlap of perimetry tests for subjects classified as WNL and ONL with respect to the ONH and IOP as classified by HRT and Goldmann applanation tonometry, respectively. The number in brackets beneath the perimetry technique indicates the number of subjects whose visual field was classified as ONL by that technique. The circles on the top represent the number of subjects in whom all 4 perimetry tests are WNL.

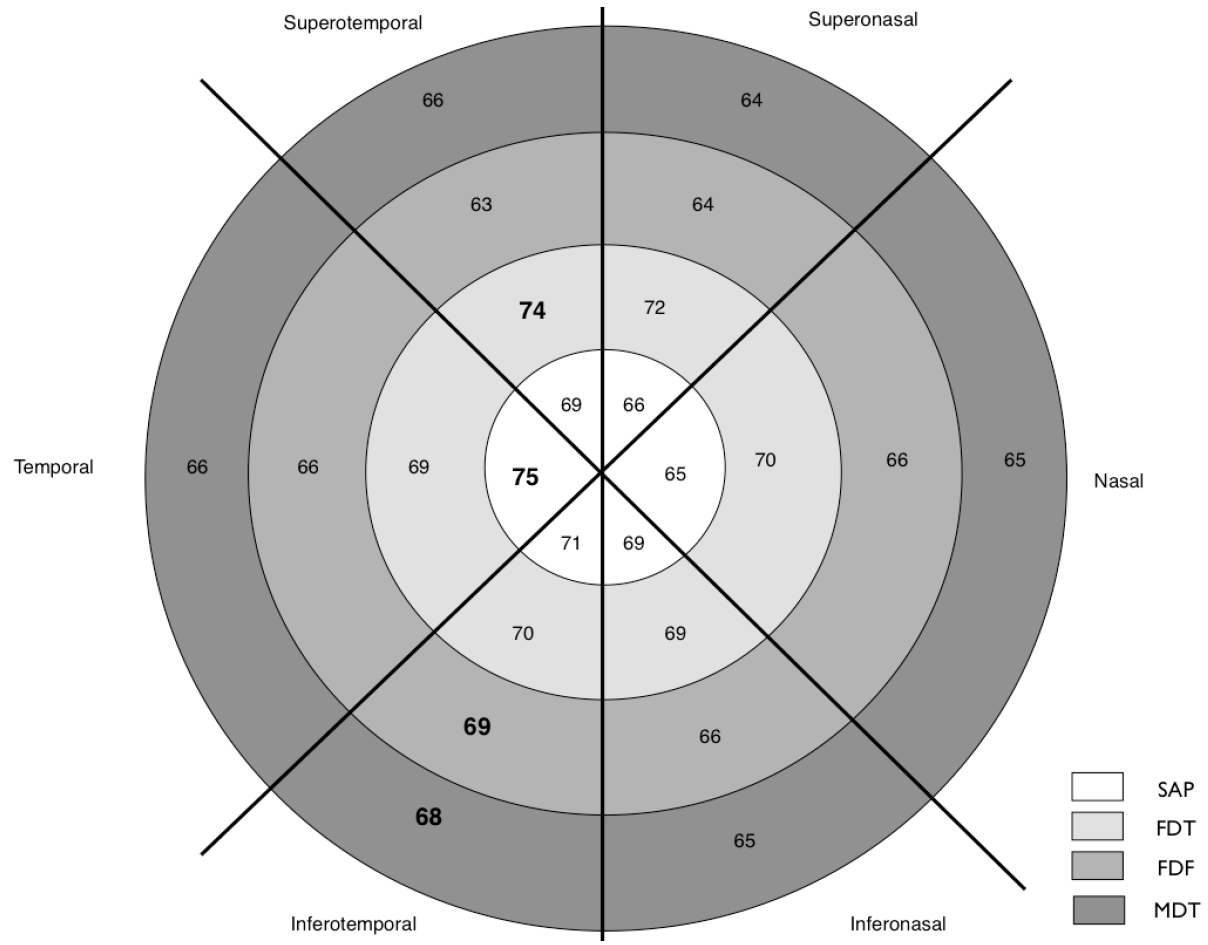

Figure 4.4: Illustration of the percentage of agreement between ONH and visual field test with respect to each sector. The numbers in bold highlight the sector with the greatest agreement within each perimetry technique.

4.5 Results

Concordance and discordance of the visual function tests to that of the HRT are shown globally and sectorally in Figure 4.1 and 4.2, respectively. Figure 4.3 are Venn diagram displaying the overlap of glaucoma classification of the perimetry techniques with respect to the classification of the HRT. All four perimetry techniques show more

agreement with the HRT when the eye was classified as glaucomatous as opposed to normal by HRT and IOP measurements. In both categories SAP, FDT and MDT showed similar agreement with the HRT; FDF showed greatest agreement when HRT classified the ONH as ONL and least agreement when the ONH was classified as WNL.

Figure 4.1 illustrates the diagnostic overlap between HRT and the perimetry techniques. In patients who were classified as WNL with respect to the HRT, there was approximately 70% agreement with SAP, FDT and MDT but only 54% agreement with FDF. In subjects classified as ONL with respect to HRT, agreement was seen with 87% of FDF data and approximately 40% with SAP, FDT and MDT. Concordance and discordance charts of HRT with VF tests also show FDF to be in greatest agreement with HRT when the ONH is classified as ONL and least agreement when ONH is classified as WNL. FDF also classifies more visual field tests as ONL than any of the three functional techniques irrespective of HRT classification.

Globally, calculations of sensitivity and specificity amongst the perimetry instruments were in the same range except for FDF, which showed a significantly higher sensitivity and lower specificity (Table 4.2). Positive and negative predictive values showed a similar trend with FDF having the highest and lowest positive and negative predictive values, respectively.

Overall there was similar ratio of agreement to disagreement in all perimetry tests. However, when looking at the distribution more closely, FDF shows greater agreement with HRT when the ONH sector is classified as glaucomatous and less agreement when the ONH is classified as normal.

Figure 4.4 displays the percentage of agreement between ONH and perimetry tests with respect to each sector. ANOVA calculations both within each perimetry test and within each sector were done to determine if any significant difference exists amongst the sectors and perimetry tests, respectively. A p-value of 0.789 was calculated for between test-within sector and a p-value of 0.001 for between sector-within test ($\alpha = 0.05$). Thus, there is a significant difference amongst the sectors with respect to each perimetry test, but there is no significant difference with respect to the perimetry tests within each sector. SAP showed greatest agreement in the temporal sector, FDT in the superiotemporal sector, and both FDF and MDT in the inferiotemporal sector.

4.6 Discussion

Clinically, the diagnosis of glaucoma involves correlating structural changes with functional deficits. Strong evidence suggests that glaucoma can progress to a moderate a stage before a visual field defect is seen on SAP (Johnson 2009; Harwerth et al. 1999; Zeyen & Caprioli 1993; Quigley et al. 1992; Tuulonen et al. 1993; Chandra et al. 2013; Hart et al. 1978; Sommer et al. 1979a) and structural changes are present before any visual field damage is detected by SAP (Kuang et al. 2015; Quigley et al.

1992; Chandra et al. 2013; Wilensky & Kolker 1976; Leung et al. 2005; Kanamori et al. 2008; Reus et al. 2006; Bowd et al. 2006a). The main objective of this study was to determine which perimetry technique showed the greatest agreement with structure of the ONH, both globally and sectorally, as measured and classified by the HRT and Goldmann applanation tonometry.

Previous studies have shown that HRT parameters are a good indicator of glaucomatous ONH damage (Iester et al. 1997) as it has shown to acquire repeatable and reliable measurements of the ONH (Mikelberg et al. 1993; Rohrschneider et al. 1994; Chauhan et al. 1994), provide reasonable levels of sensitivity and specificity (Mikelberg et al. 1995; Bathija et al. 1998; Uchida et al. 1996; Zangwill et al. 2007) and be in agreement with clinical examination (Yaghoubi et al. 2015). HRT parameters such as rim area, rim volume and mean RNFL height have been shown to be well correlated with mean deviation and corrected pattern standard deviation of SAP tests (Brigatti & Caprioli 1995; Iester, Mikelberg, et al. 1997; Iester, Swindale, et al. 1997; Tole et al. 1998). For these reasons and the purpose of this study, HRT was chosen as the gold standard for classification of the eyes.

Figure 4.3 displays Venn diagrams showing the global diagnostic overlap between HRT and the functional tests. It should be kept in mind that the structure-function relationship in glaucoma is not clear as it relies on several factors including physiological variation amongst individuals (Pan & Swanson 2006) age (Ren et al. 2014; Honjo et al. 2015)

and the stage of the disease (Harwerth et al. 2005). Studies have shown either parameter can change before the other or simultaneously (Kass et al. 2002; Heijl et al. 2002; Malik et al. 2012a). Even with the use of advanced diagnostic and analytic procedures, correlation between structural and functional changes in glaucoma can be seen in less than 50% of the cases (Drance 1985; Turpin et al. 2009; Gardiner et al. 2005; Garway-Heath, Caprioli, et al. 2000; Strouthidis, Vinciotti, et al. 2006). This explains why some subjects who were diagnosed as WNL with respect to the HRT showed functional defect on up to 4 perimetry techniques.

The sensitivity and specificity values calculated for global concordance and discordance were similar for SAP, FDT and MDT; FDT showed greater sensitivity but less specificity. The sensitivity and specificity values were expected to be similar for all perimetry techniques as they are all capable of preferentially stimulating M cells before P cells (Swanson et al. 2011). However, the fact that FDF has greater sensitivity indicates that it has the potential to identify glaucoma earlier than the other perimetry tests, making it a more suitable screening test for glaucoma. Sensitivity and specificity of diagnostic instruments may not be applicable to all subgroups of patients with the disease in question (Ransohoff & Feinstein 1978). Hence, diagnostic tests are more sensitive in advanced stages of disease and its diagnostic accuracy may not be applicable to patients in the early stages or those who are suspects (Lachs et al. 1992; Moons et al. 1997). Because no one perimetry test has both high sensitivity and high specificity in the findings of this study, it is recommended that a combination of FDF with either SAP,

FDT or MDT be used as the functional component in the diagnosis and follow-up of patients with glaucoma. Similar agreement was seen when individual sectors were compared.

Sectoral agreement with respect to each perimetry test showed SAP to have the most agreement in the temporal sector. The temporal region of the ONH is the last and the least sector of the ONH to show glaucomatous damage would have the greatest number of sectors classified as WNL. The inferior ONH sector is most likely the first sector to show structural change thus, it is expected that function tests designed to detect glaucomatous damage early would show the greatest agreement in this region. This was seen with both FDF and MDT, specifically in the inferiotemporal sector however, FDT showed its greatest agreement in the superiotemporal sector.

Ideally, in order to determine which parameter, structure or function, better detects glaucomatous damage first, there needs to be an alternate parameter that will be the gold standard for glaucoma diagnosis. In this case, we are limited by the fact that no such parameter exists and this should be kept in mind when comparing structure and function measures in glaucoma.

5 Structure and Function Relationships in Glaucoma using OCT, GDx VCC with Standard and Function Specific Perimetry

5.1 Overview

Purpose: To evaluate the structure-function relationship between measures of RNFL and visual function; specifically to determine whether or not visual function corresponds to structure and which instruments best correlate structure and function of the ONH and RNFL.

Methods: 38 subjects with early glaucoma had RNFL thickness measured with OCT and GDx and RNFL function measured with SAP, FDT, FDF and MDT during one visit. The data was recalculated to fit the 6 sectors of the ONH as divided by the HRT in order to have a common ground for comparing the measurements. Comparisons of RNFL thickness as measured by OCT and GDx were made using regression analysis. Both linear and logarithmic associations were made with OCT and GDx with each of the perimetry techniques.

Results: Both OCT and GDx showed the classic double-hump pattern as expected with the normal anatomy of the RNFL, with OCT detecting thickness to be approximately 1.5 times thicker in all sectors as compared to GDx. Logarithmic associations were stronger than that of linear associations for all function tests in both OCT and GDx comparisons. Associations with visual field sensitivity were stronger for OCT than GDx, except for FDF.

Conclusion: The difference in strength of association as seen with the two structural imaging techniques confirms that each technique is measuring a different parameter of the RNFL and cannot be used interchangeably. The strongest global structure-function correlations for OCT were seen with SAP, FDT and MDT; for GDx, the strongest association was seen with FDF. The result of this preliminary study suggests that FDF and GDx used in combination are best to detect early glaucomatous changes.

5.2 Introduction

Defining the relationship between structural and functional loss in glaucoma has been of great interest since the 1850s (Drance 1974). Several studies have shown that glaucomatous defects in RNFL usually occur before defects are seen on SAP (Airaksinen & Heijl 1983; Airaksinen & Drance 1985; Lan et al. 2003) particably, leading to the conclusion that measurement of structural changes to the ONH, and RNFL offers the prospect of improved early detection and monitoring of glaucoma (Quigley 1986; Drance 1985; Bowd et al. 2001). Various imaging techniques such as optical coherence tomography (OCT) (Schuman et al. 1995; Schuman et al. 1996), confocal scanning laser ophthalmoscopy (CSLO) (Strouthidis & Garway-Heath 2008; Fechtner et al. 1993; Uchida et al. 1996; Zangwill et al. 1996; Lemij & Reus 2008) and scanning laser polarimetry (SLP) (Zeimer et al. 1998; Medeiros et al. 2004) use different properties of light to quantitatively assess topography and other structural properties of the ONH and RNFL (Ventura et al. 2006; Weinreb et al. 1990; Weinreb et al. 1993; Weinreb 1999;

Huang et al. 1991; Hoh et al. 2000; Greenfield 2002; Kotera et al. 2008; Zangwill et al. 2000; Niessen et al. 1996; Chang & Budenz 2008).

The purpose of a visual field examination in glaucoma is to detect defects and determine the specific pattern of visual field loss for diagnostic purposes, and monitor patients for evidence of visual function defect progression (Chauhan et al. 1990; Spry et al. 2001; Spry & Johnson 2002). Standard automated perimetry (SAP) is currently the gold standard for detecting glaucomatous visual field loss (Quigley 1993; Sommer et al. 1991; Johnson 1996; Bayer & Erb 2002; Anderson 1987; Alexander 1991; Johnson & Sample 2003; Sekhar et al. 2000).

The development of second generation visual function techniques has been aimed at selectively testing subsets of ganglion cells that may be more prone to glaucomatous damage (selective loss hypothesis) (Alward 2000) or test cognitive functions driven by selective input to the visual cortex that appear to be more prone to early disease. The use of perimetric tests which utilize flicker (Johnson 2009; Harwerth et al. 1999; Tyler 1981; Lachenmayer et al. 1989; Horn et al. 1997) and motion (Silverman et al. 1990; Wall & Ketoff 1995; Bosworth et al. 1997) have been proposed for the early detection of glaucoma. Visual function techniques such as Frequency Doubling Technology (FDT), Flicker Defined Form (FDF) and Moorfields Motion Detection Test (MDT) are aimed at selectively testing ganglion cells of the magnocellular pathway, and its cortical processing (Swanson et al. 2004).

5.2.1 Structural Instruments

5.2.1.1 Optical Coherence Tomography

The Optical Coherence Tomography (OCT) is a non-invasive imaging technique which allows for quantitative examination of the optic disc and retina (Guedes et al. 2003) to evaluate ONH topography and macular thickness for diagnosis (Schuman et al. 1995a; Schumano et al. 1995b) and follow-up of patients with glaucoma (Medeiros et al. 2005). A good correlation is demonstrated between OCT NFL measurements and histology of the retina (Toth 1997). Visual field defects as measured by SAP have also been shown to correlate with RNFL measurements as measured by OCT in glaucomatous neuropathy (Harwerth et al. 2007).

Measurement of RNFL thickness by OCT has been shown to be useful in the early detection of RNFL damage, as it has been shown to qualitatively differentiate RNFL thickness in normal and glaucomatous eyes (Liu et al. 2001), and may be a useful tool in monitoring glaucomatous changes (Kanamori et al. 2003).

5.2.2 Scanning Laser Polarimetry

Scanning laser provides a good and objective method for RNFL thickness evaluation (Chen et al. 2009) and has helped improve glaucoma detection (Zhou & Weinreb 2002;

Weinreb et al. 2003; Greenfield et al. 2003; Medeiros et al. 2003; Greenfield et al. 2002; Choplin et al. 2003) as it has shown a good correlation with histological measurements (Blumenthal et al. 2009; Cohen et al. 2008).

The purpose of this study is to evaluate the structure-function relationship between measures of RNFL and visual function; specifically to determine whether or not visual function corresponds to structure and which instruments best correlate structure and function of the ONH and RNFL. The specific aims of this study were to: i) determine the relationship between RNFL measures of OCT and GDx, ii) determine whether or not visual function corresponds to RNFL structure, and iii) determine the level of agreement between structure and function of the ONH and RNFL.

5.3 Methods

The recruitment criterion was as described in Chapter 2 section. The study sample demographics are listed in Table 2.3. The procedures are explained in section 2.5. 38 subjects with early glaucoma were recruited for this preliminary study.

5.4 Analysis

In order to compare the data from the OCT, GDx and perimetry tests, the data from each instrument was recalculated to fit the 6-sector map of the HRT. Comparison amongst the instruments were based on these sectors.

Figure 5.1 gives a schematic diagram showing overlapping sectors from GDx and OCT with that of HRT. The 64 and 12 sectors from GDx and OCT, respectively, were calculated to fit the 6-sector map of the HRT. The values were averaged to give a sectoral value which corresponds with that of the HRT sector. These values were used to make comparisons between the structural tests and between structural and functional measurements from each instrument.

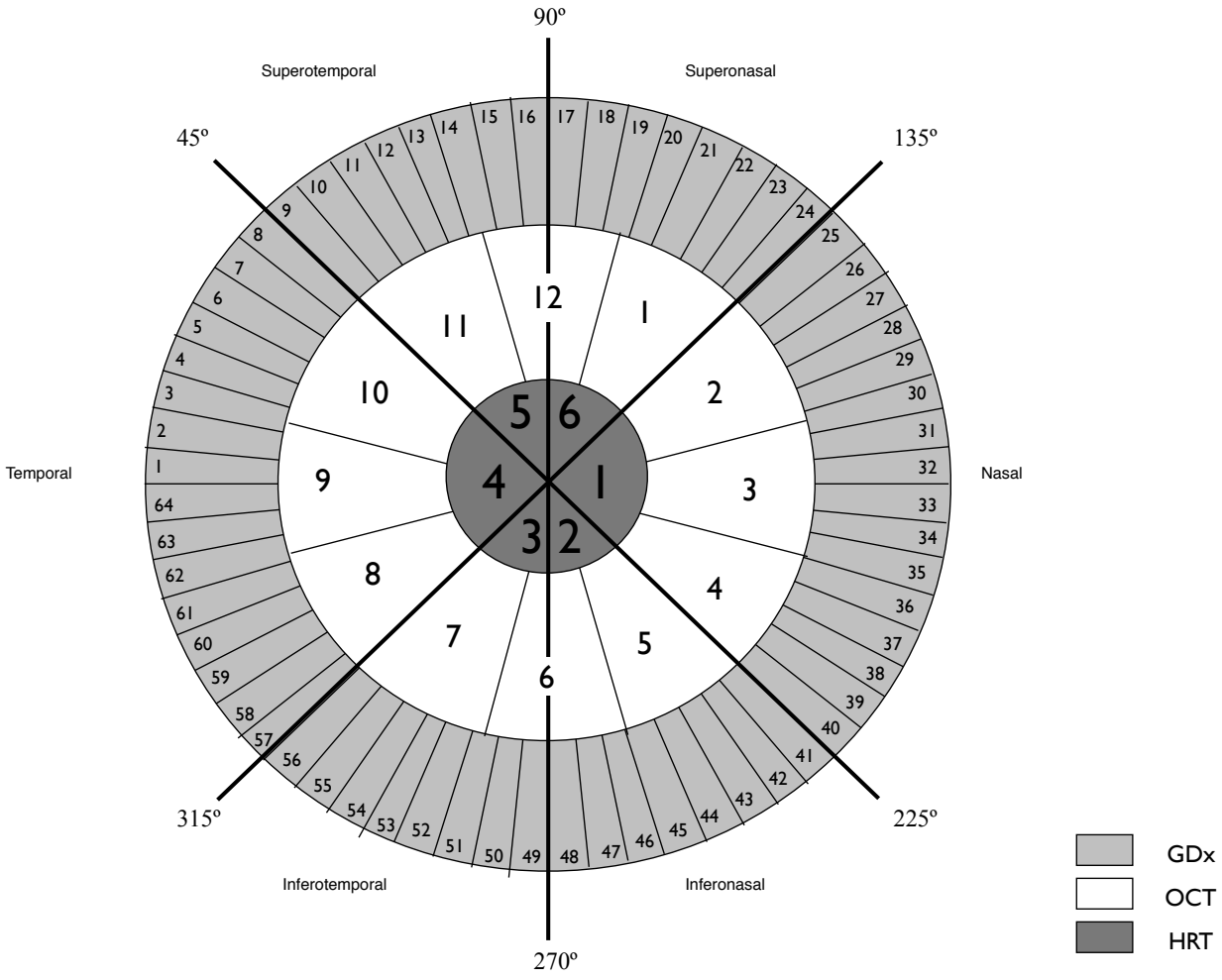

Figure 5.1: Schematic diagram showing overlapping sectors from GDx and OCT with that of HRT. The 64 and 12 sectors from GDX and OCT, respectively, were calculated to fit the 6-sector map of the HRT. The values were averaged to give a sectoral value which corresponds with that of the HRT sector.

All threshold estimates with a value less than 0 dB were given a value of 0 dB; at locations with two threshold estimates the average value was used.

Correlations between RNFL thickness measurements of OCT and GDx were performed using sectoral and global values. Figure 5.4 represents the linear regression of average thickness of OCT and GDx values as depicted by each of the 6 sectors. Correlations between structural instruments and the four visual function techniques were compared using both linear ($y=a+bx$) and logarithmic ($y=a+b \cdot \ln(x)$) associations (because visual field sensitivity is measured in logarithmic units, dB). The student's t-test was used to test the statistical significance of r.

5.5 Results

Figure 5.2 shows a scatterplot of the linear regression of RNFL thickness as measured by OCT and GDx with respect to each sector for each patient. Global and sectoral correlation coefficients of RNFL thickness between these two structural measures are listed in Table 5.1. Correlation ranged from 0.28 (temporal sector) to 0.71 (superionasal sector); all correlations were statistically significant. Measurement variability of both instruments increased in the same sectoral order: inferionasal, superiotemporal, superionasal, inferiotemporal, nasal and temporal.

Retinal thickness profiles as measured by the OCT and GDx are shown in Figure 5.3. Both OCT and GDx showed the classic double-hump pattern as expected with the normal anatomy of the RNFL, however OCT gives a thicker measurement in all sectors.

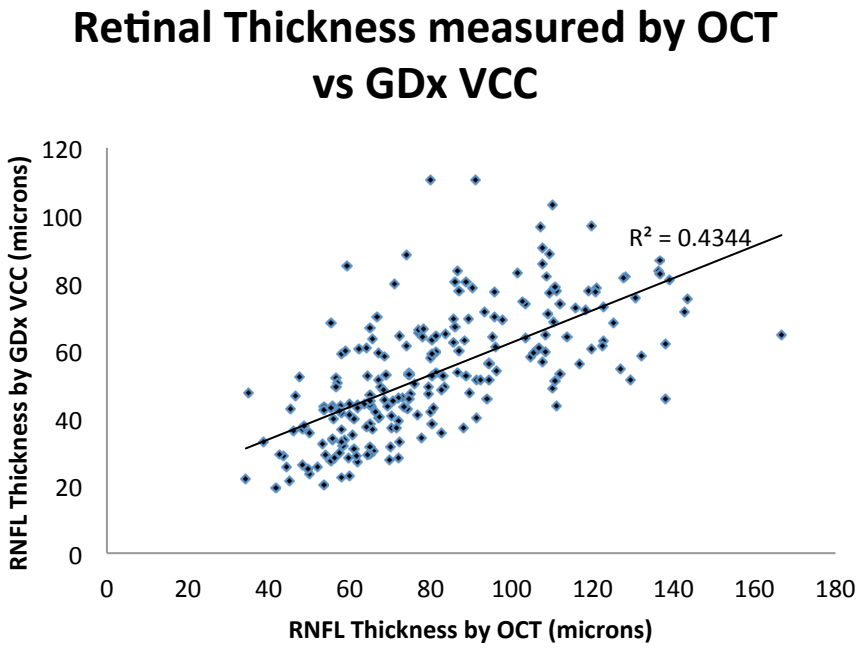

Figure 5.2: Scatterplot and linear regression line of RNFL thickness as measured by OCT and GDx VCC with respect to each of the six sectors.

Table 5.1: Global and sectoral correlation coefficient of RNFL thickness with OCT and GDx.

Sector		RNFL Thickness (ave ± SD) OCT	GDx	CC (r)	p-value
Global	**Global**	88.93 ± 21.62	59.15 ± 15.52	0.66	<0.01
1	**Nasal**	80.95 ± 25.78	53.22 ± 18.68	0.63	<0.01
2	**Inferionasal**	65.28 ±10.22	41.51 ± 8.71	0.60	<0.01
3	**Inferiotemporal**	85.93 ± 24.47	68.57 ± 17.67	0.41	<0.01
4	**Temporal**	94.45 ± 28.52	57.55 ± 19.08	0.28	<0.05
5	**Superiotemporal**	55.05 ± 10.49	34.38 ± 10.56	0.60	<0.01
6	**Superionasal**	96.01 ± 23.09	58.13 ± 14.43	0.71	<0.01

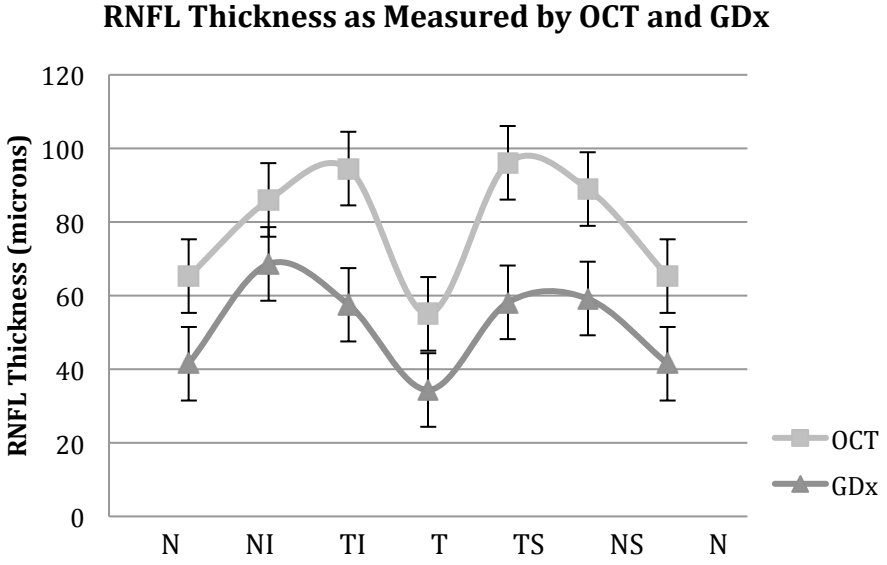

Figure 5.3: RNFL thickness profile as measured by OCT and GDx from Visit 1.

Associations of structural tests to visual field tests were calculated both linearly and logarithmically; because visual field sensitivity is measured in logarithmic units

comparing linear and logarithmic regressions is essential to detect and confirm the structure-function relationship and select the appropriate monitoring strategy to detect the change (Leung et al. 2005). R^2 values are shown in Tables 5.2 and 5.3 for GDx and Tables 5.4, 5.5, for OCT. Logarithmic associations were stronger than that of linear associations for all function tests in both OCT and GDx comparisons. Overall, both global linear and logarithmic associations with visual field sensitivity were stronger for OCT than GDx, except for FDF. OCT showed the strongest association in the inferiotemporal RNFL sector with all visual field techniques whereas with the GDx, the strongest associations were seen in the superiotemporal sector with SAP, FDT and MDT and the superionasal sector for FDT.

Table 5.2: Linear (r^2) association of GDx with Visual Function Tests.

GDx	SAP		FDT		FDF		MDT	
	r^2	p-value	r^2	p-value	r^2	p-value	r^2	p-value
Global	0.18	0.01	0.21	<0.01	0.38	<0.01	0.17	0.01
N	0.11	0.04	0.22	<0.01	0.20	<0.01	0.02	0.37
IN	0.14	0.02	0.24	<0.01	0.37	<0.01	0.21	<0.01
IT	0.12	0.03	0.10	0.06	0.19	<0.01	0.09	0.07
T	0.01	0.63	<0.00	0.86	0.03	0.34	0.02	0.34
ST	0.27	<0.01	0.29	<0.01	0.33	<0.01	0.27	<0.01
SN	0.04	0.23	0.17	0.01	0.48	<0.01	0.02	0.34

Table 5.3: Logarithmic (r^2) association of GDx with Visual Function Tests.

GDx	SAP		FDT		FDF		MDT	
	r^2	p-value	r^2	p-value	r^2	p-value	r^2	p-value
Global	0.21	<0.01	0.25	<0.01	0.41	<0.01	0.19	<0.01
N	0.12	0.03	0.23	<0.01	0.20	<0.01	0.02	0.37
IN	0.13	0.3	0.23	<0.01	0.36	<0.01	0.19	<0.01
IT	0.18	<0.01	0.13	0.03	0.26	<0.01	0.13	0.03
T	<0.00	0.68	<0.00	0.86	0.03	0.31	0.03	0.34
ST	0.34	<0.01	0.30	<0.01	0.34	<0.01	0.32	<0.01
SN	0.04	0.25	0.16	0.01	0.50	<0.01	0.02	0.34

Table 5.4: Linear (r^2) associations of OCT with Visual Function Tests.

OCT	SAP		FDT		FDF		MDT	
	r^2	p-value	r^2	p-value	r^2	p-value	r^2	p-value
Global	0.27	<0.01	0.35	<0.01	0.33	<0.01	0.19	<0.01
N	0.03	0.31	0.09	0.07	0.12	0.04	0.03	0.28
IN	0.16	0.13	0.24	<0.01	0.22	<0.01	0.21	<0.01
IT	0.40	<0.01	0.47	<0.01	0.46	<0.01	0.39	<0.01
T	0.11	0.04	0.18	<0.01	0.14	0.02	0.07	0.11
ST	0.34	<0.01	0.35	<0.01	0.33	<0.01	0.18	<0.01
SN	0.06	0.15	0.16	0.01	0.22	<0.01	<0.01	0.90

Table 5.5: Logarithmic (r^2) associations of OCT and Visual Function Tests.

OCT	SAP		FDT		FDF		MDT	
	r^2	p-value	r^2	p-value	r^2	p-value	r^2	p-value
Global	0.30	<0.01	0.40	<0.01	0.35	<0.01	0.22	<0.01
N	0.04	0.25	0.09	0.06	0.14	0.02	0.04	0.23
IN	0.19	<0.01	0.29	<0.01	0.24	<0.01	0.26	<0.01
IT	0.46	<0.01	0.54	<0.01	0.47	<0.01	0.47	<0.01
T	0.13	0.03	0.18	<0.01	0.14	0.02	0.08	0.08
ST	0.41	<0.01	0.40	<0.01	0.36	<0.01	0.23	<0.01
SN	0.08	0.09	0.20	<0.01	0.25	<0.01	<0.01	0.68

5.6 Discussion

Early detection of glaucomatous damage and its progression over time is one of the most important clinical challenges in glaucoma (Hood & Kardon 2007). Detection and

management of glaucoma is two-fold: i) observation and documentation of ONH and RNFL and, ii) measurement of visual function with automated perimeters. Several patterns of glaucomatous RNFL and optic disc damage have been described (Airaksinen & Tuulonen 1984; Drance et al. 1986; Caprioli et al. 1987; Caprioli 1989; Tuulonen & Airaksinen 1991; King et al. 2000) and correlated with different patterns of visual field loss (Caprioli et al. 1987; Jost B. Jonas et al. 1988; Bowd et al. 2001). It is therefore important to determine which techniques can accurately diagnose glaucoma and detect its progression both structurally and functionally throughout the course of the disease. For the purposes of this study, we wanted to determine which structural and functional instruments showed the strongest correlations in patients with glaucoma. Previous studies have shown significant associations between HRT II, Stratus OCT and GDx VCC with standard automated perimetry (Bowd et al. 2006a).

Correlations of OCT and GDx in this study showed a linear association between the two instruments. This was seen in previous studies comparing the measurements of these two instruments in pre-perimetric glaucoma (Kim et al. 2011). The total average RNFL thickness of the OCT is approximately 1.5 times that of the GDx despite the fact that the GDx measures RNFL closer to the optic disc than OCT. This same trend was seen in other studies comparing the two instruments (Kim et al. 2011; Leung et al. 2005). A difference in RNFL thickness was expected to be higher with OCT than that of GDx due to the difference in RNFL calculation by each instrument. OCT calculates RNFL thickness by measuring the difference in differential reflectivity signals between the

vitreoretinal interface and the posterior border of the RNFL (Schuman et al. 1995) whereas GDx measure the retardation of polarized light from the RNFL axons and converts it into a thickness value (Weinreb et al. 1995).

Looking at the sectoral correlations of this study (Table 5.1) both OCT and GDx showed the same sectoral order of increasing standard deviation in the order of inferionasal, superiotemporal, superionasal, inferiotemporal, nasal and temporal indicating that the greatest variability is seen in the nasal and temporal sectors of the peripapillary retina. Thinning of the neural rim at the superior and inferior poles has been shown to be the most reliable indicator of visual field defects (Goldberg 1981; Hoskins Jr & Gelber 1975; Gloster 1978; Hitchings & Anderson 1983). Thus, both OCT and GDx are capable of detecting RNFL damage in early glaucoma, especially in the superior and inferior sectors however, their results are not interchangeable and progressive change should be monitored with only one instrument.

Several previously published papers have compared visual field sensitivity, measured by SAP, to RNFL as measured by OCT and/or GDx. Significant correlations have been seen between visual field sensitivity and peripapillary nerve fiber layer thickness as measured with OCT (Leung et al. 2005; Kanamori et al. 2008; Wollstein et al. 2005) and SLP (Reus & Lemij 2004b; Reus et al. 2006; Bowd et al. 2006a; Mai et al. 2007; Kanamori et al. 2008; Bowd et al. 2007; Choi et al. 2008). A study by Aptel et al (2010) looked at the association of Cirrus OCT and GDx VCC in comparison to SAP; they also

found stronger structure-function associations with OCT than GDx when comparing to SAP. In the current study, r^2 values for log SAP, FDT, FDF and MDT for comparison with log OCT were 0.30, 0.49, 0.35 and 0.22, respectively; for comparison with GDx, the r^2 values were 0.21, 0.25, 0.41 and 0.19, respectively. Thus, the stronger global structure-function correlations for OCT were seen with SAP, FDT and MDT; for GDx, the stronger association was seen with FDF. This could be due to the fact that RNFL thickness as measured but the GDx is based on the birefringence of both RNFL axons and organelles from supporting structures. Thus, changes such as partial loss of supporting cell organelles or shrinkage of ganglion cells may alter the total birefringence of the RNFL before irreversible loss of axons occurs (Weber et al. 1998; Shou et al. 2003). Hence, changes in birefringence would be noted earlier than changes of axonal number. With this concept and the results from chapters 3 and 4 of this thesis which showed that FDF can detect damage earlier than the other perimetry techniques, it is not surprising that FDF showed stronger association with GDx whereas SAP, FDT and MDT were more strongly associated with OCT.

Sectorally, OCT showed the strongest association in the inferiotemporal RNFL sector with respect to all 4 visual field techniques. GDx showed greater association between superiotemporal RNFL and its corresponding visual field sector with respect to SAP, FDT and MDT; with FDF, the greatest association was seen in the superionasal sector. This analysis may be of limited value as the number of perimetric test locations that contribute to each ONH sector are quite different (Figure 2.2).

The absence of a perfect correlation between optic disc and visual field defects indicates that both structure and function measurements are essential in the diagnosis and management of glaucoma (Garway-Heath 2007; Airaksinen et al. 1985; Airaksinen & Drance 1985). The difference in strength of association as seen with the two structural imaging techniques confirms that each technique is measuring a different parameter of the RNFL and cannot be used interchangeably. SLP provides a good and objective method for RNFL thickness evaluation (Chen et al. 2009) as it has shown a good correlation with histological measurements (Blumenthal et al. 2009; Cohen et al. 2008). RNFL parameters as measured with GDx VCC present a weak to moderate correlation with SAP VF indices in patients with glaucoma (Lopez-Pena et al. 2010) and may be a useful tool in distinguishing between normal and glaucomatous eyes (Chen et al. 2007; Chen et al. 2009; Reus & Lemij 2004b; Da Pozzo et al. 2006). A recent study showed progression in RNFL retardance and function before loss of RNFL thickness and optic nerve axon counts in early experimental glaucoma in non-human primate models (Fortune et al. 2015).

Clinically, it is important to determine the structure-function relationship with currently available techniques that measure structural and functional deficits as the combination of these two modalities is used for assessing the severity and progression of glaucoma. The results of this preliminary study suggest that FDF and GDx used in combination are best to detect early glaucomatous changes.

6 Study of Repeatability After 1 year for SAP, FDT, FDF and MDT

6.1 Overview

Purpose: Preliminary study to determine which perimetry technique, SAP, FDT, FDF or MDT, is better able to detect repeatability after 1 year in early glaucoma.

Methods: 38 subjects with early glaucoma had perimetry testing with SAP, FDT, FDF and MDT on two separate visits, approximately 1 year apart. Pattern deviation probability maps were used to compare the threshold estimates. Ordinal scores of 0, 2 and 5 were assigned to PD values labeled as $p>0.05$, $p<0.05$ and $p<0.02$, respectively. Differences in ordinal scoring between the two visits with respect to each perimetry test were used to make comparisons amongst the techniques.

Results: FDF showed the greatest number of points with no change in ordinal scoring between visits, the majority of which were at $p<0.02$, i.e. had severe defect. With SAP, FDT and MDT, the majority of test locations which showed no progression were at the level of $p>0.05$, i.e. had earlier defect. More improvement was detected than progression in nearly all stages of disease severity with all techniques.

Conclusion: No one technique showed clear or better detection of disease progression. Further studies are required to determine which technique is best suited to monitor glaucomatous disease progression.

6.2 Introduction

Progressive glaucomatous loss of retinal ganglion cells causes characteristic optic nerve, RNFL and visual field abnormalities (Epstein 1997; Johnson 2009; Nicolela et al. 2001; Quigley 1993). Management of glaucoma requires the detection and monitoring of progression (Haymes et al. 2005; Vesti et al. 2003) which relies on the detection of a deteriorating structural and/or functional measurement. Early detection of glaucoma progression is just as important as early detection of the disease (Ansari et al. 2000) as progression of the disease can significantly impact visual function (Gupta & Weinreb 1997) and quality of life (Gutierrez et al. 1997; Parrish et al. 1997; Sherwood et al. 1998; Jampel et al. 2002; Nelson et al. 2003; Hyman et al. 2005). Automated perimeters along with standard thresholding algorithms (Anderson 1987) have improved our ability to quantify visual function and determine if visual function is deteriorating (Chauhan et al. 1990).

For progression to be detected on any instrument, measurement “noise” must be distinguished from change due to glaucoma (Strouthidis et al. 2006). Thus, detection of visual field progression depends on accuracy and reproducibility of threshold values at each visual field location tested (Artes et al. 2002).

The purpose of a visual field examination in glaucoma is to detect defects and determine the specific pattern of visual field loss for diagnostic purposes, and monitor

patients for evidence of visual function defect progression (Chauhan et al. 1990; Spry et al. 2001; Spry & Johnson 2002). The stimulus employed by SAP is non-selective for any particular ganglion cell subtype thus, SAP has shown to be a poor diagnostic test for patients with early glaucoma however, its performance improves (Spry et al. 2003) and variability increases (Harwerth et al. 2002; Weber & Rau 1992; Olsson et al. 1993; Wall et al. 1997; Chauhan et al. 1993; Henson et al. 1997) as sensitivity is reduced. For this reason, it is an ideal measure for glaucoma progression.

The key to managing a patient with glaucoma is to determine whether or not the patient's visual status has progressed (Johnson 2009); changes in visual field have been used to determine progression of glaucoma (AGIS 1994; Anderson et al. 1998; Gordon & Kass 1999; Leske et al. 1999; CGS Group 2006; Musch et al. 1999). Detecting progression on visual fields is dependent on the instruments' variability, the amount of change that is considered clinically significant and the number of follow-up examinations required to detect this change (Chauhan et al. 2008). Small amounts of clinically significant visual field change can be detected with a sufficient number of examinations and follow-up time (Heijl et al. 2003; Vesti et al. 2003). However, in everyday clinical practice, this may be difficult to achieve. Thus, more accurate and reliable techniques are needed for glaucoma management.

There is weak evidence supporting the notion that SWAP and FDT are more sensitive than SAP at detecting progression (Demirel & Johnson 2001; Haymes et al. 2005).

Several major glaucoma studies have looked at the progression of glaucoma but each uses different criteria to define it and the criteria used for one study may only be applicable to the study population of that particular study and not for the other. These differences in methodology give rise to difficulties in comparing the results of these studies to each other in addition to the absence of a gold standard (Nouri-Mahdavi et al. 1997; McNaught et al. 1996).

The purpose of this research was to conduct a preliminary study to determine which perimetry technique(s) is better able to detect event-based progression.

6.3 Methods

The recruitment criterion was as described in Chapter 2 in section 2.2. The study sample demographics are listed in Table 2.4. The procedures are explained in section 2.5.

6.4 Analysis

Because each visual field instrument uses a different scale to measure threshold values, pattern deviation probability plots were used to compare progression. Only values of $p>0.05$, $p<0.05$ and $p<0.02$ were used as this was limited to the values that were calculated by the MDT. Ordinal scores of 0, 2 and 5 were assigned to each of the

probability scores, respectively, an approach similar to that used to weight the Glaucoma Hemifield scores (Asman & Heijl 1992). Scores from Visit A and Visit B were compared to detect progression.

The difference between ordinal scores for each point was calculated to compare the average versus the difference of each point from Visit A to Visit B with respect the ordinal scores assigned. Because only one follow-up data set was available for this study, a point-by-point analysis was performed and change was defined based on event-analysis.

6.5 Results

According to the frequency histogram (Figure 6.1), FDF showed the greatest number of points with no change and FDT showed the least number of points with no change.

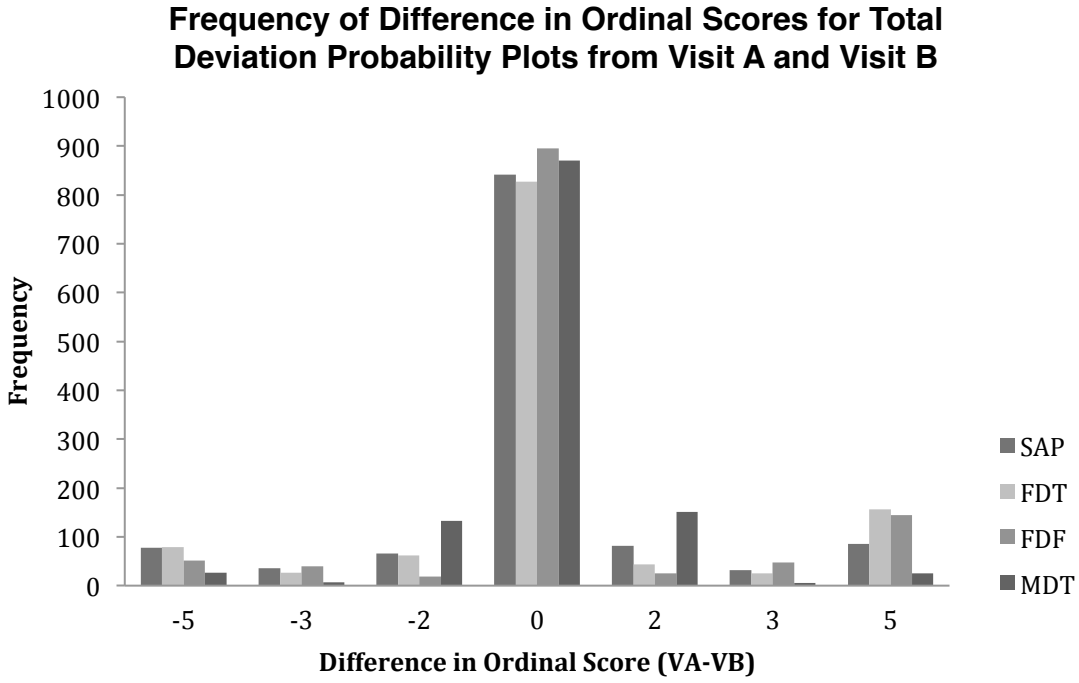

Figure 6.1: Frequency distribution of difference in ordinal score between Visit A and Visit B.

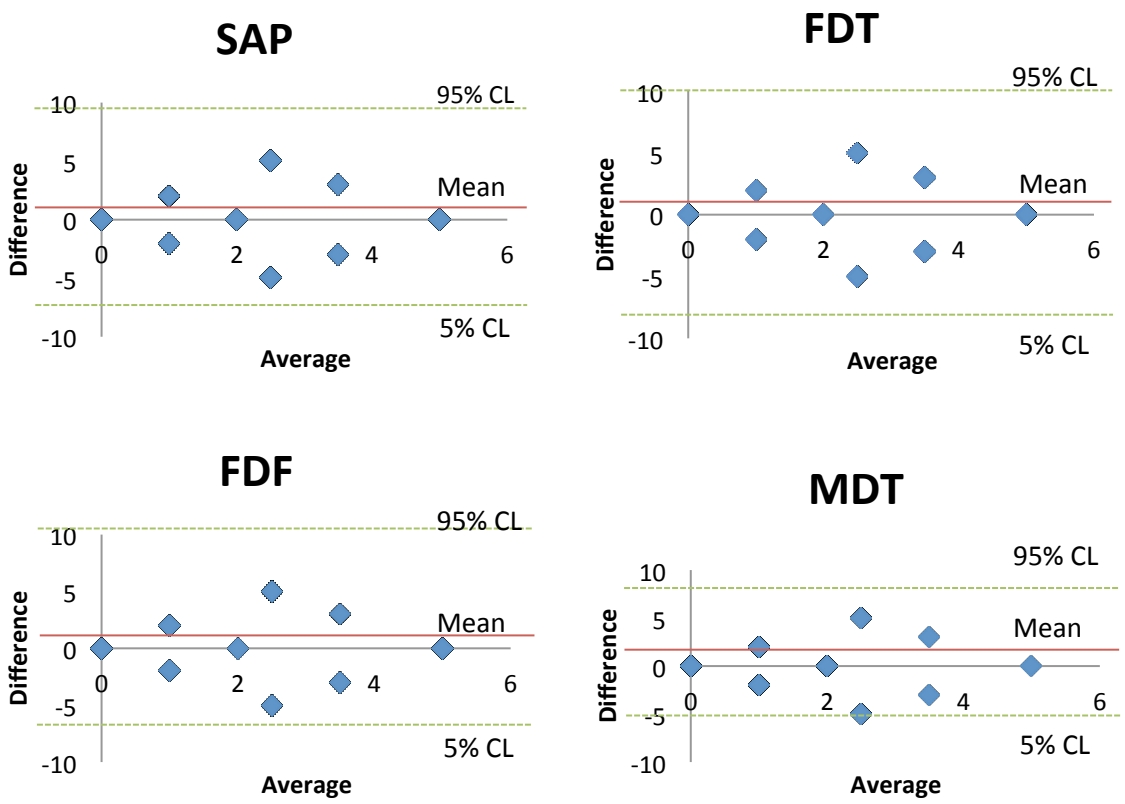

Figure 6.2: Bland-Altman plots for comparing ordinal scores from Visit A to Visit B.

Bland-Altman plots of visual field tests were done comparing Visit A to Visit B using the ordinal scoring system described above (Figure 6.2); this was performed using a point-by-point analysis. Table 6.2 illustrates that FDF showed the greatest number of test locations without change, in the most abnormal category, i.e. a difference of 0 but a severity score of 5 ($p<0.02$). The majority of the remaining three perimetry tests showed no progression in normal locations, i.e. a difference of 0 but a normal "severity" score of 0 ($p>0.05$). This tells us that FDF showed more abnormality at baseline, but similar

levels of stability over the one-year study period. MDT showed almost no change over the one-year study period, where as SAP was between the two.

Table 6.1: Total number of points showing the difference between Visit A and Visit B. The differences are categorized into 0, mild (±2), moderate (±3), and severe (±5) change.

	no change (0)	mild change (±2)	moderate change (±3)	severe change (±5)
SAP	841	148	66	161
FDT	827	106	49	234
FDF	895	42	85	194
MDT	870	284	11	51

Table 6.2: Showing the average of the two visits as a function of the differences defined in Table 6.1.

change	none			mild		moderate		severe	
	(0, 0)	**(2, 0)**	**(5, 0)**	**(1, 2)**	**(1, -2)**	**(3.5, 3)**	**(3.5, -3)**	**(2.5, 5)**	**(2.5, -5)**
SAP	636	18	187	82	66	32	34	86	75
FDT	620	25	182	44	62	24	25	156	78
FDF	211	13	671	24	18	47	38	144	50
MDT	680	186	4	151	133	5	6	25	26

(x, y) = (average, difference) as calculated from Visit A to Visit B.

6.6 Discussion

In glaucoma, quality of life is directly associated with the amount of the visual field damage (Gutierrez et al. 1997; Parrish et al. 1997; Sherwood et al. 1998; Jampel et al. 2002; Nelson et al. 2003; Hyman et al. 2005) and is therefore important to detect and monitor progression of this disease. Early detection of glaucomatous damage and its progression over time is one of the most important clinical challenges in glaucoma (Hood & Kardon 2007). It is crucial to determine which techniques can accurately diagnose and detect glaucomatous progression throughout the course of the disease.

Thus, when comparing tests over time, it is crucial to distinguish between change due to progression of the disease and change due to variability of the algorithm.

The majority of the test locations for all techniques showed no change in probability values from Visit A to Visit B. This was expected as the subjects were well controlled with their glaucoma treatment. When looking at the distribution with respect to severity of these test locations (Table 6.1), FDF showed the majority of its stable points classified as severe defect, whereas the majority of stable points from SAP, FDT and MDT were classified as near-normal. Thus, FDF is better at detecting defect earlier than the other perimetry tests and it can repeatedly detect this defect as time progresses; however, there is also a notable number of points that show "improvement" with the FDF with locations originally detected as severely depressed which is attributed to the variability of the technique.

FDT was the only technique that showed more points as progressing than improving in mild disease but more points as improving in severe disease. This should be kept in mind when looking for signs of disease progression with these techniques.

Overall, more improvement was detected than progression in nearly all stages of disease severity with all techniques except for mild changes with the FDT.

The results of this preliminary study suggest that FDF detects more defect than any other technique. What the study does not tell us is the technique that most accurately and precisely illustrates disease progression. We can conclude that FDF determines the most abnormality at baseline in patients with early glaucoma, and that MDT shows the

least abnormality and the greatest variability in early glaucoma defect. No one technique showed clear detection of disease progression. Factors such as too few ordinal scores, only one follow-up visit and only one year duration contribute to the limitations of this study. Further studies with longer follow-up periods and more frequent testing are required to determine whether either of these techniques are suitable for monitoring disease and determining progression. Detecting progression on visual fields is dependent on the instruments' variability, the amount of change that is considered clinically significant and the number of follow-up examinations required to detect this change (Chauhan et al. 2008). Theoretically, small amounts of clinically significant visual field change can be detected with a sufficient number of examinations and follow-up time (Heijl et al. 2003; Vesti et al. 2003). However, in everyday clinical practice, this may be difficult to achieve.

Progressive optic neuropathy is the hallmark of glaucoma (Fechtner & Lama 1999). Detection of visual field progression depends on accuracy and reproducibility of threshold values at each visual field location tested (Artes et al. 2002). Thus, accurately detecting glaucomatous change will be an asset to the diagnosis and management of this disease.

7 Discussion

One of the most important clinical challenges in glaucoma is the early detection of glaucomatous damage and its progression (Hood & Kardon 2007). It is crucial to determine which techniques can accurately diagnose and detect glaucomatous progression throughout the course of the disease. The aim of this thesis was just that: to determine which perimetry technique, SAP, FDT, FDF or MDT, is better able to detect early changes in glaucoma and whether or not visual function as measured by these techniques corresponds to measures of ONH and RNFL structure as determined by HRT, OCT and GDx.

The development of new perimetry techniques are aimed at selectively stimulating various properties of the retina which are lost in the early stages of glaucoma, before significant, irreversible impairment of vision. Repeatability of SAP, FDT, FDF and MDT were compared in patients with early stage glaucoma and controls. Test-retest variability was determined by comparing visual field indices and threshold estimates. Each patient was examined on two separate occasions with each of the four techniques.

Overall, both SAP and MDT showed similar trend in variability: it increased as sensitivity decreased. This is in agreement with previously published studies (Henson et al. 1997; Russell et al. 2012). FDT and FDF also showed a similar trend in variability: both had uniform variability throughout the dynamic range, with FDF having a narrower

95% confidence interval throughout. These findings were also in agreement with previously published studies (Heidelberg Edge Perimeter 2010; Artes, Hutchison, et al. 2005).

Global indices were used to compare the overall severity of each visual field test. MDT was not included in this analysis as it does not calculate MD or PSD. Overall, FDF showed the greatest amount of defect, and SAP showed the least. No significant difference was found in PSD of FDT and FDF, however, they show slightly greater localized reduction of sensitivity when compared to SAP. Frequency of differences between visits showed FDT as having the highest fraction of 0 dB difference. This is attributed to the fact that FDT has a smaller number of final threshold estimates compared to the other techniques (i.e. 15 vs 29 or 39). These findings suggest that SAP may not be suitable to detect or monitor functional damage caused by glaucoma in the early stages as readily as FDT and/or FDF.

The ability to detect change after one year was measured by comparing the pattern deviation probability maps from each of these instruments. Both FDF and FDT showed the same number of points with little or no change. SAP and MDT showed greater stability than either of the aforementioned techniques with MDT having almost no points with significant change. These results suggest that both FDT and FDF are equally capable of detecting changes in the early stages of the disease and MDT is unlikely to

provide any advantage in clinical performance when compared to SAP, FDT and FDF. FDF showed deeper defect at baseline.

Agreement between HRT and the perimetry tests were analyzed using both global and sectoral comparisons. The maps created by Garway-Heath (2000) were used to group the functional test locations to the six ONH sectors. Visual field sectors were then classified into WNL and ONL and compared to the Moorfields Regression Analysis classification of the HRT.

With all perimetry tests, the greatest agreement was seen in eyes that were classified as glaucomatous based on this study inclusion/exclusion criterion. In both the glaucoma and control group, global classifications of SAP, FDT and MDT showed similar agreement with HRT however, FDF showed the greatest agreement when HRT classified the ONH as ONL and least agreement when the ONH was classified as WNL. Thus, calculations of sensitivity and specificity showed FDT to have a significantly higher sensitivity and lower specificity than the remaining three perimetry tests which had their values in roughly the same range. Because no one perimetry test has ideal sensitivity and specificity, it is recommended that a combination of FDF with either SAP or FDT be used as the functional component in the diagnosis and management of patients with glaucoma.

The structure-function analysis was taken a step further by adding data from OCT and GDx VCC. Again, the data from both OCT and GDx VCC was recalculated to fit the 6-sector ONH map from the HRT. Initially, RNFL thickness comparisons were made between the two imaging techniques using regression analysis. The four perimetry tests were then compared to the OCT and GDx RNFL values.

Both imaging techniques showed the classic double-hump pattern with the normal anatomy of the RNFL. The measurements of the OCT were approximately 1.5 times thicker than that of the GDx in all 6 sectors; this was seen in previously published studies comparing these two instruments (Kim et al. 2011; Leung et al. 2005). The standard deviations from each sector increased in the same sectoral order for both instruments; inferionasal, superiotemporal, superionasal, inferiotemporal, nasal and temporal. Although both instruments have comparable ability to detect early glaucoma damage, the results are not interchangeable and progressive change should be monitored with only one instrument.

The strongest structure-function correlations for OCT were seen with SAP, FDT and MDT, and GDx with FDF. RNFL thickness as measured by the GDx is based on the birefringence of both RNFL axons and organelles from supporting structures; changes such as partial loss of supporting cell organelles or shrinkage of ganglion cells may alter the total birefringence of the RNFL before irreversible loss of axons occurs (Weber et al. 1998; Shou et al. 2003). Hence, changes in birefringence would be noted earlier than

changes of axonal number. With this concept and the results from test-retest analysis, it is not surprising that FDF showed stronger association with GDx whereas SAP, FDT and MDT were more strongly associated with OCT.

The results from this thesis suggest that both FDF and GDx be used in combination to detect changes in the early stages of glaucoma. SAP and FDT are likely better at monitoring change as the disease advances.

8 Limitations of the Study

Despite the fact that this study was carried through as precisely as possible, there were several limitations, most of which have to do with the data analysis. First of all, each instrument, whether functional or structural, has a normal database that is unique to it. This affects the indices and the probability calculations. For the functional tests, each technique uses a different dB scale, which makes direct comparisons of these techniques very difficult. The structural instruments each utilize a different property of light to measure thickness of the retina making direct comparisons of these data very difficult as well.

Second was the difference in test location co-ordinates amongst the functional and structural instruments of which data points had to be recalculated for any comparison to be made. Not all sectors overlap to the same number of data points and some sectors have a greater density of RGCs than others.

The data collected was only limited to patients with early glaucoma and controls thus, in areas where sectors of perimetry tests and/or structural tests were analyzed, there were far more sectors that were classified as WNL in comparison to ONL.

The change after one year data had a small sample size and only one follow-up visit.

References

Abe, R.Y. et al., 2015. Lamina Cribrosa in Glaucoma: Diagnosis and Monitoring. *Current ophthalmology reports*, 3(2), pp.74–84. Available at: http://www.ncbi.nlm.nih.gov/pubmed/26052477 [Accessed May 31, 2016].

Abe, R.Y. et al., 2016. The impact of location of progressive visual field loss on longitudinal changes in quality of life of patients with glaucoma. *Ophthalmology*, 123(3), pp.552–557. Available at: http://dx.doi.org/10.1016/j.ophtha.2015.10.046.

Airaksinen, P.J. et al., 1984. Diffuse and localized nerve fiber loss in glaucoma. *American journal of ophthalmology*, 98(5), pp.566–571.

Airaksinen, P.J. et al., 1985. Visual field and retinal nerve fiber layer comparisons in glaucoma. *Archives of ophthalmology*, 103(2), pp.205–207. Available at: http://www.ncbi.nlm.nih.gov/pubmed/3977691.

Airaksinen, P.J. & Alanko, H.I., 1983. Effect of retinal nerve fibre loss on the optic nerve head configuration in early glaucoma. *Graefe's Archive for Clinical and Experimental Ophthalmology*, 220(4), pp.193–196.

Airaksinen, P.J. & Drance, S.M., 1985. Neuroretinal rim area and retinal nerve fiber layer in glaucoma. *Archives of ophthalmology*, 103(2), pp.203–204. Available at: http://www.ncbi.nlm.nih.gov/pubmed/3977690.

Airaksinen, P.J. & Heijl, a, 1983. Visual field and retinal nerve fibre layer in early glaucoma after optic disc haemorrhage. *Acta ophthalmologica*, 61(2), pp.186–194.

Airaksinen, P.J. & Tuulonen, A., 1984. Early glaucoma changes in patients with and without an optic disc haemorrhage. *Acta Ophthalmol (Copenh)*, 62(2), pp.197–202. Available at: http://www.ncbi.nlm.nih.gov/pubmed/6720285.

Alencar, L.M. et al., 2010. A comparison of rates of change in neuroretinal rim area and retinal nerve fiber layer thickness in progressive glaucoma. *Investigative Ophthalmology and Visual Science*, 51(7), pp.3531–3539.

Alexander, L.J., 1991. Diagnosis and management of primary open-angle glaucoma. *Optom Clin*, 1, pp.19–102.

Allingham, R. et al., 2005. *Shield's Textbook of Glauocma* 5th ed., Lippincott Williams & Wilkins.

Almasieh, M. et al., 2012. The molecular basis of retinal ganglion cell death in glaucoma. *Progress in Retinal and Eye Research*, 31(2), pp.152–181.

Alward, W.L.M., 2000. Frequency doubling technology perimetry for the detection of glaucomatous visual filed loss. *American Journal of Ophthalmology*, 129(3), pp.376–378.

Anderson, A.J. & Johnson, C. a., 2002. Mechanisms isolated by frequency-doubling technology perimetry. *Investigative Ophthalmology & Visual Science*, 43, pp.398–401. Available at: http://www.ncbi.nlm.nih.gov/pubmed/11818383.

Anderson, D.R., 1987. *Perimetry: with and without automation* 2nd ed., St. Louis: CV Mosby, Co.

Anderson, D.R., Drance, S.M. & Schulzer, M., 1998. Comparison of glaucomatous progression between untreated patients with normal-tension glaucoma and patients with therapeutically reduced intraocular pressures. *American Journal of*

Ophthalmology, 126(4), pp.487–497.
Ansari, I. et al., 2000. Comparison of conventional and pattern discrimination perimetry in a prospective study of glaucoma patients. *Investigative Ophthalmology and Visual Science*, 41(13), pp.4150–4157.
Anton, A. et al., 2007. Usefulness of optical coherence tomography parameters of the optic disc and the retinal nerve fiber layer to differentiate glaucomatous, ocular hypertensive, and normal eyes. *J Glaucoma*, 16(1), pp.1–8.
Aptel, F. et al., 2010. Structure-Function Relationships Using Spectral-Domain Optical Coherence Tomography: Comparison With Scanning Laser Polarimetry. *American Journal of Ophthalmology*, 150(6), pp.825–833. Available at: <Go to ISI>://000285367900009.
Aref, B.A.A., 2013. Measuring Macular Thickness in Glaucoma. , (april), pp.28–30.
Artes, P.H., 2008. Progression: things we need to remember but often forget to think about. *Optometry and vision science : official publication of the American Academy of Optometry*, 85(6), pp.380–5. Available at: http://www.ncbi.nlm.nih.gov/pubmed/18521009.
Artes, P.H. et al., 2002. Properties of perimetric threshold estimates from full threshold, SITA standard, and SITA fast strategies. *Investigative Ophthalmology and Visual Science*, 43(8), pp.2654–2659.
Artes, P.H. et al., 2011. Properties of the Statpac visual field index. *Investigative Ophthalmology and Visual Science*, 52(7), pp.4030–4038.
Artes, P.H., Hutchison, D.M., et al., 2005. Threshold and variability properties of matrix frequency-doubling technology and standard automated perimetry in glaucoma. *Investigative Ophthalmology and Visual Science*, 46(7), pp.2451–2457.
Artes, P.H., Nicolela, M.T., et al., 2005. Visual field progression in glaucoma: Total versus pattern deviation analyses. *Investigative Ophthalmology and Visual Science*, 46(12), pp.4600–4606.
Artes, P.H. & Chauhan, B.C., 2005a. Longitudinal changes in the visual field and optic disc in glaucoma. *Progress in Retinal and Eye Research*, 24(3), pp.333–354.
Artes, P.H. & Chauhan, B.C., 2005b. Longitudinal changes in the visual field and optic disc in glaucoma. *Progress in Retinal and Eye Research*, 24(3), pp.333–354.
Asman, P. & Heijl, A., 1992. Glaucoma Hemifield Test. Automated visual field evaluation. *Archives of ophthalmology*, 110(6), pp.812–9.
Asrani, S. et al., 2003. Correlation among retinal thickness, optic disc, and visual field in glaucoma patients and suspects: a pilot study. *Journal of glaucoma*, 12(2), pp.119–28. Available at: http://www.ncbi.nlm.nih.gov/pubmed/12671466.
AW, D. & Bailey, E., 1993. Assessment of the retinal nerve fiber layer by scanning-laser polarimetry. *SPIE*, (266–271).
Baez, K.A. et al., 1995. Motion detection threshold and field progression in normal tension glaucoma. *The British journal of ophthalmology*, 79(2), pp.125–128. Available at: http://www.ncbi.nlm.nih.gov/pubmed/7696230.
Bagga, H. et al., 2003. Scanning laser polarimetry with variable corneal compensation and optical coherence tomography in normal and glaucomatous eyes. *American Journal of Ophthalmology*, 135(4), pp.521–529.

Bagga, H., Greenfield, D.S. & Feuer, W.J., 2005. Quantitative assessment of atypical birefringence images using scanning laser polarimetry with variable corneal compensation. *American Journal of Ophthalmology*, 139(3), pp.437–446.

Balazsi, A.G. et al., 1984. The effect of age on the nerve fiber population of the human optic nerve. *Am J Ophthalmol*, 97(6), pp.760–6. Available at: http://www.ncbi.nlm.nih.gov/pubmed/6731540.

Banegas, S.A. et al., 2016. Evaluation of the Retinal Nerve Fiber Layer Thickness, the Mean Deviation, and the Visual Field Index in Progressive Glaucoma. *Journal of glaucoma*, 25(3), pp.e229-35. Available at: http://www.ncbi.nlm.nih.gov/pubmed/26020689 [Accessed June 29, 2016].

Bartz-Schmidt, K.U. et al., 1999. Quantitative morphologic and functional evaluation of the optic nerve head in chronic open-angle glaucoma. *Survey of Ophthalmology*, 44(2 SUPPL. 1).

Bartz-Schmidt, K.U. & Weber, J., 1993. Comparison of spatial thresholds and intensity thresholds in glaucoma. *International Ophthalmology*, 17(4), pp.171–178.

Bathija, R. et al., 1998. Detection of early glaucomatous structural damage with confocal scanning laser tomography. *Journal of Glaucoma*, 7, pp.121–127.

Bayer, A.U. & Erb, C., 2002. Short wavelength automated perimetry, frequency doubling technology perimetry, and pattern electroretinography for prediction of progressive glaucomatous standard visual field defects. *Ophthalmology*, 109(5), pp.1009–1017.

Bebie, H., Fankhauser, F. & Spahr, J., 1976. Static perimetry: accuracy and fluctuations. *Acta Ophthalmologica*, 54(3), pp.339–348.

Beck, R.W. et al., 1985. Is there a racial difference in physiologic cup size? *Ophthalmology*, 92(7), pp.873–6. Available at: http://www.ncbi.nlm.nih.gov/pubmed/4022570.

Bengtsson, B., Olsson, J., et al., 1997. A new generation of algorithms for computerized threshold perimetry, SITA. *Acta ophthalmologica Scandinavica*, 75(4), pp.368–375.

Bengtsson, B., 1990. Optic disc haemorrhages preceding manifest glaucoma. *Acta ophthalmologica*, 68(4), pp.450–454.

Bengtsson, B., Lindgren, A., et al., 1997. Perimetric probability maps to separate change caused by glaucoma from that caused by cataract. *Acta ophthalmologica Scandinavica*, 75, pp.184–188.

Bengtsson, B., 2000. Reliability of computerized perimetric threshold tests as assessed by reliability indices and threshold reproducibility in patients with suspect and manifest glaucoma. *Acta Ophthalmologica Scandinavica*, 78(5), pp.519–522. Available at: http://www.scopus.com/inward/record.url?eid=2-s2.0-0033828907&partnerID=tZOtx3y1\nhttp://onlinelibrary.wiley.com/store/10.1034/j.1600-0420.2000.078005519.x/asset/j.1600-0420.2000.078005519.x.pdf?v=1&t=i1c8flkq&s=e4b1e055134289b92d4f60499899b7e41f0f4ebc\nh.

Bengtsson, B., 1976. The variation and covariation of cup and disc diameters. *Acta ophthalmologica*, 54, pp.804–818.

Bengtsson, B. & Heijl, A., 2008. A Visual Field Index for Calculation of Glaucoma Rate of Progression. *American Journal of Ophthalmology*, 145(2), pp.343–353.

Bengtsson, B., Heijl, a & Olsson, J., 1998. Evaluation of a new threshold visual field strategy, SITA, in normal subjects. Swedish Interactive Thresholding Algorithm. *Acta ophthalmologica Scandinavica*, 76(2), pp.165–169.

Bengtsson, B., Patella, V.M. & Heijl, A., 2009. Prediction of glaucomatous visual field loss by extrapolation of linear trends. *Archives of ophthalmology (Chicago, Ill.: 1960)*, 127(12), pp.1610–5. Available at: http://www.ncbi.nlm.nih.gov/pubmed/20008716 [Accessed June 29, 2016].

Bergin, C. et al., 2011. The effect of induced intraocular straylight on perimetric tests. *Investigative Ophthalmology and Visual Science*, 52(6), pp.3676–3682.

Bernhard, J., Lachenmayer, P. & Vivell, P.M., 1993. *Perimetry and its clinical correlation*, New York: Thieme Medical Publishers, Inc.. New York.

Bickler-Bluth, M. et al., 1989. Assessing the utility of reliability indices for automated visual fields. Testing ocular hypertensives. *Ophthalmology*, 96(5), pp.616–619. Available at: http://www.ncbi.nlm.nih.gov/pubmed/2748118.

Blumenthal, E.Z. et al., 2000. Reproducibility of nerve fiber layer thickness measurements by use of optical coherence tomography. *Ophthalmology*, 107(12), pp.2278–2282.

Blumenthal, E.Z. et al., 2009. Retinal nerve fibre layer imaging compared with histological measurements in a human eye. *Eye (London, England)*, 23(1), pp.171–5. Available at: http://www.ncbi.nlm.nih.gov/pubmed/17721504.

de Boer, R.W. et al., 1982. Concepts for automatic perimetry, as applied to the Scoperimeter, an experimental automatic perimeter. *International Ophthalmology*, 5(3), pp.181–191.

Bosworth, C.F., Sample, P.A. & Weinreb, R.N., 1997. Motion perception thresholds in areas of glaucomatous visual field loss. *Vision Research*, 37(3), pp.355–364.

Bowd, C. et al., 2001. Detecting early glaucoma by assessment of retinal nerve fiber layer thickness and visual function. *Investigative Ophthalmology and Visual Science*, 42(9), pp.1993–2003.

Bowd, C. et al., 2006. Structure-function relationships using confocal scanning laser ophthalmoscopy, optical coherence tomography, and scanning laser polarimetry. *Investigative Ophthalmology & Visual Science*, 47(7), pp.2889–2895. Available at: <Go to ISI>://000238688600022.

Brandt, J.D., 2004. Corneal thickness in glaucoma screening, diagnosis, and management. *Current opinion in ophthalmology*, 15(2), pp.85–89.

Brenton, R.S. & Argus, W.A., 1987. Fluctuations on the Humphrey and Octopus perimeters. *Investigative Ophthalmology and Visual Science*, 28(5), pp.767–771.

Breton, M. & Drum, B., 1989. Functional testing in glaucoma: visual psychophysics and electropphysiology. In *The Glaucomas*. St. Louis: CV Mosby, Co., pp. 179–197.

Breusegem, C. et al., 2011. Agreement and accuracy of non-expert ophthalmologists in assessing glaucomatous changes in serial stereo optic disc photographs. *Ophthalmology*, 118(4), pp.742–746.

Brigatti, L. & Caprioli, J., 1995. Correlation of visual field with scanning confocal laser optic disc measurements in glaucoma. *Archives of ophthalmology (Chicago, Ill.: 1960)*, 113(9), pp.1191–4. Available at:

http://www.ncbi.nlm.nih.gov/pubmed/7661755.
Budenz, D.L. et al., 2002. Comparison of glaucomatous visual field defects using standard full threshold and Swedish interactive threshold algorithms. *Archives of ophthalmology*, 120(9), pp.1136–41. Available at: http://www.ncbi.nlm.nih.gov/pubmed/12215086.
Bullimore, M.A., Wood, J.M. & Swenson, K., 1993. Motion perception in glaucoma. *Investigative Ophthalmology and Visual Science*, 34(13), pp.3526–3533.
Burgoyne, C.F., 2011. A biomechanical paradigm for axonal insult within the optic nerve head in aging and glaucoma. *Experimental Eye Research*, 93(2), pp.120–132.
Burgoyne, C.F., 2004. Image analysis of optic nerve disease. *Eye (London, England)*, 18(11), pp.1207–13. Available at: http://www.ncbi.nlm.nih.gov/pubmed/15534606.
Caprioli, J., 1989. Correlation of visual function with optic nerve and nerve fiber layer structure in glaucoma. *Survey of ophthalmology*, 33 Suppl, pp.319–330.
Caprioli, J., Sears, M. & Miller, J.M., 1987. Patterns of early visual field loss in open-angle glaucoma. *American journal of ophthalmology*, 103(4), pp.512–517. Available at: http://www.ncbi.nlm.nih.gov/pubmed/3565511.
Carkeet, A., 2015. Comment on: statistical methods for conducting agreement (comparison of clinical tests) and precision (repeatability or reproducibility) studies in optometry and ophthalmology. *Ophthalmic and Physiological Optics*, 35, pp.345–346.
Carpineto, P. et al., 2003. Reliability of nerve fiber layer thickness measurements using optical coherence tomography in normal and glaucomatous eyes. *Ophthalmology*, 110(1), pp.190–195.
Cello, K.E., Nelson-Quigg, J.M. & Johnson, C.A., 2000. Frequency doubling technology perimetry for detection of glaucomatous visual field loss. *American Journal of Ophthalmology*, 129(3), pp.314–322.
Chandra, A., Bandyopadhyay, A.K. & Bhaduri, G., 2013. A comparative study of two methods of optic disc evaluation in patients of glaucoma. *Oman journal of ophthalmology*, 6(2), pp.103–7. Available at: http://www.pubmedcentral.nih.gov/articlerender.fcgi?artid=3779406&tool=pmcentrez&rendertype=abstract.
Chang, R. & Budenz, D.L., 2008. New developments in optical coherence tomography for glaucoma. *Current opinion in ophthalmology*, 19(2), pp.127–135.
Chauhan, B.C. et al., 1993. Characteristics of frequency-of-seeing curves in normal subjects, patients with suspected glaucoma, and patients with glaucoma. *Investigative ophthalmology & visual science*, 34(13), pp.3534–3540.
Chauhan, B.C. et al., 2001. Optic disc and visual field changes in a prospective longitudinal study of patients with glaucoma: comparison of scanning laser tomography with conventional perimetry and optic disc photography. *Archives of ophthalmology*, 119, pp.1492–1499.
Chauhan, B.C. et al., 2008. Practical recommendations for measuring rates of visual field change in glaucoma. *The British journal of ophthalmology*, 92(4), pp.569–73. Available at: http://bjo.bmj.com/content/92/4/569.abstract.
Chauhan, B.C. et al., 2000. Technique for detecting serial topographic changes in the

optic disc and peripapillary retina using scanning laser tomography. *Investigative Ophthalmology and Visual Science*, 41(3), pp.775–782.
Chauhan, B.C. et al., 1994. Test-retest variability of topographic measurements with confocal scanning laser tomography in patients with glaucoma and control subjects. *American journal of ophthalmology*, 118(1), pp.9–15.
Chauhan, B.C., Drance, S.M. & Douglas, G.R., 1990. The use of visual field indices in detecting changes in the visual field in glaucoma. *Investigative ophthalmology & visual science*, 31(3), pp.512–520.
Chauhan, B.C. & Johnson, C.A., 1999. Test-retest variability of frequency-doubling perimetry and conventional perimetry in glaucoma patients and normal subjects. *Investigative Ophthalmology and Visual Science*, 40(3), pp.648–656.
Chen, H.-Y., Huang, M.-L. & Huang, W.-C., 2009. Evaluating Glaucomatous Retinal Nerve Fiber Damage by GDx VCC Polarimetry in Taiwan Chinese Population. *Journal of Optometry*, 2(4), pp.197–206. Available at: http://linkinghub.elsevier.com/retrieve/pii/S1888429609700470.
Chi, T. et al., 1989. Racial differences in optic nerve head parameters. *Archives of ophthalmology*, 107(6), pp.836–9. Available at: http://www.ncbi.nlm.nih.gov/pubmed/24160971.
Choplin, N., 2007. Psychological and elctrophysiological testing in glaucoma: visual fields and other functional tests. In *Atlas of Glaucoma*. Informa Healthcare.
Choplin, N.T., Zhou, Q. & Knighton, R.W., 2003. Effect of individualized compensation for anterior segment birefringence on retinal nerve fiber layer assessments as determined by scanning laser polarimetry. *Ophthalmology*, 110(4), pp.719–725.
Cohen, M.J. et al., 2008. Morphometric analysis of human peripapillary retinal nerve fiber layer thickness. *Investigative ophthalmology & visual science*, 49(3), pp.941–4. Available at: http://www.ncbi.nlm.nih.gov/pubmed/18326716.
Coops, A. et al., 2006. Automated analysis of Heidelberg retina tomograph optic disc images by glaucoma probability score. *Investigative Ophthalmology and Visual Science*, 47(12), pp.5348–5355.
Dandona, L., Hendrickson, A. & Quigley, H.A., 1991. Selective effects of experimental glaucoma on axonal transport by retinal ganglion cells to the dorsal lateral geniculate nucleus. *Invest Ophthalmol Vis Sci*, 32(5), pp.1593–1599. Available at: http://www.ncbi.nlm.nih.gov/entrez/query.fcgi?cmd=Retrieve&db=PubMed&dopt=Citation&list_uids=1707861.
DeLeón Ortega, J.E. et al., 2007. Effect of glaucomatous damage on repeatability of confocal scanning laser ophthalmoscope, scanning laser polarimetry, and optical coherence tomography. *Investigative Ophthalmology and Visual Science*, 48(3), pp.1156–1163.
Delgado, M.F. et al., 2002. Automated perimetry: A report by the American Academy of Ophthalmology. *Ophthalmology*, 109(12), pp.2362–2374.
Demirel, S. & Johnson, C.A., 2001. Incidence and prevalence of short wavelength automated perimetry deficits in ocular hypertensive patients. *American Journal of Ophthalmology*, 131(6), pp.709–715.
Dichtl, A., Jonas, J.B. & Naumann, G.O., 1999. Retinal nerve fiber layer thickness in

human eyes. *Graefes Arch Clin Exp Ophthalmol*, 237(6), pp.474–479. Available at: http://www.ncbi.nlm.nih.gov/pubmed/10379607\nhttp://www.springerlink.com/content/ju7um5kpmpwh4vxa/fulltext.pdf.
Diehl, D.L. et al., 1990. Prevalence and significance of optic disc hemorrhage in a longitudinal study of glaucoma. *Archives of ophthalmology*, 108(4), pp.545–550. Available at: http://www.ncbi.nlm.nih.gov/pubmed/2322157.
Drance, S., 1975. Doyne Memorial Lecture: correlation of optic nerve and visual field defect in simple glaucoma. *Trasactions of the Ophthalmological Society of the United Kingdom*, 95, pp.288–296.
Drance, S., 1974. The optic disc and visual field in glaucoma. *Canadian Journal of Ophthalmology*, 9, pp.389–390.
Drance, S. & Anderson, D., 1985. *Automatic Perimetry in Glaucoma: A Practical Guide*, Grune & Stratton, Inc.
Drance, S.M. et al., 1986. The correlation of functional and structural measurements in glaucoma patients and normal subjects. *American journal of ophthalmology*, 102(5), pp.612–616. Available at: http://www.ncbi.nlm.nih.gov/pubmed/3777081.
Drance, S.M., 1985. The early structural and functional disturbances of chronic open-angle glaucoma. Robert N. Shaffer lecture. *Ophthalmology*, 92(7), pp.853–857. Available at: http://www.ncbi.nlm.nih.gov/pubmed/4022568.
Drance, S.M. et al., 1977. The importance of disc hemorrhage in the prognosis of chronic open angle glaucoma. *Archives of ophthalmology*, 95(2), pp.226–228.
Drexler, W. et al., 2003. Enhanced visualization of macular pathology with the use of ultrahigh-resolution optical coherence tomography. *Archives of ophthalmology*, 121(5), pp.695–706.
Drexler, W. et al., 1999. In vivo ultrahigh-resolution optical coherence tomography. *Optics letters*, 24(17), pp.1221–1223.
Duke-Elder, W., 1941. Diseases of the inner eye. Anomalies of the intraocular pressure. In *Textbook of Ophthalmology*. St. Louis: Mosby.
Eid, T.M. et al., 1997. Quantitative estimation of retinal nerve fiber layer height in glaucoma and the relationship with optic nerve head topography and visual field. *Journal of glaucoma*, 6(4), pp.221–230. Available at: http://www.ncbi.nlm.nih.gov/pubmed/9264301.
Emdadi, a et al., 1998. Patterns of optic disk damage in patients with early focal visual field loss. *American journal of ophthalmology*, 126(6), pp.763–771.
Epstein, D., 1997. Primary open-angle glaucoma. In D. Epstein, R. Allingham, & J. Schuman, eds. *Chandler and Grant's Glaucoma*. Williams & Wilkins, pp. 183–189.
Ernest, P.J.G. et al., 2016. Prediction of Glaucomatous Visual Field Progression Using Baseline Clinical Data. *Journal of glaucoma*, 25(2), pp.228–235. Available at: http://www.ncbi.nlm.nih.gov/pubmed/25265001.
European Glaucoma Society, 2008. *Terminology and Guidelines for Glaucoma* 3rd Editio., Savona, Italy.
Faridi, O. et al., 2014. Effect of focal lamina cribrosa defect on glaucomatous visual field progression. *Ophthalmology*, 121(8), pp.1524–1530.
Fechtner, R., Dreher, A. & Weinreb, R., 1993. The laser scanning ophthalmoscope. In

R. Varma & G. Speath, eds. *The optic nerve in glaucoma*. Philadelphia: JB Lippincott, pp. 269–276.
Fechtner, R.D. & Lama, P., 1999. Advances in optic nerve head analysis in glaucoma. [Review] [43 refs]. *Seminars in ophthalmology*, 14(3), pp.180–188.
Ferreras, A. et al., 2007. Diagnostic Ability of Heidelberg Retina Tomograph 3 Classifications. Glaucoma Probability Score versus Moorfields Regression Analysis. *Ophthalmology*, 114(11), pp.525–532.
Fingeret, M., Medeiros, F.A., et al., 2005. Five rules to evaluate the optic disc and retinal nerve fiber layer for glaucoma. *Optometry*, 76(11), pp.661–668.
Fingeret, M., Flanagan, J.G. & Liebmann, J.M., 2005. *The Essential HRT Primer*, San Ramon: Jocoto Advertising.
Fitzke, F. et al., 1989. Peripheral displacement thresholds in glaucoma and ocular hypertension. In A. Heijl, ed. *Perimetry Update*. The Hague, The Netherlands: Kugler & Ghedini, pp. 399–405.
Fitzke, F.W. et al., 1996. Analysis of visual field progression in glaucoma. *Investigative Ophthalmology and Visual Science*, 80, pp.40–48.
Fitzke, F.W. et al., 1987. Peripheral displacement thresholds in normals, ocular hypertensives and glaucoma. In E. Greve & A. Heijl, eds. *Perimetry Update*. The Hague, The Netherlands: Kugler & Ghedini, pp. 447–452.
Flammer, J., 1985. Fluctuations in the visual field. In S. M. Drance & D. R. Anderson, eds. *Automated Perimetry in Glaucoma*. Orlando, FL: Grune & Stratton, Inc., pp. 161–173.
Flammer, J. et al., 1985. Quantification of glaucomatous visual field defects with automated perimetry. *Investigative Ophthalmology and Visual Science*, 26(2), pp.176–181.
Flammer, J., Drance, S. & Zulauf, M., 1984. Differential light threshold. Short- and long-term fluctuation in patients with glaucoma, normal controls, and patients with suspected glaucoma. *Arch Ophthalmol*, 102(5), pp.704–6.
Flanagan, J. et al., 1994. The phantom contour illusion letter test: A new psychophysical test for glaucoma? In *Perimetry Update*.
Flanagan, J.G., Wild, J.M. & Trope, G.E., 1993. The visual field indices in primary open-angle glaucoma. *Investigative ophthalmology & visual science*, 34(7), pp.2266–2274. Available at: http://www.ncbi.nlm.nih.gov/pubmed/8505208.
Ford, B.A. et al., 2003. Comparison of data analysis tools for detection of glaucoma with the Heidelberg retina tomograph. *Ophthalmology*, 110(6), pp.1145–1150.
Forte, R. et al., 2009. Comparison of time domain Stratus OCT and spectral domain SLO/OCT for assessment of macular thickness and volume. *Eye (London, England)*, 23(11), pp.2071–2078. Available at: http://www.ncbi.nlm.nih.gov/pubmed/19079147.
Fortune, B. et al., 2012. Structural and functional abnormalities of retinal ganglion cells measured in vivo at the onset of optic nerve head surface change in experimental glaucoma. *Investigative ophthalmology & visual science*, 53(7), pp.3939–50. Available at: http://www.ncbi.nlm.nih.gov/pubmed/22589428\nhttp://www.iovs.org/content/53/7/3

939.short.
FrisÉn, L., 1993. High-pass resolution perimetry - A clinical review. *Documenta Ophthalmologica*, 83(1), pp.1–25.
Gandolfi, S.A. et al., 2005. Improvement of spatial contrast sensitivity threshold after surgical reduction of intraocular pressure in unilateral high-tension glaucoma. *Investigative Ophthalmology and Visual Science*, 46(1), pp.197–201.
Garcia-Valenzuela, E. et al., 1995. Programmed cell death of retinal ganglion cells during experimental glaucoma. *Experimental Eye Research*, 61(1), pp.33–44.
Gardiner, S.K., Johnson, C.A. & Cioffi, G.A., 2005. Evaluation of the structure-function relationship in glaucoma. *Investigative Ophthalmology and Visual Science*, 46(10), pp.3712–3717.
Garway-Heath, D.F., 2007. Correlation of visual changes with disc morphology. *Eye*, 21, pp.S29–S33.
Garway-Heath, D.F., Poinoosawmy, D., et al., 2000. Mapping the visual field to the optic disc in normal tension glaucoma eyes. *Ophthalmology*, 107(10), pp.1809–1815.
Garway-Heath, D.F. et al., 2002. Relationship between electrophysiological, psychophysical, and anatomical measurements in glaucoma. *Investigative Ophthalmology and Visual Science*, 43(7), pp.2213–2220.
Garway-Heath, D.F., Caprioli, J., et al., 2000. Scaling the hill of vision: The physiological relationship between light sensitivity and ganglion cell numbers. *Investigative Ophthalmology and Visual Science*, 41(7), pp.1774–1782.
GDX VCC Primer, 2004. *Retinal Nerve Fiber Laser Analysis with GDx VCC: A Primer and Clinical Guide*, Laser Diagnostic Technologies, Inc.
Giraud, J.M. et al., 2010. [Analysis of a new visual field index, the VFI, in Ocular Hypertension and Glaucoma]. *Journal français d'ophtalmologie*, 33(1), pp.2–9. Available at: http://www.ncbi.nlm.nih.gov/pubmed/20005005.
Glaucoma, C. & Group, S., 2006. Canadian Glaucoma Study: 1. Study design, baseline characteristics, and preliminary analyses. *Canadian journal of ophthalmology. Journal canadien d'ophtalmologie*, 41(5), pp.566–75. Available at: http://www.ncbi.nlm.nih.gov/pubmed/17016527.
Glovinsky, Y., Quigley, H., et al., 1991. Large ganglion cells are selectively damaged in experimental glaucoma. *Investigative ophthalmology & visual science*, 32.
Glovinsky, Y., Quigley, H. a & Dunkelberger, G.R., 1991. Retinal ganglion cell loss is size dependent in experimental glaucoma. *Investigative ophthalmology & visual science*, 32(3), pp.484–91. Available at: http://www.ncbi.nlm.nih.gov/pubmed/2001923.
Gordon, M.O. & Kass, M. a, 1999. The Ocular Hypertension Treatment Study: design and baseline description of the participants. *Arch Ophthalmol*, 117(May 1999), pp.573–583.
Greaney, M.J. et al., 2002. Comparison of optic nerve imaging methods to distinguish normal eyes from those with glaucoma. *Investigative Ophthalmology and Visual Science*, 43(1), pp.140–145.
Greenfield, D.S. et al., 2002. Correction for corneal polarization axis improves the discriminating power of scanning laser polarimetry. *American Journal of*

Ophthalmology, 134(1), pp.27–33.
Greenfield, D.S., Knighton, R.W., et al., 2003. Normative retardation data corrected for the corneal polarization axis with scanning laser polarimetry. *Ophthalmic surgery, lasers & imaging : the official journal of the International Society for Imaging in the Eye*, 34(2), pp.165–171. Available at: http://www.ncbi.nlm.nih.gov/pubmed/12665235.
Greenfield, D.S., 2002. Optic nerve and retinal nerve fiber layer analyzers in glaucoma. *Current opinion in ophthalmology*, 13(2), pp.68–76. Available at: http://www.ncbi.nlm.nih.gov/pubmed/11880718.
Greenfield, D.S., Bagga, H. & Knighton, R.W., 2003. Macular thickness changes in glaucomatous optic neuropathy detected using optical coherence tomography. *Archives of ophthalmology*, 121(1), pp.41–46.
Greenfield, D.S. & Weinreb, R.N., 2008. Role of Optic Nerve Imaging in Glaucoma Clinical Practice and Clinical Trials. *American Journal of Ophthalmology*, 145(4).
Grillo, L.M. et al., 2016. The 24-2 Visual Field Test Misses Central Macular Damage Confirmed by the 10-2 Visual Field Test and Optical Coherence Tomography. *Translational vision science & technology*, 5(2), p.15. Available at: http://www.ncbi.nlm.nih.gov/pubmed/27134774\nhttp://www.pubmedcentral.nih.gov/articlerender.fcgi?artid=PMC4849532.
Guedes, V. et al., 2003. Optical coherence tomography measurement of macular and nerve fiber layer thickness in normal and glaucomatous human eyes. *Ophthalmology*, 110(1), pp.177–189.
Gupta, D. & Chen, P., 2016. Glaucoma. *American Family Physician*, 93(8), pp.668–674.
Gupta, N. & Weinreb, R.N., 1997. New definitions of glaucoma. *Current opinion in ophthalmology*, 8(2), pp.38–41.
Gutierrez, P. et al., 1997. Influence of glaucomatous visual field loss on health-related quality of life. *Archives of ophthalmology*, 115(6), pp.777–84. Available at: http://www.ncbi.nlm.nih.gov/pubmed/9194730.
Hart, W.M. et al., 1990. Glaucomatous visual field damage. Luminance and color-contrast sensitivities. *Investigative Ophthalmology and Visual Science*, 31(2), pp.359–367.
Hart, W.M. et al., 1978. Quantitative visual field and optic disc correlates early in glaucoma. *Archives of ophthalmology*, 96(12), pp.2209–2211. Available at: http://www.ncbi.nlm.nih.gov/pubmed/718511.
Harwerth, R.S., 2008. Charles F. Prentice Award Lecture 2006: a neuron doctrine for glaucoma. *Optometry and vision science : official publication of the American Academy of Optometry*, 85(6), pp.436–44. Available at: http://www.ncbi.nlm.nih.gov/pubmed/18521013.
Harwerth, R.S. et al., 1999. Ganglion cell losses underlying visual field defects from experimental glaucoma. *Investigative Ophthalmology and Visual Science*, 40(10), pp.2242–2250.
Harwerth, R.S. et al., 2004. Neural losses correlated with visual losses in clinical perimetry. *Investigative Ophthalmology and Visual Science*, 45(9), pp.3152–3160.
Harwerth, R.S. et al., 2005. Scaling the structure-function relationship for clinical

perimetry. *Acta Ophthalmologica Scandinavica*, 83(4), pp.448–455.
Harwerth, R.S. et al., 2005. Scaling the structure – function relationship for clinical perimetry. *Acta Ophthalmologica*, pp.448–455.
Harwerth, R.S. et al., 2007. The relationship between nerve fiber layer and perimetry measurements. *Investigative Ophthalmology and Visual Science*, 48(2), pp.763–773.
Harwerth, R.S. et al., 2002. *Visual field defects and neural losses from experimental glaucoma*,
Harwerth, R.S. & Quigley, H.A., 2010. Visual Field Defects and Retinal Ganglion Cell Losses in Patients With Glaucoma. , 124(June 2006).
Harwerth, R.S. & Quigley, H. a, 2006. Visual field defects and retinal ganglion cell losses in patients with glaucoma. *Archives of ophthalmology*, 124(June 2006), pp.853–859.
Hasler, S. & Stürmer, J., 2012. [First experience with the Heidelberg Edge Perimeter® on patients with ocular hypertension and preperimetric glaucoma]. *Klinische Monatsblätter für Augenheilkunde*, 229(4), pp.319–22. Available at: http://www.ncbi.nlm.nih.gov/pubmed/22495996 [Accessed June 29, 2016].
Haymes, S.A. et al., 2005. Glaucomatous visual field progression with frequency-doubling technology and standard automated perimetry in a longitudinal prospective study. *Investigative Ophthalmology and Visual Science*, 46(2), pp.547–554.
Hee, M.R. et al., 1995. Optical coherence tomography of the human retina. *Archives of ophthalmology*, 113(3), pp.325–32. Available at: http://www.ncbi.nlm.nih.gov/pubmed/7887846.
Heidelberg Engineering, 2010. Heidelberg Edge Perimeter Operating Instructions Software Version 2.1. , E-002(20930).
Heijl, A. et al., 1991. Extended empirical statistical package for evaluation of single and multiple fields: Statpac 2. In *Perimetry Update*. New York, NY: Kugler & Ghedini, pp. 303–315.
Heijl, A. et al., 2003. Measuring visual field progression in the Early Manifest Glaucoma Trial. *Acta ophthalmologica Scandinavica*, 81(3), pp.286–93. Available at: http://www.ncbi.nlm.nih.gov/pubmed/12780410.
Heijl, A. et al., 2002. Reduction of intraocular pressure and glaucoma progression: results from the Early Manifest Glaucoma Trial. *Archives of ophthalmology (Chicago, Ill.: 1960)*, 120(10), pp.1268–79. Available at: http://www.ncbi.nlm.nih.gov/pubmed/12365904.
Heijl, A. et al., 1989. Visual field interpretation with empiric probability maps. *Archives of ophthalmology (Chicago, Ill.: 1960)*, 107(2), pp.204–8. Available at: http://www.ncbi.nlm.nih.gov/pubmed/2916973.
Heijl, A. & Drance, S.M., 1983. Changes in differential threshold in patients with glaucoma during prolonged perimetry. *The British journal of ophthalmology*, 67(8), pp.512–516. Available at: http://www.ncbi.nlm.nih.gov/pubmed/6871143.
Heijl, A., Drance, S.M. & Douglas, G.R., 1980. Automatic perimetry (COMPETER). Ability to detect early glaucomatous field defects. *Archives of ophthalmology*, 98(9),

pp.1560–1563. Available at: http://www.ncbi.nlm.nih.gov/pubmed/7425915.
Heijl, A. & Patella, V.M., 2002. *The Field Analyzer Primer: Essential Perimetry* 3rd ed., Carl Zeiss Meditech Inc.
Heijl, a, Bengtsson, B. & Patella, V.M., 2000. Glaucoma follow-up when converting from long to short perimetric threshold tests. *Archives of ophthalmology*, 118(4), pp.489–493. Available at: http://www.ncbi.nlm.nih.gov/pubmed/10766134.
Heijl, a, Lindgren, a & Lindgren, G., 1989. Test-retest variability in glaucomatous visual fields. *American journal of ophthalmology*, 108(2), pp.130–135.
Heijl, a, Lindgren, G. & Olsson, J., 1987. Normal variability of static perimetric threshold values across the central visual field. *Archives of ophthalmology*, 105(11), pp.1544–1549.
Hemenger, R.P., 1989. Birefringence of a medium of tenuous parallel cylinders. *Applied optics*, 28(18), pp.4030–4. Available at: http://www.ncbi.nlm.nih.gov/pubmed/20555816.
Henson, D., Chaudry, S. & Artes, P., 1997. The relationship between sensitivity and variability in normal and glaucomatous visual fields. In M. Wall, ed. *Perimetry Update*. Amsterdam: Kugler & Ghedini.
Hess, D.B. et al., 2005. Macular and retinal nerve fiber layer analysis of normal and glaucomatous eyes in children using optical coherence tomography. *American Journal of Ophthalmology*, 139(3), pp.509–517.
Hoh, S.T. et al., 2000. Optical coherence tomography and scanning laser polarimetry in normal, ocular hypertensive, and glaucomatous eyes. *American journal of ophthalmology*, 129(2), pp.129–135.
Holmin, C. & Krakau, C.E., 1979. Variability of glaucomatous visual field defects in computerized perimetry. *Albrecht von Graefes Archiv fur klinische und experimentelle Ophthalmologie. Albrecht von Graefe's archive for clinical and experimental ophthalmology*, 210(4), pp.235–250.
Honjo, M. et al., 2015. Retinal thickness and the structure/function relationship in the eyes of older adults with glaucoma. *PLoS ONE*, 10(10), pp.1–16.
Hood, D.C. et al., 2007. Structure versus function in glaucoma: An application of a linear model. *Investigative Ophthalmology and Visual Science*, 48(8), pp.3662–3668.
Hood, D.C. & Kardon, R.H., 2007. A framework for comparing structural and functional measures of glaucomatous damage. *Progress in Retinal and Eye Research*, 26(6), pp.688–710.
Horn, F.K. et al., 2016. Comparison of frequency doubling and flicker defined form perimetry in early glaucoma. *Graefe's archive for clinical and experimental ophthalmology = Albrecht von Graefes Archiv für klinische und experimentelle Ophthalmologie*, 254(5), pp.937–46. Available at: http://www.ncbi.nlm.nih.gov/pubmed/26883356 [Accessed June 29, 2016].
Horn, F.K. et al., 1997. The full-field flicker test in early diagnosis of chronic open-angle glaucoma. *American journal of ophthalmology*, 123(3), pp.313–9. Available at: http://www.ncbi.nlm.nih.gov/pubmed/9063240.
Hoyt, W.F. & Newman, N.M., 1972. The Earliest Observable Defect in Galucoma? , pp.692–693.

Huang, D. et al., 1991. Optical coherence tomography. *Science*, 254(5035), pp.1178–81. Available at: http://www.sciencemag.org/content/254/5035/1178\nhttp://www.sciencemag.org/content/254/5035/1178.short\nhttp://www.ncbi.nlm.nih.gov/pubmed/1957169.

Huang, X.-R. et al., 2004. Variation of peripapillary retinal nerve fiber layer birefringence in normal human subjects. *Investigative ophthalmology & visual science*, 45(9), pp.3073–80. Available at: http://www.ncbi.nlm.nih.gov/pubmed/15326123.

Hudson, C., Wild, J.M. & O'Neill, E.C., 1994. Fatigue effects during a single session of automated static threshold perimetry. *Investigative Ophthalmology and Visual Science*, 35(1), pp.268–280.

Hyman, L.G. et al., 2005. Treatment and vision-related quality of life in the early manifest glaucoma trial. *Ophthalmology*, 112(9), pp.1505–1513.

Iester, M. et al., 1997. Correlation between the visual field indices and Heidelberg retina tomograph parameters. *Journal of glaucoma*, 6(2), pp.78–82. Available at: http://journals.lww.com/glaucomajournal/abstract/1997/04000/correlation_between_the_visual_field_indices_and.2.aspx\nhttp://www.ncbi.nlm.nih.gov/pubmed/9098814.

Iester, M., Mikelberg, F.S. & Drance, S.M., 1996. The effect of disc size on diagnostic precision with the Heidelberg Retina Tomograph. *Investigative Ophthalmology and Visual Science*, 37(3).

Investigators, T.A., 1994. The Advanced Glaucoma Intervention Study (AGIS): 1. Study design and methods and baseline characteristics of study patients. *Control Clin Trials*, 15(4), pp.299–325. Available at: http://linkinghub.elsevier.com/retrieve/pii/0197245694900469.

J, P., 1971. Early signs of the glaucomatous disc. *British Journal of Ophthalmology*, 55, pp.820–825.

Jampel, H.D. et al., 2002. Correlation of the binocular visual field with patient assessment of vision. *Investigative Ophthalmology and Visual Science*, 43(4), pp.1059–1067.

Jeoung, J.W. et al., 2014. Diagnostic Ability of Spectral-domain Versus Time-domain Optical Coherence Tomography in Preperimetric Glaucoma. *Journal of glaucoma*, 23(5), pp.299–306. Available at: http://www.ncbi.nlm.nih.gov/pubmed/23377582.

Jia, Y. et al., Optical Coherence Tomography Angiography of Optic Disc Perfusion in Glaucoma.

Johnson, C., 2009. Determining progression in glaucoma: An overview of current methods and difficulties and a look at the future. *Glaucoma Today*, pp.22–26.

Johnson, C., 1996. Standardizing the measurement of visual fields. *Ophthalmology*, 103(1), pp.186–189. Available at: http://dx.doi.org/10.1016/S0161-6420(96)30740-9.

Johnson, C.A., 2009. Determining Progression in Glaucoma. *Technology Today*, (November/December), pp.22–26.

Johnson, C.A., 1994. Selective versus nonselective losses in glaucoma. *Journal of glaucoma*, 3 Suppl 1, pp.S32–S44.

Johnson, C.A. et al., 2003. Structure and function evaluation (SAFE): II. Comparison of

optic disk and visual field characteristics. *American Journal of Ophthalmology*, 135(2), pp.148–154.
Johnson, C.A. et al., 2000. The relationship between structural and functional alterations in glaucoma: a review. *Seminars in ophthalmology*, 15(4), pp.221–233.
Johnson, C.A. & Samuels, S.J., 1997. Screening for glaucomatous visual field loss with frequency-doubling perimetry. *Investigative Ophthalmology and Visual Science*, 38(2), pp.413–425.
Johnson, C. & Sample, P., 2003. Perimetry and visual field testing. In P. Kaufmann & A. Alm, eds. *Adler's Physiology of the Eye*. St. Louis: CV Mosby, pp. 552–577.
Jonas, J.B. et al., 1992. Human optic nerve fiber count and optic disc size. *Investigative Ophthalmology and Visual Science*, 33(6), pp.2012–2018.
Jonas, J.B. & Grundler, A.E., 1997. Correlation between mean visual field loss and morphometric optic disk variables in the open-angle glaucomas. *AMERICAN JOURNAL OF OPHTHALMOLOGY*, 124(4), pp.488–497.
Jonas, J.B., Gusek, G.C. & Naumann, G.O.H., 1988. Optic disc, cup and neuroretinal rim size, configuration and correlations in normal eyes. *Investigative Ophthalmology and Visual Science*, 29(7), pp.1151–1158.
Jonas, J.B., Gusek, G.C. & Naumann, G.O.H., 1988. Optic disc morphometry in chronic primary open-angle glaucoma - I. Morphometric intrapapillary characteristics. *Graefe's Archive for Clinical and Experimental Ophthalmology*, 226(6), pp.522–530.
Jonas, J.B., Nguyen, N.X. & Naumann, G.O., 1989. The retinal nerve fiber layer in normal eyes. *Ophthalmology*, 96(5), pp.627–632. Available at: http://www.ncbi.nlm.nih.gov/pubmed/2748120.
Jung, K.I., Park, H.Y.L. & Park, C.K., 2012. Characteristics of optic disc morphology in glaucoma patients with parafoveal scotoma compared to peripheral scotoma. *Investigative Ophthalmology and Visual Science*, 53(8), pp.4813–4820.
Kanamori, A. et al., 2006. Comparison of confocal scanning laser ophthalmoscopy, scanning laser polarimetry and optical coherence tomography to discriminate ocular hypertension and glaucoma at an early stage. *Graefe's archive for clinical and experimental ophthalmology = Albrecht von Graefes Archiv für klinische und experimentelle Ophthalmologie*, 244(1), pp.58–68. Available at: http://www.ncbi.nlm.nih.gov/pubmed/16044326.
Kanamori, A. et al., 2003. Evaluation of the glaucomatous damage on retinal nerve fiber layer thickness measured by optical coherence tomography. *American Journal of Ophthalmology*, 135(4), pp.513–520.
Kanamori, A. et al., 2008. Regional relationship between retinal nerve fiber layer thickness and corresponding visual field sensitivity in glaucomatous eyes. *Archives of ophthalmology*, 126(11), pp.1500–1506.
Kaplan, E. & Shapley, R.M., 1986. The primate retina contains two types of ganglion cells, with high and low contrast sensitivity. *Proceedings of the National Academy of Sciences of the United States of America*, 83(8), pp.2755–7. Available at: http://www.pubmedcentral.nih.gov/articlerender.fcgi?artid=323379&tool=pmcentrez&rendertype=abstract.
Kass, M.A. et al., 2002. The Ocular Hypertension Treatment Study: a randomized trial

determines that topical ocular hypotensive medication delays or prevents the onset of primary open-angle glaucoma. *Archives of ophthalmology (Chicago, Ill. : 1960)*, 120(6), pp.701-13-30. Available at: http://www.ncbi.nlm.nih.gov/pubmed/12049574.

Katsumori, N., Okubo, K. & Mizokami, K., 1985. The changes of visual field sensitivity accompanied with enlargement of optic cup. *Japanese Journal of Clinical Ophthalmology*, 89, pp.928–933.

Katz, J. et al., 1991. Comparison of analytic algorithms for detecting glaucomatous visual field loss. *Archives of ophthalmology*, 109(12), pp.1684–1689.

Katz, J. et al., 1997. Estimating Progression of Visual Field Loss in Glaucoma. *Ophthalmology*, 104(6), pp.1017–1025. Available at: http://www.sciencedirect.com/science/article/pii/S0161642097301924.

Katz, J., 1999. Scoring systems for measuring progression of visual field loss in clinical trials of glaucoma treatment. *Ophthalmology*, 106(2), pp.391–395.

Katz, J. & Sommer, A., 1986. Asymmetry and variation in the normal hill of vision. *Archives of ophthalmology*, 104(1), pp.65–8. Available at: http://www.ncbi.nlm.nih.gov/pubmed/3942546.

Keltner, J.L. et al., 2006. The association between glaucomatous visual fields and optic nerve head features in the Ocular Hypertension Treatment Study. *Ophthalmology*, 113(9), pp.1603–1612. Available at: http://www.ncbi.nlm.nih.gov/pubmed/16949445.

Kerrigan-Baumrind, L.A. et al., 2000. Number of ganglion cells in glaucoma eyes compared with threshold visual field tests in the same persons. *Investigative Ophthalmology and Visual Science*, 41(3), pp.741–748.

Kim, H.-G., Heo, H. & Park, S.-W., 2011. Comparison of scanning laser polarimetry and optical coherence tomography in preperimetric glaucoma. *Optometry and vision science : official publication of the American Academy of Optometry*, 88(1), pp.124–9. Available at: http://www.ncbi.nlm.nih.gov/pubmed/21037496.

Kim, T.W. et al., 2007. Retinal Nerve Fiber Layer Damage as Assessed by Optical Coherence Tomography in Eyes with a Visual Field Defect Detected by Frequency Doubling Technology Perimetry but Not by Standard Automated Perimetry. *Ophthalmology*, 114(6), pp.1053–1057.

King-Smith, P.E. et al., 1994. Efficient and unbiased modifications of the QUEST threshold method: Theory, simulations, experimental evaluation and practical implementation. *Vision Research*, 34(7), pp.885–912.

King, A.J.W. et al., 2000. Measurement of peripapillary retinal nerve fiber layer volume in glaucoma. *American Journal of Ophthalmology*, 129(5), pp.599–607.

Knight, O.J. et al., 2009. Comparison of Retinal Nerve Fiber Layer Measurements Using Time Domain and Spectral Domain Optical Coherent Tomography. *Ophthalmology*, 116(7), pp.1271–1277.

Koizumi, H. et al., 2008. Three-Dimensional Evaluation of Vitreomacular Traction and Epiretinal Membrane Using Spectral-Domain Optical Coherence Tomography. *American Journal of Ophthalmology*, 145(3).

Kotera, Y. et al., 2008. Comparison of spectral domain optical coherence tomography and color photographic imaging of the optic nerve head in management of

glaucoma. *Ophthalmic surgery, lasers & imaging : the official journal of the International Society for Imaging in the Eye*, 40, pp.255–263.
Kourkoutas, D. et al., 2007. Comparison of glaucoma progression evaluated with Heidelberg retina tomograph II versus optic nerve head stereophotographs. *Canadian journal of ophthalmology. Journal canadien d'ophtalmologie*, 42(1), pp.82–8. Available at: http://www.ncbi.nlm.nih.gov/pubmed/17361246.
Kuang, T. et al., 2015. Estimating Lead Time Gained by Optical Coherence Tomography in Detecting Glaucoma before Development of Visual Field Defects. *Ophthalmology*, 122(10), pp.2002–2009.
Kwon, Y.H. et al., 2009. Primary open-angle glaucoma. *The New England Journal of Medicine*, 360(11), pp.1113–1124. Available at: http://www.pubmedcentral.nih.gov/articlerender.fcgi?artid=3207715&tool=pmcentrez&rendertype=abstract.
Lachenmayer, B., Rothbacher, H. & Gleissner, M., 1989. Automated flicker perimetry versus quantitative static perimetry in early glaucoma. In A. Heijl, ed. *Perimetry Update*. pp. 359–368.
Lan, Y.-W., Henson, D.B. & Kwartz, a J., 2003. The correlation between optic nerve head topographic measurements, peripapillary nerve fibre layer thickness, and visual field indices in glaucoma. *The British journal of ophthalmology*, 87(9), pp.1135–1141. Available at: http://bjo.bmj.com/cgi/doi/10.1136/bjo.87.9.1135.
Landers, J. a, Goldberg, I. & Graham, S.L., 2003. Detection of early visual field loss in glaucoma using frequency-doubling perimetry and short-wavelength automated perimetry. *Archives of ophthalmology*, 121(12), pp.1705–1710.
Lemij, H.G. & Reus, N.J., 2008. New developments in scanning laser polarimetry for glaucoma. *Current opinion in ophthalmology*, 19(2), pp.136–40. Available at: http://www.ncbi.nlm.nih.gov/pubmed/18301287.
Leske, M.C. et al., 1999. Early manifest glaucoma trial. *Ophthalmology*, 106(11), pp.2144–2153. Available at: http://www.sciencedirect.com/science/article/pii/S0161642099904979.
Leung, C.K.S. et al., 2005. Comparative study of retinal nerve fiber layer measurement by StratusOCT and GDx VCC, II: Structure/function regression analysis in glaucoma. *Investigative Ophthalmology and Visual Science*, 46(10), pp.3702–3711.
Leung, C.K.S. et al., 2010. Evaluation of retinal nerve fiber layer progression in glaucoma: A study on optical coherence tomography guided progression analysis. *Investigative Ophthalmology and Visual Science*, 51(1), pp.217–222.
Leung, C.K.S. et al., 2010. Retinal nerve fiber layer imaging with spectral-domain optical coherence tomography: Analysis of the retinal nerve fiber layer map for glaucoma detection. *Ophthalmology*, 117(9), pp.1684–1691. Available at: http://dx.doi.org/10.1016/j.ophtha.2010.01.026.
Lewis, R.A. et al., 1986. Variability of Quantitative Automated Perimetry in Normal Observers. *Ophthalmology*, 93(7), pp.878–881. Available at: http://www.sciencedirect.com/science/article/pii/S0161642086336479.
Lichter, P.R., 1976. Variability of expert observers in evaluating the optic disc. *Transactions of the American Ophthalmological Society*, 74, pp.532–72. Available

at:
http://www.pubmedcentral.nih.gov/articlerender.fcgi?artid=1311528&tool=pmcentrez&rendertype=abstract.
Lim, J.H. et al., 2016. Incidence of and risk factors for glaucoma in lost-to-follow-up normal-tension glaucoma suspect patients. *BMC ophthalmology*, 16(1), p.62. Available at:
http://www.pubmedcentral.nih.gov/articlerender.fcgi?artid=4880870&tool=pmcentrez&rendertype=abstract [Accessed June 3, 2016].
Lindenmuth, K.A. et al., 1990. Effects of Pupillary Dilation on Automated Perimetry in Normal Patients. *Ophthalmology*, 97(3), pp.367–370. Available at:
http://www.sciencedirect.com/science/article/pii/S0161642090325800.
Liu, L. et al., 2015. Optical Coherence Tomography Angiography of the Peripapillary Retina in Glaucoma. *JAMA ophthalmology*, 4197(9), pp.1045–1052. Available at:
http://www.ncbi.nlm.nih.gov/pubmed/26203793.
Liu, X. et al., 2001. Optical coherence tomography in measuring retinal nerve fiber layer thickness in normal subjects and patients with open-angle glaucoma. *Chinese medical journal*, 114(5), pp.524–9. Available at:
http://www.ncbi.nlm.nih.gov/pubmed/11780419.
Livingstone, M.S. & Hubel, D.H., 1987. Psychophysical evidence for separate channels for the perception of form, color, movement, and depth. *The Journal of neuroscience : the official journal of the Society for Neuroscience*, 7(11), pp.3416–3468.
Mai, T.A., Reus, N.J. & Lemij, H.G., 2007. Structure-function relationship is stronger with enhanced corneal compensation than with variable corneal compensation in scanning laser polarimetry. *Investigative Ophthalmology and Visual Science*, 48(4), pp.1651–1658.
Malik, R., Swanson, W.H. & Garway-Heath, D.F., 2012a. “Structure-function relationship” in glaucoma: Past thinking and current concepts. *Clinical and Experimental Ophthalmology*, 40(4), pp.369–380.
Malik, R., Swanson, W.H. & Garway-Heath, D.F., 2012b. “Structure-function relationship” in glaucoma: Past thinking and current concepts. *Clinical and Experimental Ophthalmology*, 40(4), pp.369–380.
Mardin, C.Y. et al., 2006. Improving glaucoma diagnosis by the combination of perimetry and HRT measurements. *J Glaucoma*, 15(4), pp.299–305.
Martin Bland, J. & Altman, D., 1986. STATISTICAL METHODS FOR ASSESSING AGREEMENT BETWEEN TWO METHODS OF CLINICAL MEASUREMENT. *The Lancet*, 327(8476), pp.307–310.
Matsumoto, C. et al., 2003. Study of retinal nerve fiber layer thickness within normal hemivisual field in primary open-angle glaucoma and normal-tension glaucoma. *Japanese Journal of Ophthalmology*, 47(1), pp.22–27.
McKendrick, A.M., 2005. Recent developments in perimetry: Test stimuli and procedures. *Clinical and Experimental Optometry*, 88(2), pp.73–80.
McNaught, A.I. et al., 1996. Visual field progression: comparison of Humphrey Statpac2 and pointwise linear regression analysis. *Graefe’s archive for clinical and*

experimental ophthalmology = Albrecht von Graefes Archiv f{ü}r klinische und experimentelle Ophthalmologie, 234(7), pp.411–418. Available at: http://www.ncbi.nlm.nih.gov/pubmed/8817283.

Medeiros, F.A. et al., 2007. Detection of glaucoma using scanning laser polarimetry with enhanced corneal compensation. *Investigative Ophthalmology and Visual Science*, 48(7), pp.3146–3153.

Medeiros, F.A. et al., 2005. Evaluation of retinal nerve fiber layer, optic nerve head, and macular thickness measurements for glaucoma detection using optical coherence tomography. *American Journal of Ophthalmology*, 139(1), pp.44–55.

Medeiros, F.A. et al., 2003. Fourier analysis of scanning laser polarimetry measurements with variable corneal compensation in glaucoma. *Investigative Ophthalmology and Visual Science*, 44(6), pp.2606–2612.

Medeiros, F.A., Sample, P.A. & Weinreb, R.N., 2004. Frequency doubling technology perimetry abnormalities as predictors of glaucomatous visual field loss. *American Journal of Ophthalmology*, 137(5), pp.863–871.

Medeiros, F. a et al., 2006. A statistical approach to the evaluation of covariate effects on the receiver operating characteristic curves of diagnostic tests in glaucoma. *Investigative ophthalmology & visual science*, 47, pp.2520–2527.

Medeiros, F. a et al., 2004. Comparison of scanning laser polarimetry using variable corneal compensation and retinal nerve fiber layer photography for detection of glaucoma. *Archives of ophthalmology*, 122(May 2004), pp.698–704.

Medeiros, F. & Weinreb, R., 2002. Medical backgrounders: glaucoma. *Drugs Today*, 38, pp.563–570.

Meira-Freitas, D. et al., 2014. Predicting progression of glaucoma from rates of frequency doubling technology perimetry change. *Ophthalmology*, 121(2), pp.498–507.

Membrey, L., Kogure, S. & Fitzke, F., 1998. A comparison of the effects of neutral density filters and diffusing filters on motion perimetry, white on white perimetry and frequency doubling perimetry. In M. Wall & J. Wild, eds. *Perimetry Update*. The Hague, The Netherlands: Kugler Publications, pp. 75–83.

Michelessi, M. et al., 2015. Optic nerve head and fibre layer imaging for diagnosing glaucoma. *The Cochrane database of systematic reviews*, (11), p.CD008803. Available at: http://www.ncbi.nlm.nih.gov/pubmed/26618332 [Accessed June 29, 2016].

Miglior, S., 2005. Results of the European Glaucoma Prevention Study. *Ophthalmology*, 112(3), pp.366–375.

Mikelberg, F.S. et al., 1995. Ability of the heidelberg retina tomograph to detect early glaucomatous visual field loss. *Journal of glaucoma*, 4(4), pp.242–7. Available at: http://www.ncbi.nlm.nih.gov/pubmed/19920681.

Mikelberg, F.S. et al., 1989. The normal human optic nerve. Axon count and axon diameter distribution. *Ophthalmology*, 96(9), pp.1325–8. Available at: http://www.ncbi.nlm.nih.gov/pubmed/2780002.

Mikelberg, F.S., Wijsman, K. & Schulzer, M., 1993. Reproducibility of topographic parameters obtained with the heidelberg retina tomograph. *Journal of glaucoma*,

2(2), pp.101–3. Available at: http://www.ncbi.nlm.nih.gov/pubmed/19920494.
Minckler, D.S., Bunt, A.H. & Johanson, G.W., 1977. Orthograde and retrograde axoplasmic transport during acute ocular hypertension in the monkey. *Invest Ophthalmol Vis Sci*, 16(5), pp.426–441. Available at: http://www.ncbi.nlm.nih.gov/pubmed/67096.
Mistlberger, a et al., 1999. Heidelberg retina tomography and optical coherence tomography in normal, ocular-hypertensive, and glaucomatous eyes. *Ophthalmology*, 106(10), pp.2027–2032.
Mohammadi, K. et al., 2004. Retinal nerve fiber layer thickness measurements with scanning laser polarimetry predict glaucomatous visual field loss. *American Journal of Ophthalmology*, 138(4), pp.592–601.
Moorfield Eye Hospital, 2015. Moorfields MDT. Available at: http://www.moorfieldsmdt.co.uk [Accessed June 5, 2015].
Morgan-Davies, J. et al., 2004. Three dimensional analysis of the lamina cribrosa in glaucoma. *The British journal of ophthalmology*, 88(10), pp.1299–304. Available at: http://www.scopus.com/inward/record.url?eid=2-s2.0-4744367562&partnerID=tZOtx3y1.
Morgan, J.E. & Waldock, A., 2000. Scanning laser polarimetry of the normal human retinal nerve fiber layer: a quantitative analysis. *American journal of ophthalmology*, 129(1), pp.76–82. Available at: http://www.ncbi.nlm.nih.gov/pubmed/10653416.
Musch, D.C. et al., 1999. The Collaborative Initial Glaucoma Treatment Study: study design, methods, and baseline characteristics of enrolled patients. *Ophthalmology*, 106(4), pp.653–62. Available at: http://www.sciencedirect.com/science/article/pii/S0161642099901471\nhttp://www.ncbi.nlm.nih.gov/pubmed/10201583.
Nelson, P. et al., 2003. Quality of Life in Glaucoma and Its Relationship with Visual Function. *Journal of Glaucoma*, 12(2), pp.139–150.
Nicolela, M.T. et al., 2001. Agreement among clinicians in the recognition of patterns of optic disk damage in glaucoma. *American Journal of Ophthalmology*, 132(6), pp.836–844.
Nicolela, M.T. et al., 2001. Scanning laser polarimetry in a selected group of patients with glaucoma and normal controls. *American journal of ophthalmology*, 132, pp.845–854.
Niessen, A.G. et al., 1996. Retinal nerve fiber layer assessment by scanning laser polarimetry and standardized photography. *American journal of ophthalmology*, 121(5), pp.484–493. Available at: http://www.ncbi.nlm.nih.gov/pubmed/8610791.
Nouri-Mahdavi, K. et al., 1997. Comparison of methods to detect visual field progression in glaucoma . *Ophthalmology*, 104(8), pp.1228–1236.
Öhnell, H. et al., 2016. Structural and Functional Progression in the Early Manifest Glaucoma Trial. *Ophthalmology*, 123(6), pp.1173–1180.
Okubo, K., 1986. Correlation between glaucomatous optic disc and visual field defects. IV. Mode of cupping formation. *The Kobe Journal of Medical Sciences*, 32, pp.197–202.
Olsson, J. et al., 1997. An improved method to estimate frequency of false positive

answers in computerized perimetry. *Acta Ophthalmologica Scandinavica*, 75(2), pp.181–183.
Olsson, J., Heijl, A. & Rootsen, H., 1993. Frequency-of-seeing in computerised perimetry. In R. Mills, ed. *Perimetry Update*. Amsterdam: Kugler, pp. 551–556.
Olsson, J., Rootzén, H. & Heijl, A., 1988. Maximum likelihood estimation of the frequency of false positive and false negative answers from the up-and-down staircases of computerized threshold perimetry. In A. Heijl, ed. *Perimetry Update*. Amsterdam: Kugler & Ghedini, pp. 245–251.
Pan, F. & Swanson, W.H., 2006. A cortical pooling model of spatial summation for perimetric stimuli. *Journal of vision*, 6(11), pp.1159–1171.
Park, S.C. et al., 2011. Initial parafoveal versus peripheral scotomas in glaucoma: Risk factors and visual field characteristics. *Ophthalmology*, 118(9), pp.1782–1789. Available at: http://dx.doi.org/10.1016/j.ophtha.2011.02.013.
Parrish, R.K. et al., 1997. Visual function and quality of life among patients with glaucoma. *Archives of ophthalmology*, 115(11), pp.1447–55. Available at: http://www.ncbi.nlm.nih.gov/pubmed/9366678.
Pederson, J.E. & Anderson, D.R., 1980. The Mode of Progressive Disc Cupping in Ocular Hypertension and Glaucoma. *Archives of ophthalmology*, 98(3), pp.490–495.
Perry, V.H., Oehler, R. & Cowey, A., 1984. Retinal ganglion cells that project to the dorsal lateral geniculate nucleus in the macaque monkey. *Neuroscience*, 12(4), pp.1101–1123.
Poinoosawmy, D. et al., 1992. Discrimination between progression and non-progression visual field loss in low tension glaucoma using MDT. In R. Mills, ed. *Perimetry Update*. Kugler Publications, pp. 109–114.
Poinoosawmy, D. et al., 1997. Variation of nerve fibre layer thickness measurements with age and ethnicity by scanning laser polarimetry. *The British journal of ophthalmology*, 81(5), pp.350–4. Available at: http://www.pubmedcentral.nih.gov/articlerender.fcgi?artid=1722182&tool=pmcentrez&rendertype=abstract.
Pons, M.E. et al., 2000. Assessment of retinal nerve fiber layer internal reflectivity in eyes with and without glaucoma using optical coherence tomography. *Arch Ophthalmol*, 118, pp.1044–1047.
Prum, B.E. et al., 2016. Primary Open-Angle Glaucoma Preferred Practice Pattern® Guidelines. *Ophthalmology*, 123(1), pp.P41–P111.
Puliafito, C.A. et al., 1995. Imaging of Macular Diseases with Optical Coherence Tomography. *Ophthalmology*, 102(2), pp.217–229. Available at: http://www.sciencedirect.com/science/article/pii/S0161642095310329.
Quaid, P.T. & Flanagan, J.G., 2005. Defining the limits of flicker defined form: Effect of stimulus size, eccentricity and number of random dots. *Vision Research*, 45(8), pp.1075–1084.
Quaid, P.T., Simpson, T.L. & Flanagan, J.G., 2005. Frequency doubling illusion: detection vs. form resolution. *Optometry and vision science : official publication of the American Academy of Optometry*, 82(1), pp.36–42. Available at:

http://www.ncbi.nlm.nih.gov/pubmed/15630402.
Quigley, H.A. et al., 1987. Chronic glaucoma selectively damages large optic nerve fibers. *Investigative Ophthalmology and Visual Science*, 28(6), pp.913–920.
Quigley, H.A., 1998. Identification of glaucoma-related visual field abnormality with the screening protocol of frequency doubling technology. *American Journal of Ophthalmology*, 125(6), pp.819–829.
Quigley, H.A., 1993. Open-angle glaucoma. *New England Journal of Medicine*, 328, pp.1097–1106.
Quigley, H.A. et al., 1981. Optic nerve damage in human glaucoma. II. The site of injury and susceptibility to damage. *Archives of ophthalmology (Chicago, Ill. : 1960)*, 99(4), pp.635–49. Available at: http://archopht.jamanetwork.com/article.aspx?doi=10.1001/archopht.1981.03930010635009\nhttp://www.ncbi.nlm.nih.gov/pubmed/6164357.
Quigley, H.A. et al., 1995. Retinal ganglion cell death in experimental glaucoma and after axotomy occurs by apoptosis. *Investigative Ophthalmology and Visual Science*, 36(5), pp.774–786.
Quigley, H.A. et al., 1994. Risk factors for the development of glaucomatous visual field loss in ocular hypertension. *Archives of ophthalmology*, 112(5), pp.644–649.
Quigley, H.A. et al., 1990. The size and shape of the optic disc in normal human eyes. *Archives of ophthalmology*, 108(1), pp.51–7. Available at: http://europepmc.org/abstract/MED/2297333/reload=0.
Quigley, H.A., Addicks, E.M. & Green, W.R., 1982. Optic nerve damage in human glaucoma. III. Quantitative correlation of nerve fiber loss and visual field defect in glaucoma, ischemic neuropathy, papilledema, and toxic neuropathy. *Archives of ophthalmology*, 100(1), pp.135–146.
Quigley, H.A. & Broman, A.T., 2006. The number of people with glaucoma worldwide in 2010 and 2020. *The British journal of ophthalmology*, 90(3), pp.262–7. Available at: http://www.pubmedcentral.nih.gov/articlerender.fcgi?artid=1856963&tool=pmcentrez&rendertype=abstract.
Quigley, H.A., Coleman, A.L. & Dorman-Pease, M.E., 1991. Larger optic nerve heads have more nerve fibers in normal monkey eyes. *Archives of Ophthalmology*, 109(10), pp.1441–1443. Available at: http://www.ncbi.nlm.nih.gov/pubmed/1929937.
Quigley, H.A., Dunkelberger, G.R. & Green, W.R., 1989. Retinal ganglion cell atrophy correlated with automated perimetry in human eyes with glaucoma. *American Journal of Ophthalmology*, 107(5), pp.453–464.
Quigley, H. a et al., 1992. An evaluation of optic disc and nerve fiber layer examinations in monitoring progression of early glaucoma damage. *Ophthalmology*, 99(1), pp.19–28. Available at: http://www.ncbi.nlm.nih.gov/pubmed/1741133.
Quigley, H. a, 1986. Examination of the retinal nerve fiber layer in the recognition of early glaucoma damage. *Transactions of the American Ophthalmological Society*, 84, pp.920–966. Available at: http://www.pubmedcentral.nih.gov/articlerender.fcgi?artid=1298755&tool=pmcentrez&rendertype=abstract.

Quigley, H. & Anderson, D.R., 1976. The dynamics and location of axonal transport blockade by acute intraocular pressure elevation in primate optic nerve. *Investigative ophthalmology*, 15(8), pp.606–16. Available at: http://www.ncbi.nlm.nih.gov/pubmed/60300.

Quigley, H., Dunkelberger, GR. & Green, W., 1988. Chronic Human Glaucoma Causing Selectively Greater Loss of Large Optic Nerve Fibers. *Ophthalmology*, 95(3), pp.357–363. Available at: http://www.sciencedirect.com/science/article/pii/S0161642088331763.

Ramchandran, V. & Rogers-Ramchandaran, D., 1991. Phantom contours: A new class of visual patterns that selectively activates the magnocellular pathway in man. *Bulletin of the Psychonomic Society*, 29, pp.391–394.

Rao, H.L. et al., 2011. Effect of disease severity and optic disc size on diagnostic accuracy of rtvue spectral domain optical coherence tomograph in glaucoma. *Investigative Ophthalmology and Visual Science*, 52(3), pp.1290–1296.

Ren, R. et al., 2014. Anterior lamina cribrosa surface depth, age, and visual field sensitivity in the Portland progression project. *Investigative Ophthalmology and Visual Science*, 55(3), pp.1531–1539.

Repka, M. & Quigley, H.A., 1989. The effect of age on normal human optic nerve fiber number and diameter. *Ophthalmology*, 96(1), pp.26–32. Available at: http://www.ncbi.nlm.nih.gov/pubmed/2919049.

Reus, N.J., de Graaf, M. & Lemij, H.G., 2007. Accuracy of GDx VCC, HRT I, and clinical assessment of stereoscopic optic nerve head photographs for diagnosing glaucoma. *The British journal of ophthalmology*, 91(3), pp.313–8. Available at: http://www.ncbi.nlm.nih.gov/pubmed/17035283 [Accessed August 16, 2016].

Reus, N.J. & Lemij, H.G., 2004a. Diagnostic accuracy of the GDx VCC for glaucoma. *Ophthalmology*, 111(10), pp.1860–1865.

Reus, N.J. & Lemij, H.G., 2004b. The relationship between standard automated perimetry and GDx VCC measurements. *Investigative Ophthalmology and Visual Science*, 45(3), pp.840–845.

Reus, N.J., Zhou, Q. & Lemij, H.G., 2006. Enhanced imaging algorithm for scanning laser polarimetry with variable corneal compensation. *Investigative Ophthalmology and Visual Science*, 47(9), pp.3870–3877.

Reznicek, L. et al., 2015. Flicker defined form perimetry in glaucoma suspects with normal achromatic visual fields. *Current eye research*, 40(7), pp.683–9. Available at: http://www.ncbi.nlm.nih.gov/pubmed/25207744 [Accessed June 29, 2016].

Rohrschneider, K. et al., 1994. Reproducibility of the optic nerve head topography with a new laser tomographic scanning device. *Ophthalmology*, 101(6), pp.1044–1049. Available at: http://europepmc.org/abstract/MED/8008345\nhttp://www.ncbi.nlm.nih.gov/pubmed/8008345.

Ruben, S. & Fitzke, F., 1994. Correlation of peripheral displacement thresholds and optic disc parameters in ocular hypertension. *The British journal of ophthalmology*, 78(4), pp.291–294.

Russell, R.A. et al., 2012. The relationship between variability and sensitivity in large-

scale longitudinal visual field data. *Investigative Ophthalmology and Visual Science*, 53(10), pp.5985–5990.
Samarawickrama, C. et al., 2012. Measurement of Normal Optic Nerve Head Parameters. *Survey of Ophthalmology*, 57(4), pp.317–336.
Sample, P.A., 2001. What does functional testing tell us about optic nerve damage? *Survey of Ophthalmology*, 45(6), pp.319–324.
Sample, P.A., Juang, P.S.C. & Weinreb, R.N., 1991. Isolating the effects of primary open-angle glaucoma on the contrast sensitivity function. *American Journal of Ophthalmology*, 112(3), pp.308–316. Available at: http://www.scopus.com/inward/record.url?eid=2-s2.0-0025875855&partnerID=40&md5=6f1c73c8a10360da425ec8d82028ef7d.
Sanchez-Galeana, C. et al., 2001. Using optical imaging summary data to detect glaucoma. *Ophthalmology*, 108(10), pp.1812–1818.
Schiller, P.H., Logothetis, N.K. & Charles, E.R., 1994. Role of the color-opponent and broad-band channels in vision. *Visual Neuroscience*, 5(4), pp.321–346.
Schlottmann, P.G. et al., 2004. Relationship between visual field sensitivity and retinal nerve fiber layer thickness as measured by scanning laser polarimetry. *Investigative ophthalmology & visual science*, 45(6), pp.1823–1829. Available at: http://www.ncbi.nlm.nih.gov/pubmed/15161846.
Schrems, W.A. et al., 2015. Predicted and measured retinal nerve fiber layer thickness from time-domain optical coherence tomography compared with spectral-domain optical coherence tomography. *JAMA ophthalmology*, 133(10), pp.1135–43. Available at: http://www.ncbi.nlm.nih.gov/pubmed/26225533 [Accessed August 16, 2016].
Schuman, J.S., Hee, M.R., Arya, A. V, et al., 1995. Optical coherence tomography: a new tool for glaucoma diagnosis. *Current opinion in ophthalmology*, 6(2), pp.89–95. Available at: http://www.ncbi.nlm.nih.gov/pubmed/10150863.
Schuman, J.S., Hee, M.R., Puliafito, C.A., et al., 1995. Quantification of nerve fiber layer thickness in normal and glaucomatous eyes using optical coherence tomography. *Archives of ophthalmology*, 113(5), pp.586–596. Available at: http://www.ncbi.nlm.nih.gov/pubmed/7748128.
Schuman, J.S. et al., 1996. Reproducibility of nerve fiber layer thickness measurements using optical coherence tomography. *Ophthalmology*, 103(11), pp.1889–98. Available at: http://www.pubmedcentral.nih.gov/articlerender.fcgi?artid=1939724&tool=pmcentrez&rendertype=abstract.
Schwartz, B., 1976. The optic disc in glaucoma: introduction. *Transactions of the American Academy of Ophthalmology and Otolaryngology*, 81, p.191.
Scobey, R.P. & Horowitz, J.M., 1976. Detection of image displacement by phasic cells in peripheral visual fields of the monkey. *Vision Research*, 16(1), pp.15–24.
Sekhar, G.C. et al., 2000. Sensitivity of Swedish interactive threshold algorithm compared with standard full threshold algorithm in Humphrey visual field testing. *Ophthalmology*, 107(7), pp.1303–1308.
Sherwood, M.B. et al., 1998. Glaucoma's impact on quality of life and its relation to

clinical indicators. *Ophthalmology*, 105(3), pp.561–566. Available at: http://www.aaojournal.org/article/S0161-6420(98)93043-3/abstract.
Shou, T. et al., 2003. Differential dendritic shrinkage of ?? and ?? retinal ganglion cells in cats with chronic glaucoma. *Investigative Ophthalmology and Visual Science*, 44(7), pp.3005–3010.
Silverman, S.E., Trick, G.L. & Hart, W.M., 1990. Motion perception is abnormal in primary open-angle glaucoma and ocular hypertension. *Investigative ophthalmology & visual science*, 31(4), pp.722–9. Available at: http://www.ncbi.nlm.nih.gov/pubmed/2335439.
Smith, S.D., Katz, J. & Quigley, H.A., 1996. Analysis of progressive change in automated visual fields in glaucoma. *Investigative Ophthalmology and Visual Science*, 37(7), pp.1419–1428.
Sommer, A. et al., 1977. The nerve fiber layer in the diagnosis of glaucoma. *Archives of ophthalmology (Chicago, Ill.: 1960)*, 95(12), pp.2149–2156.
Sommer, A., Pollack, I. & Maumenee, A.E., 1979a. Optic disc parameters and onset of glaucomatous field loss. I. Methods and progressive changes in disc morphology. *Archives of ophthalmology*, 97(8), pp.1444–1448. Available at: http://www.ncbi.nlm.nih.gov/pubmed/464866.
Sommer, A., Pollack, I. & Maumenee, A.E., 1979b. Optic disc parameters and onset of glaucomatous field loss. II. Static screening criteria. *Archives of ophthalmology*, 97(8), pp.1449–1454. Available at: http://www.ncbi.nlm.nih.gov/pubmed/464867.
Sommer, a et al., 1991. Clinically detectable nerve fiber atrophy precedes the onset of glaucomatous field loss. *Archives of ophthalmology*, 109(1), pp.77–83.
Spaeth, G.L., Hitchings, R.A. & Sivalingam, E., 1976. The optic disc in glaucoma: pathogenetic correlation of five patterns of cupping in chronic open-angle glaucoma. *Transactions. Section on Ophthalmology. American Academy of Ophthalmology and Otolaryngology*, 81(2), pp.217–223. Available at: http://www.ncbi.nlm.nih.gov/pubmed/936393.
Sponsel, W.E. et al., 1998. Clinical classification of glaucomatous visual field loss by frequency doubling perimetry. *American Journal of Ophthalmology*, 125(6), pp.830–836.
Spry, P.G.D. et al., 2003. Measurement error of visual field tests in glaucoma. *The British journal of ophthalmology*, 87, pp.107–112. Available at: http://www.pubmedcentral.nih.gov/articlerender.fcgi?artid=1771451&tool=pmcentrez&rendertype=abstract.
Spry, P.G.D. et al., 2001. Variability components of standard automated perimetry and frequency-doubling technology perimetry. *Investigative Ophthalmology and Visual Science*, 42(6), pp.1404–1410.
Spry, P.G.D. & Johnson, C.A., 2002. Identification of progressive glaucomatous visual field loss. *Survey of Ophthalmology*, 47(2), pp.158–173.
Stein, J.D. et al., 2012. Trends in Use of Ancillary Glaucoma Tests for Patients with Open-Angle Glaucoma from 2001 to 2009. *Ophthalmology*, 119(4), pp.748–758. Available at: http://linkinghub.elsevier.com/retrieve/pii/S0161642011009316 [Accessed July 10, 2016].

Stewart, W., 1990. *Clinical Practice of Glaucoma*, Thorafare, NJ: Slack Inc.
Stewart, W.C. & Hunt, H.H., 1993. Threshold variation in automated perimetry. *Survey of Ophthalmology*, 37(5), pp.353–361.
Strouthidis, N.G., Scott, A., et al., 2006. Optic disc and visual field progression in ocular hypertensive subjects: Detection rates, specificity, and agreement. *Investigative Ophthalmology and Visual Science*, 47(7), pp.2904–2910.
Strouthidis, N.G., Vinciotti, V., et al., 2006. Structure and function in glaucoma: The relationship between a functional visual field map and an anatomic retinal map. *Investigative Ophthalmology and Visual Science*, 47(12), pp.5356–5362.
Strouthidis, N.G. & Garway-Heath, D.F., 2008. New developments in Heidelberg retina tomograph for glaucoma. *Current opinion in ophthalmology*, 19(2), pp.141–148.
Study, A.G.I., 1994. Advanced Glaucoma Intervention Study (AGIS): 2. Visual Field Test Scoring and Reliability. *Ophthalmology*, 101(8), pp.1445–1455.
Suh, M.H. et al., 2012. Glaucoma Progression After the First-detected Optic Disc Hemorrhage by Optical Coherence Tomography. *Journal of Glaucoma*, 21(6), pp.358–366.
Sung, K.R. et al., 2011. Retinal nerve fiber layer normative classification by optical coherence tomography for prediction of future visual field loss. *Investigative ophthalmology & visual science*, 52(5), pp.2634–9. Available at: http://www.ncbi.nlm.nih.gov/pubmed/21282570.
Susanna, R. & Medeiros, F., 2006. Enhanced Corneal Compensation (ECC). In *The Optic Nerve in Glaucoma*. Rio de Janeiro, Brazil: Cultura Medica.
Swanson, E. a et al., 1993. In vivo retinal imaging by optical coherence tomography. *Optics letters*, 18(21), pp.1864–6. Available at: http://www.ncbi.nlm.nih.gov/pubmed/19829430.
Swanson, W.H., Sun, H., Lee, B.B. & Cao, D., 2011. Responses of primate retinal ganglion cells to perimetric stimuli. *Investigative Ophthalmology and Visual Science*, 52(2), pp.764–771.
Swanson, W.H., Sun, H., Lee, B.B., Cao, D., et al., 2011. Responses of Primate Retinal Ganglion Cells to Perimetric Stimuli. *Investigative Opthalmology & Visual Science*, 52(2), p.764. Available at: http://iovs.arvojournals.org/article.aspx?doi=10.1167/iovs.10-6158 [Accessed August 2, 2016].
Swanson, W.H., Felius, J. & Pan, F., 2004. Perimetric Defects and Ganglion Cell Damage: Interpreting Linear Relations Using a Two-Stage Neural Model. *Investigative Ophthalmology and Visual Science*, 45(2), pp.466–472.
Swindale, N. V. et al., 2000. Automated analysis of normal and glaucomatous optic nerve head topography images. *Investigative Ophthalmology and Visual Science*, 41(7), pp.1730–1742.
Tanna, A. et al., 2011. Interobserver agreement and intraobserver reproducibility of the subjective determination of glaucomatous visual field progression. *Ophthalmology*, 118(1), pp.60–65.
Tate, G., 1985. The physiological basis for perimetry. In S. Drance & D. Anderson, eds. *Automated Perimetry in Glaucoma: A Practical Guide*. Orlando: Grune & Stratton,

Inc., pp. 1–28.
Teal, P.K., Morin, J.D. & McCulloch, C., 1972. Assessment of the normal disc. *Transactions of the American Ophthalmological Society*, 70, pp.164–177. Available at: http://www.ncbi.nlm.nih.gov/pubmed/4663666.
Thomas, D. & Duguid, G., 2004. Optical coherence tomography--a review of the principles and contemporary uses in retinal investigation. *Eye (London, England)*, 18(6), pp.561–570.
Tjon-Fo-Sang, M.J., de Vries, J. & Lemij, H.G., 1996. Measurement by nerve fiber analyzer of retinal nerve fiber layer thickness in normal subjects and patients with ocular hypertension. *American journal of ophthalmology*, 122(2), pp.220–227.
Toth, C.A., 1997. A Comparison of Retinal Morphology Viewed by Optical Coherence Tomography and by Light Microscopy. *Archives of Ophthalmology*, 115(11), p.1425. Available at: http://www.ncbi.nlm.nih.gov/pubmed/9366674.
Trible, J.R. et al., 2000. Accuracy of glaucoma detection with frequency-doubling perimetry. *American Journal of Ophthalmology*, 129(6), pp.740–745.
Turpin, A. et al., 2002a. Development of efficient threshold strategies for frequency doubling technology perimetry using computer simulation. *Investigative Ophthalmology and Visual Science*, 43(2), pp.322–331.
Turpin, A. et al., 2002b. Performance of efficient test procedures for frequency-doubling technology perimetry in normal and glaucomatous eyes. *Investigative Ophthalmology and Visual Science*, 43(3), pp.709–715.
Turpin, A., Sampson, G.P. & Mckendrick, A.M., 2009. Combining ganglion cell topology and data of patients with glaucoma to determine a structure-function map. *Investigative Ophthalmology and Visual Science*, 50(7), pp.3249–3256.
Tuulonen, A. & Airaksinen, P.J., 1991. Initial glaucomatous optic disk and retinal nerve fiber layer abnormalities and their progression. *American journal of ophthalmology*, 111(4), pp.485–490. Available at: http://www.ncbi.nlm.nih.gov/pubmed/2012151.
Tuulonen, A., Lehtola, J. & Airaksinen, P.J., 1993. Nerve fiber layer defects with normal visual fields. Do normal optic disc and normal visual field indicate absence of glaucomatous abnormality? *Ophthalmology*, 100(5), pp.587-597-598.
Tyler, C.W., 1981. Specific deficits of flicker sensitivity in glaucoma and ocular hypertension. *Investigative Ophthalmology and Visual Science*, 20(2), pp.204–212.
Tyrrell, R. a. & Owens, D.A., 1988. A rapid technique to assess the resting states of the eyes and other threshold phenomena: The Modified Binary Search (MOBS). *Behavior Research Methods, Instruments, & Computers*, 20(2), pp.137–141.
Uchida, H., Brigatti, L. & Caprioli, J., 1996. Detection of structural damage from glaucoma with confocal laser image analysis. *Investigative ophthalmology & visual science*, 37(12), pp.2393–401. Available at: http://www.ncbi.nlm.nih.gov/pubmed/8933756.
Varma, R. et al., 1994. Race-, Age-, Gender-, and Refractive Error--Related Differences in the Normal Optic Disc. *Arch Ophthalmol*, 112(8), pp.1068–1076. Available at: http://archopht.ama-assn.org/cgi/content/abstract/112/8/1068.
Varma, R., Skaf, M. & Barron, E., 1996. Retinal nerve fiber layer thickness in normal human eyes. *Ophthalmology*, 103, pp.2114–2119.

Ventura, L.M. et al., 2006. The relationship between retinal ganglion cell function and retinal nerve fiber thickness in early glaucoma. *Investigative Ophthalmology and Visual Science*, 47(9), pp.3904–3911.
Ventura, L.M. & Porciatti, V., 2005. Restoration of retinal ganglion cell function in early glaucoma after intraocular pressure reduction: A pilot study. *Ophthalmology*, 112(1), pp.20–27.
Verdon-Roe, G.M. et al., 2006. Exploration of the psychophysics of a motion displacement hyperacuity stimulus. *Investigative Ophthalmology and Visual Science*, 47(11), pp.4847–4855.
Vesti, E., Johnson, C. a & Chauhan, B.C., 2003. Comparison of different methods for detecting glaucomatous visual field progression. *Investigative ophthalmology & visual science*, 44(9), pp.3873–3879. Available at: http://www.ncbi.nlm.nih.gov/pubmed/12939303.
Viswanathan, A.C., Fitzke, F.W. & Hitchings, R.A., 1997. Early detection of visual field progression in glaucoma: a comparison of PROGRESSORT and STATPAC2T. *British Journal of Ophthalmology*, 81, pp.1037–1042.
Vizzeri, G. et al., 2010. Determinants of agreement between the confocal scanning laser tomograph and standardized assessment of glaucomatous progression. *Ophthalmology*, 117(10), pp.1953–1959.
Wall, M. et al., 2010. The effective dynamic ranges of standard automated perimetry sizes III and V and motion and matrix perimetry. *Archives of ophthalmology*, 128(5), pp.570–576.
Wall, M. & Ketoff, K.M., 1995. Random dot motion perimetry in patients with glaucoma and in normal subjects. *American journal of ophthalmology*, 120(5), pp.587–596. Available at: http://dx.doi.org/10.1016/S0002-9394(14)72205-6.
Wall, M., Kutzko, K.E. & Chauhan, B.C., 1997. Variability in patients with glaucomatous visual field damage is reduced using size V stimuli. *Investigative Ophthalmology and Visual Science*, 38(2), pp.426–435.
Walsh, T., 1990. Visual Fileds: Examination and Interpretation. In *American Academy of Ophthalmology*. La Jolla: Palace Press.
Weber, A.J., Kaufman, P.L. & Hubbard, W.C., 1998. Morphology of single ganglion cells in the glaucomatous primate retina. *Investigative Ophthalmology and Visual Science*, 39(12), pp.2304–2320.
Weber, J. & Rau, S., 1992. The properties of perimetric thresholds in normal and glaucomatous eyes. *German journal of ophthalmology*, 1(2), pp.79–85. Available at: http://www.ncbi.nlm.nih.gov/pubmed/1477630.
Weber, J., Schultze, T. & Ulrich, H., 1989. The visual field in advanced glaucoma. *International Ophthalmology*, 13(1–2), pp.47–50.
Weinreb, R.N., Shakiba, S., Sample, P.A., et al., 1995. Association between quantitative nerve fiber layer measurement and visual field loss in glaucoma. *American journal of ophthalmology*, 120, pp.732–738.
Weinreb, R.N. et al., 1993. Effect of repetitive imaging on topographic measurements of the optic nerve head. *Archives of ophthalmology (Chicago, Ill. : 1960)*, 111(5), pp.636–8. Available at: http://www.ncbi.nlm.nih.gov/pubmed/8489444.

Weinreb, R.N., 1999. Evaluating the retinal nerve fiber layer in glaucoma with scanning laser polarimetry. *Archives of ophthalmology*, 117, pp.1403–1406.
Weinreb, R.N. et al., 1990. Histopathologic validation of Fourier-ellipsometry measurements of retinal nerve fiber layer thickness. *Archives of ophthalmology*, 108(4), pp.557–60. Available at: http://www.ncbi.nlm.nih.gov/pubmed/2322159.
Weinreb, R.N., 1993. Laser scanning tomography to diagnose and monitor glaucoma. *Current opinion in ophthalmology*, 4(2), pp.3–6. Available at: http://www.ncbi.nlm.nih.gov/pubmed/10148455.
Weinreb, R.N., Bowd, C. & Zangwill, L.M., 2003. Glaucoma detection using scanning laser polarimetry with variable corneal polarization compensation. *Archives of ophthalmology*, 121, pp.218–224.
Weinreb, R.N., Shakiba, S. & Zangwill, L., 1995. Scanning laser polarimetry to measure the nerve fiber layer of normal and glaucomatous eyes. *American journal of ophthalmology*, 119(5), pp.627–636.
Werner, E.B. et al., 1989. Variability of automated visual fields in clinically stable glaucoma patients. *Investigative Ophthalmology and Visual Science*, 30(6), pp.1083–1089.
Werner, E.B., Saheb, N. & Thomas, D., 1982. Variability of static visual threshold responses in patients with elevated IOPs. *Archives of ophthalmology*, 100(10), pp.1627–31.
White, A.J.R. et al., 2002. An examination of physiological mechanisms underlying the frequency-doubling illusion. *Investigative Ophthalmology and Visual Science*, 43(11), pp.3590–3599.
Wild, J.M. et al., 1999. Between-algorithm, between-individual differences in normal perimetric sensitivity: Full Threshold, FASTPAC, and SITA. *Investigative Ophthalmology and Visual Science*, 40(6), pp.1152–1161.
Wild, J.M. et al., 1989. The influence of the learning effect on automated perimetry in patients with suspected glaucoma. *Acta ophthalmologica*, 67(5), pp.537–545.
Wilensky, J. & Joondeph, B., 1984. Variation in visual field measurements with an automated perimeter. *American Journal of Ophthalmology*, 97, pp.328–331.
Wilensky, J.T. & Kolker, A.E., 1976. Peripapillary changes in glaucoma. *American journal of ophthalmology*, 81(3), pp.341–345. Available at: http://www.ncbi.nlm.nih.gov/pubmed/943951.
Wojtkowski, M. et al., 2005. Three-dimensional retinal imaging with high-speed ultrahigh-resolution optical coherence tomography. *Ophthalmology*, 112(10), pp.1734–1746.
Wojtkowski, M. et al., 2004. Ultrahigh-resolution, high-speed, Fourier domain optical coherence tomography and methods for dispersion compensation. *Optics Express*, 12(11), pp.2404–2422. Available at: http://www.opticsexpress.org/abstract.cfm?URI=oe-12-11-2404\nhttp://www.opticsinfobase.org/DirectPDFAccess/8511D535-90DD-89F2-4FE778535B38C101_80147/oe-12-11-2404.pdf?da=1&id=80147&seq=0&mobile=no\nhttp://www.opticsinfobase.org/oe/abstract.cfm?uri=OE-12-1.

Wollstein, G. et al., 2000. Identifying early glaucomatous changes: Comparison between expert clinical assessment of optic disc photographs and confocal scanning ophthalmoscopy. *Ophthalmology*, 107(12), pp.2272–2277.
Wollstein, G., Garway-Heath, D.F. & Hitchings, R.A., 1998. Identification of early glaucoma cases with the scanning laser ophthalmoscope. *Ophthalmology*, 105(8), pp.1557–1563.
Yaghoubi, M. et al., 2015. Confocal scan laser ophthalmoscope for diagnosing glaucoma: a systematic review and meta-analysis. *Asia-Pacific journal of ophthalmology (Philadelphia, Pa.)*, 4(1), pp.32–9. Available at: http://www.ncbi.nlm.nih.gov/pubmed/26068611 [Accessed August 16, 2016].
Yu, J.J.H. et al., 2003. Correlation between frequency doubling technology perimetry and temporal frequency characteristics in early glaucoma. *Documenta Ophthalmologica*, 107(2), pp.93–99.
Yucel, Y.H. et al., 1998. Relationship of optic disc topography to optic nerve fiber number in glaucoma. *Arch Ophthalmol*, 116(4), pp.493–497. Available at: http://www.ncbi.nlm.nih.gov/pubmed/9565048\nhttp://archopht.jamanetwork.com/data/Journals/OPHTH/6594/els7584.pdf.
Zalta, a H., 1991. Use of a central 10 degrees field and size V stimulus to evaluate and monitor small central islands of vision in end stage glaucoma. *The British journal of ophthalmology*, 75(3), pp.151–4. Available at: http://www.pubmedcentral.nih.gov/articlerender.fcgi?artid=1042294&tool=pmcentrez&rendertype=abstract.
Zangwill, L.M. et al., 2000. A comparison of optical coherence tomography and retinal nerve fiber layer photography for detection of nerve fiber layer damage in glaucoma. *Ophthalmology*, 107, pp.1309–1315.
Zangwill, L.M. et al., 2001. Discriminating between normal and glaucomatous eyes using the Heidelberg Retina Tomograph, GDx Nerve Fiber Analyzer, and Optical Coherence Tomograph. *Arch Ophthalmol*, 119(July), pp.985–993.
Zangwill, L.M. et al., 1996. Optic nerve head topography in ocular hypertensive eyes using confocal scanning laser ophthalmoscopy. *American journal of ophthalmology*, 122(4), pp.520–525. Available at: http://www.ncbi.nlm.nih.gov/pubmed/8862049.
Zangwill, L.M. et al., 2007. The effect of disc size and severity of disease on the diagnostic accuracy of the Heidelberg retina tomograph glaucoma probability score. *Investigative Ophthalmology and Visual Science*, 48(6), pp.2653–2660.
Zangwill, L.M. & Bowd, C., 2006. Retinal nerve fiber layer analysis in the diagnosis of glaucoma. *Current opinion in ophthalmology*, 17, pp.120–131.
Zeimer, R. et al., 1998. Quantitative detection of glaucomatous damage at the posterior pole by retinal thickness mapping: A pilot study. *Ophthalmology*, 105(2), pp.224–231.
Zeyen, T. et al., 2003. Reproducibility of evaluation of optic disc change for glaucoma with stereo optic disc photographs. *Ophthalmology*, 110(2), pp.340–344.
Zeyen, T. & Caprioli, J., 1993. Progression of disc and field damage in early glaucoma. *Archives of Ophthalmology*, 111(1), pp.62–65.
Zhou, Q. & Knighton, R., 1997. Light scattering and form birefringence of parallel

cylindrical arrays that represent cellular organelles of the retinal nerve fiber layer. *Applied Optics*, 36, pp.2273–2285.

Zhou, Q. & Weinreb, R.N., 2002. Individualized compensation of anterior segment birefringence during scanning laser polarimetry. *Investigative Ophthalmology and Visual Science*, 43(7), pp.2221–2228.

Zueva, M. V et al., 2016. [Distinctive morphological and functional changes in retinal ganglion cells associated with normal aging and early stage of glaucoma]. *Vestnik oftalmologii*, 132(1), pp.36–42. Available at: http://www.ncbi.nlm.nih.gov/pubmed/27030432 [Accessed June 29, 2016].